

AD-A155 142

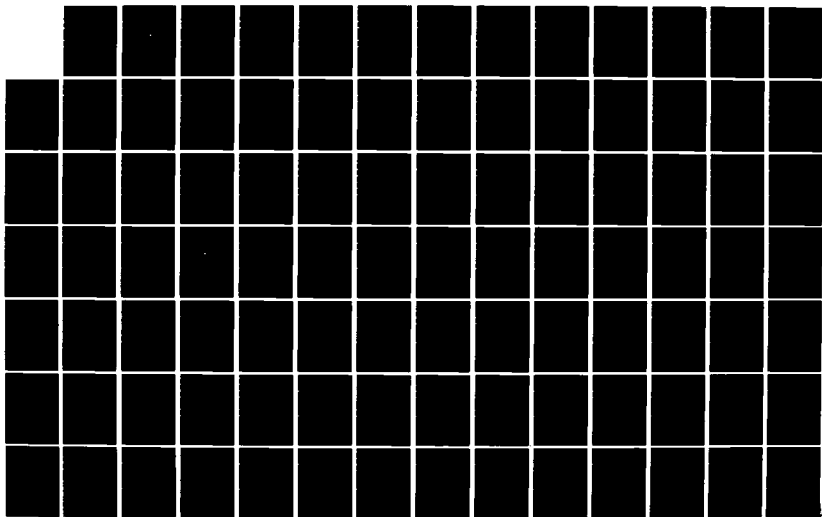
THE EFFECT OF ALLOY ADDITIONS ON SUPERPLASTICITY IN  
THERMOECHANICALLY PR. (U) NAVAL POSTGRADUATE SCHOOL  
MONTEREY CA R J SELF DEC 84

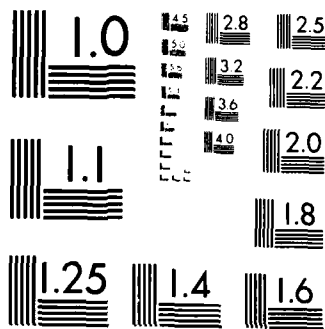
1/2

UNCLASSIFIED

F/G 11/6

NL

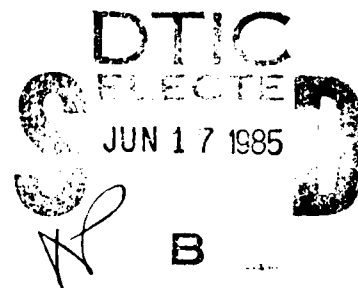




MICROCOPY RESOLUTION TEST CHART  
NATIONAL BUREAU OF STANDARDS 1963-A

AD-A155 142

NAVAL POSTGRADUATE SCHOOL  
Monterey, California



THESIS

THE EFFECT OF ALLOY ADDITIONS ON SUPERPLASTICITY  
IN THERMOMECHANICALLY PROCESSED HIGH MAGNESIUM  
ALUMINUM-MAGNESIUM ALLOYS

by

Richard J. Self

December 1984

Thesis Advisor:

Terry McNelley

Approved for public release; distribution is unlimited

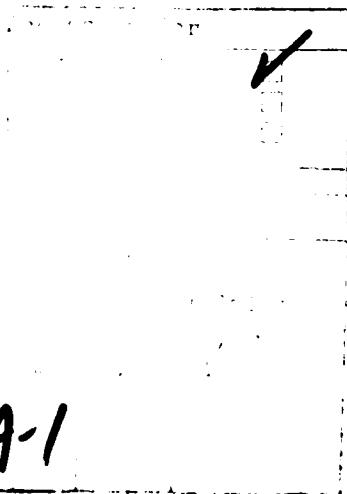
DTIC FILE COPY

85 5 22 031

REPORT DOCUMENTATION PAGE		READ INSTRUCTIONS BEFORE COMPLETING FORM
1. REPORT NUMBER	2. GOVT ACCESSION NO. AD 4155142	3. RECIPIENT'S CATALOG NUMBER
4. TITLE (and Subtitle) The Effects of Alloy Additions on Superplasticity in Thermomechanically Processed High Magnesium Aluminum- Magnesium Alloys		5. TYPE OF REPORT & PERIOD COVERED Master's Thesis; December 1984
7. AUTHOR(s) Richard J. Self		6. PERFORMING ORG. REPORT NUMBER
9. PERFORMING ORGANIZATION NAME AND ADDRESS Naval Postgraduate School Monterey, California 93943		8. CONTRACT OR GRANT NUMBER(s)
11. CONTROLLING OFFICE NAME AND ADDRESS Naval Postgraduate School Monterey, California 93943		10. PROGRAM ELEMENT, PROJECT, TASK AREA & WORK UNIT NUMBERS
14. MONITORING AGENCY NAME & ADDRESS (if different from Controlling Office)		12. REPORT DATE December 1984
		13. NUMBER OF PAGES 126
		15. SECURITY CLASS. (of this report) Unclassified
		15a. DECLASSIFICATION/DOWNGRADING SCHEDULE
16. DISTRIBUTION STATEMENT (of this Report)  Approved for public release; distribution is unlimited		
17. DISTRIBUTION STATEMENT (of the abstract entered in Block 20, if different from Report)		
18. SUPPLEMENTARY NOTES		
19. KEY WORDS (Continue on reverse side if necessary and identify by block number) Superplasticity High Mg Al-Mg Alloys		
20. ABSTRACT (Continue on reverse side if necessary and identify by block number)  This research extends previous thesis work by Becker and Mills, and is concurrent with that of Stengel on the superplastic behavior of warm rolled high-Mg, Al-Mg alloys. In this work, the effect of various alloy additions were investigated. The following Al-Mg alloy compositions were studied: 8% Mg; 8% Mg-0.4% Cu; 8% Mg-0.4% Cu-0.5% Mn; 10% Mg; 10% Mg-0.4% Cu; 10% Mg-0.2% Mn. These materials were solution treated and hot worked at 440°C and then warm rolled at 300°C.		

20. (Continued)

to 94% reduction. Tensile testing was then conducted for the as-rolled condition. The alloys were tested at temperatures ranging from room temperature to 300°C and at strain rates from  $5.6 \times 10^{-5}/\text{sec}^{-1}$  to  $1.4 \times 10^{-1}/\text{sec}^{-1}$ . The copper addition has, on the same weight percentage basis, the same effect on superplasticity as does the addition of manganese to the alloy. The addition of small amounts (i.e., approximately 0.2 weight percent) of manganese appears to offer little advantage over the binary compositions in terms of superplasticity.



Approved for public release; distribution is unlimited

The Effect of Alloy Additions on Superplasticity  
in Thermomechanically Processed High Magnesium  
Aluminum-Magnesium Alloys

by

Richard J. Self  
Lieutenant, United States Navy  
B.S., University of California, Los Angeles, 1977

Submitted in partial fulfillment of the  
requirements for the degree of

MASTER OF SCIENCE IN ENGINEERING SCIENCE


from the

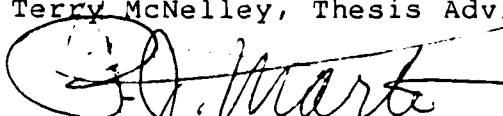
NAVAL POSTGRADUATE SCHOOL  
December 1984

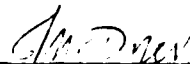
Author:

  
Richard J. Self

Approved by:

  
Terry McNelley, Thesis Advisor

  
P. J. Marto, Chairman,  
Department of Mechanical Engineering

  
John N. Dyer, Dean of Science and Engineering

## ABSTRACT

This research extends previous thesis work by Becker and Mills, and is concurrent with that of Stengel on the superplastic behavior of warm rolled high-Mg, Al-Mg alloys. In this work, the effects of various alloy additions were investigated. The following Al-Mg alloy compositions were studied: 8% Mg; 8% Mg-0.4% Cu; 8% Mg-0.4% Cu-0.5% Mn; 10% Mg; 10% Mg-0.4% Cu; 10% Mg-0.2 Mn. These materials were solution treated and hot worked at 440°C and then warm rolled at 300°C to 94% reduction. Tensile testing was then conducted for the as-rolled condition. The alloys were tested at temperatures ranging from room temperature to 300°C and at strain rates from  $5.6 \times 10^{-5} \text{ sec}^{-1}$  to  $1.4 \times 10^{-1} \text{ sec}^{-1}$ . The copper addition has, on the same weight percentage basis, the same effect on superplasticity as does the addition of manganese to the alloy. The addition of small amounts (i.e., approximately 0.2 weight percent) of manganese appears to offer little advantage over the binary compositions in terms of superplasticity.

## TABLE OF CONTENTS

I.	INTRODUCTION . . . . .	13
II.	BACKGROUND . . . . .	16
	A. ALUMINUM-MAGNESIUM ALLOYS . . . . .	16
	B. PREVIOUS WORK . . . . .	16
	C. SUPERPLASTIC BEHAVIOR . . . . .	19
	D. ALLOYING ADDITIONS . . . . .	22
III.	EXPERIMENTAL PROCEDURE . . . . .	28
	A. MATERIAL PROCESSING . . . . .	28
	B. WARM ROLLING . . . . .	29
	C. TENSILE SPECIMEN TESTING . . . . .	31
	D. DATA REDUCTION . . . . .	34
	E. METALLOGRAPHY . . . . .	35
IV.	RESULTS AND DISCUSSION . . . . .	36
	A. OPTICAL MICROSCOPY . . . . .	36
	1. General Results . . . . .	36
	2. Binary Alloys . . . . .	37
	3. Manganese Alloying Additions . . . . .	40
	4. Copper Alloying Additions . . . . .	42
	5. Copper and Manganese Addition . . . . .	44
	B. MECHANICAL TEST RESULTS . . . . .	47
	1. General Remarks . . . . .	47
	2. Magnesium Alloying Additions . . . . .	55



3.	Manganese Alloying Additions . . . . .	61
4.	Copper Alloying Additions . . . . .	68
5.	Copper and Manganese Addition . . . . .	77
6.	Summary of Mechanical Test Data . . . . .	82
V.	CONCLUSIONS . . . . .	85
APPENDIX A:	Mechanical Test Data on Al-8% Mg Alloy . .	87
APPENDIX B:	Mechanical Test Data on Al-10% Mg Alloy . .	94
APPENDIX C:	Mechanical Test Data on Al-10% Mg-0.4% Cu Alloy . . . . .	101
APPENDIX D:	Mechanical Test Data on Al-10% Mg-0.2% Mn Alloy . . . . .	108
APPENDIX E:	Mechanical Test Data on Al-8% Mg-0.4% Cu-0.5% Mn Alloy . . . . .	114
APPENDIX F:	Mechanical Test Data on the Effect of Mn Addition on Al-10% Mg Alloy . . . . .	120
	LIST OF REFERENCES . . . . .	124
	INITIAL DISTRIBUTION LIST . . . . .	126

# LIST OF TABLES

I.	Alloy Composition (Weight Percent)	28
II.	Mechanical Properties of Al-8% Mg Alloy	48
III.	Mechanical Properties of Al-10% Mg Alloy	49
IV.	Mechanical Properties of Al-10% Mg-0.4% Cu Alloy	50
V.	Mechanical Properties of Al-8% Mg-0.4% Cu Alloy	51
VI.	Mechanical Properties of Al-8% Mg-0.4% Cu-0.5% Mn Alloy	52
VII.	Mechanical Properties of Al-10% Mg-0.2% Mn Alloy	53
VIII.	Mechanical Properties of Al-10% Mg-0.5% Mn Alloy	54

## LIST OF FIGURES

2.1	Phase Diagram for Al-Mg Alloy System . . . . .	24
2.2	Phase Diagram for Al-Mg-Cu Alloy System . . . . .	26
2.3	Phase Diagram for Al-Mg-Mn Alloy System . . . . .	26
3.1	Test Specimen Geometry . . . . .	32
4.1	Triplanar Photomicrograph of Al-8% Mg Binary Alloy in the As-Rolled Condition, Showing Banding in Transverse and Longitudinal Planes, and Inhomogeneous Microstructure in the Rolling Plane. Graf-Sargent Etch, x250 . . . . .	38
4.2	Triplanar Photomicrograph of Al-10% Mg Binary Alloy in the As-Rolled Condition, Again Showing Banding and Inhomogeneous Microstructure. Graf-Sargent Etch, x250 . . . . .	39
4.3	Triplanar Photomicrograph of Al-10% Mg-0.2% Mn Alloy in the As-Rolled Condition Showing the Homogenizing Effect of the Manganese Addition; However, the Rolling Plane Microstructure is Still Slightly Inhomogeneous at this Mn Content. Graf-Sargent Etch, x250 . . . . .	41
4.4	Triplanar Photomicrograph of Al-10% Mg-0.4% Cu Alloy in the As-Rolled Condition Showing the Homogenizing Effect of the Copper Addition. Graf-Sargent Etch, x250 . . . . .	43
4.5	Triplanar Photomicrograph of Al-8% Mg-0.4% Cu-0.5% Mn Alloy in the As-Rolled Condition Showing the Homogenizing Effect of the Copper and Manganese Additions; Slight Banding in the Transverse and Longitudinal Planes. Graf-Sargent Etch, x250 . . . . .	45
4.6	Phase Diagram for the Al-Cu-Mg-Mn Alloy System . . . . .	46
4.7	True Stress at 0.1 Strain versus Strain Rate for Tensile Tests on Al-8% Mg Alloy Conducted at 250 and 300°C. The Al-8% Mg Alloy is Slightly Stronger at 250°C than it is at 300°C . .	56

4.8	True Stress at 0.1 Strain versus Strain Rate for Tensile Tests on Al-10% Mg Alloy Conducted at 250 and 300°C Again Showing that the 10% Mg Alloy is Slightly Stronger at 250°C than it is at 300°C . . . . .	57
4.9	True Stress at 0.1 Strain versus Strain Rate for Tensile Tests at 300°C Comparing the Effect of Magnesium Addition at 8% and 10% Levels; Showing that the 8% Mg Alloy is Slightly Stronger . . . . .	58
4.10	True Stress at 0.1 Strain versus Strain Rate for Tensile Tests at 250°C Comparing the Effect of Magnesium Addition at 8% and 10% Levels; Showing that the 8% Alloy is Slightly Stronger . . . . .	59
4.11	Ductility versus Strain Rate for Tensile Tests at 300°C Comparing the Effect of the Magnesium Addition at the 8% and 10% Levels Showing that the 8% Mg Alloy is Slightly More Ductile . . . . .	60
4.12	True Stress at 0.1 Strain versus Strain Rate for Tensile Tests on Al-10% Mg-0.2% Mn Alloy Conducted at 250 and 300°C. This Alloy is Stronger at 250°C than it is at 300°C . . . . .	62
4.13	Ductility versus Strain Rate for Tensile Tests on Al-10% Mg-0.2% Mn Alloy, Tests Conducted at Room Temperature, 250°C, and 300°C . . . . .	63
4.14	True Stress at 0.1 Strain versus Strain Rate for Tensile Tests on Al-10% Mg-0.5% Mn Alloy Conducted at 250 and 300°C. This Alloy is Stronger at 250°C than it is at 300°C . . . . .	64
4.15	Ductility versus Strain Rate for Tensile Tests on Al-10% Mg-0.5% Mn Alloy, Tests Conducted at Room Temperature, 250°C, and 300°C, Showing the Large Increase in Ductility at 300°C . . . . .	65
4.16	True Stress at 0.1 Strain versus Strain Rate for Tensile Tests Conducted at 300°C Showing the Comparative Effects of Increasing Mn Content on Strength in the 10% Mg Alloy . . . . .	66

4.17	Ductility versus Strain Rate for Tensile Tests Conducted at 300°C Showing the Comparative Effects of Increasing Mn Content on Ductility. There is a Pronounced Increase in Ductility in the 10% Mg Alloy for a 0.5% Mn Addition . . . . .	67
4.18	True Stress at 0.1 Strain versus Strain Rate for Tensile Tests on Al-8% Mg-0.4% Cu Alloy Conducted at 250 and 300°C Showing that the Alloy is Stronger at 250°C than it is at 300°C . . . . .	69
4.19	True Stress at 0.1 Strain versus Strain Rate for Tensile Tests on Al-10% Mg-0.4% Cu Alloy Conducted at 250 and 300°C Showing that the Alloy is Stronger at 250°C than it is at 300°C . . . . .	70
4.20	True Stress at 0.1 Strain versus Strain Rate for Tensile Tests Conducted at 300°C Comparing the Effects of Copper Addition on Strength in the 10% Mg Alloy, and also Showing that the 10% Mg Binary Alloy is Slightly Stronger than the 10% Mg Alloy with Copper Addition . . . . .	71
4.21	True Stress at 0.1 Strain versus Strain Rate for Tensile Tests Conducted at 300°C Comparing the Effect of Increasing Magnesium Content on Strength of the Al-Mg Alloy with a 0.4% Cu Addition, Showing that the 8% Alloy is Slightly Stronger than is the 10% Alloy . . . . .	72
4.22	Ductility versus Strain Rate for Tensile Tests Conducted at 300°C Comparing the 8% Mg and the 8% Mg-0.4% Cu Alloys. The 8% Mg-0.4% Cu Alloy is Slightly more Ductile . . . . .	73
4.23	Ductility versus Strain Rate for Tensile Tests Conducted at 300°C Comparing the 10% Mg and the 10% Mg-0.4% Cu Alloys Showing the Pronounced Ductility Increase in the 10% Mg-0.4% Cu Alloy . . . . .	74
4.24	Ductility versus Strain Rate for Tensile Tests Conducted at 300°C Comparing the 8% Mg-0.4% Cu and the 10% Mg-0.4% Cu Alloys. Again Showing the Pronounced Increase in Ductility Observed in the 10% Mg-0.4% Cu Alloy . . . . .	75

4.25	Ductility versus Strain Rate for Tensile Tests Conducted at 300°C Comparing the Effects of Cu and Mn Additions on the 10% Mg Alloy, and also Showing that the Cu Addition Results in a Slightly Enhanced Ductility . . . . .	78
4.26	True Stress at 0.1 Strain versus Strain Rate for Tensile Tests on Al-8% Mg-0.4% Cu-0.5% Mn Alloy Conducted at 250 and 300°C Showing that the Alloy is Slightly Stronger at 250°C than it is at 300°C . . . . .	79
4.27	True Stress at 0.1 Strain versus Strain Rate for Tensile Tests Conducted at 300°C Comparing the 8% Mg and the 8% Mg-0.4% Cu-0.5% Mn Alloys Showing that the 8% Mg Alloy is Slightly Stronger than is the 8% Mg-0.4% Cu-0.5% Mn Alloy . . . . .	80
4.28	Ductility versus Strain Rate for Tensile Tests on Al-8% Mg-0.4% Cu-0.5% Mn Alloy, Tests Conducted at Room Temperature, 250°C, and 300°C, Showing the Large Increase in Ductility Observed at 300°C . . . . .	81
4.29	Ductility versus Strain Rate for Tensile Tests Conducted at 300°C Comparing the 8% Mg and the 8% Mg-0.4% Cu-0.5% Mn Alloys Showing the Pronounced Ductility Increase in the 8% Mg-0.4% Cu-0.5% Mn Alloy . . . . .	83

particles or as a continuous network at the grain boundaries. Dissolved copper produces the highest increase in strength while still retaining substantial ductility. Copper is a grain refiner in aluminum alloys. At the temperatures and compositions considered here, the composition of the intermetallic phase present would be  $\text{CuMg}_4\text{Al}_6$ . A phase diagram for the Al-Mg-Cu system is present in Figure 2.2. The solid solubility of copper in aluminum is decreased by magnesium addition especially in the 7-15% magnesium range [Ref. 16]. In the Al-Mg-Cu alloy system the hardness, ultimate tensile strength, yield strength, and percentage elongation are strongly dependent on heat treatment. Superplasticity has been previously investigated in the Al-Cu system by Holt [Ref. 17], and in the Al-Mg-Cu system by Becker [Ref. 10].

A phase diagram for the Al-Mg-Mn system can be found in Figure 2.3. At the alloying levels considered in this research, the apparent intermetallic phase present would be  $\text{MnAl}_6$ . This result was confirmed by selected area diffraction work conducted by Garg on these alloys [Ref. 9]. Finely dispersed particles of  $\text{MnAl}_6$  facilitate formation of subgrains and hinder grain growth in aluminum alloys. Manganese in solution has little or no effect on grain size; recrystallization, and precipitation overlap, and interact strongly with the magnesium addition. At temperatures below

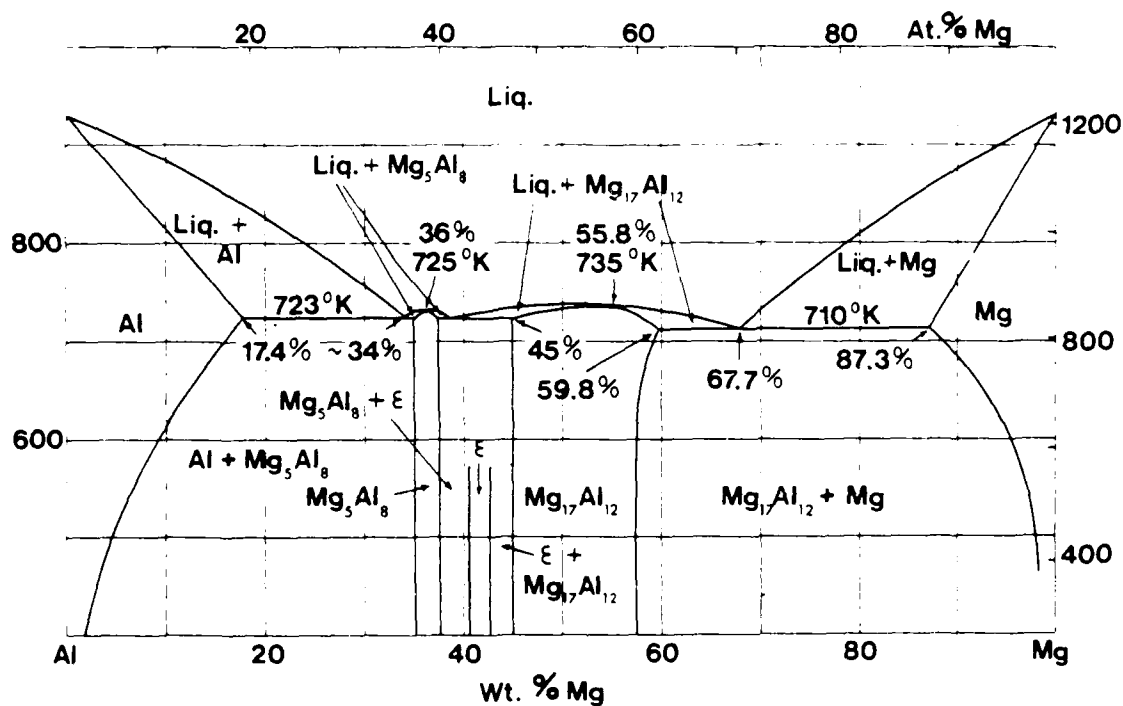


Figure 2.1. Phase Diagram for Al-Mg Alloy System



in Figure 2.1. All phase diagrams are after Mondolfo [Ref. 13]. From this diagram, it can be seen that the solubility of magnesium in aluminum varies from 0.8 weight percent at 100°C to a maximum of approximately 15 weight percent at the eutectic temperature of 451°C. The difference in solubility as a function of temperature provides a driving force for second phase(s) particle formation when the temperature is reduced to a value below the solvus for the amount of magnesium present in the alloy. The beta phase ( $\text{Al}_8\text{Mg}_5$ ) is the intermetallic that exists above five weight percent magnesium. A major problem with this alloying addition is that the beta phase has a tendency to form at grain boundaries. The strength of the alloy increases and the ductility decreases as the magnesium content is increased from five to fourteen weight percent. Alloys with magnesium contents in excess of fourteen weight percent have been found to be too brittle to determine tensile properties [Ref. 16].

Copper is added to the aluminum- alloys to increase the strength of the alloy at low temperatures by heat treatment, and at high temperatures through the formation of compounds with other metals. As the copper content of an alloy increases, there is a continuous increase of hardness, but strength and ductility depend on whether the copper is in solid solution, as spheroidized and evenly distributed

Values for the activation energy may be obtained from the log strain rate versus inverse temperature plot for data at constant stress. Activation energy may be constant for a range of stress, but may change to a different value for a different range of stress. Values for the deformation activation energy are frequently the same as those for lattice diffusion, suggesting lattice diffusion control of deformation, and this is noted in particular for dislocation climb controlled plastic flow [Ref. 15]. Lower values for the activation energy may be observed when grain boundary sliding controls the deformation process. Diffusion in the grain boundaries, the rate controlling process, may occur more readily than diffusion in the grain interior, and hence may be characterized by the lower activation energy. Measurement of the activation energy may provide information concerning the mode of deformation at work in a material.

#### D. ALLOYING ADDITIONS

The magnesium addition to aluminum alloys results in lower density, and increased strength. Most of the strength in these alloys is due to magnesium in solid solution, although precipitation does occur. Strength can be increased by cold or warm working. Aluminum-magnesium alloys with minor other alloying elements added, are capable of obtaining good strength, corrosion resistance, and toughness. The phase diagram for this system is illustrated

elevated temperatures. For a thermally activated process, the flow stress is a function of strain, strain rate, and temperature. Stress is often assumed to depend upon strain rate at constant strain and temperature according to the relation:

$$\sigma = k\dot{\epsilon}^m \quad (\text{eqn. 2.2})$$

where  $\sigma$  is the stress,  $\dot{\epsilon}$  is the strain rate,  $k$  is a temperature dependent constant, and  $m$  is the strain rate sensitivity coefficient. In general,  $m$  increases with increasing temperature. In most metals, superplastic behavior usually occurs at high  $m$  values of 0.3 to 0.5, and is the greatest at the maximum value for  $m$ . The value for  $m$  can be found by plotting log stress vs. log strain rate for data obtained at constant strain and temperature. A large value for  $m$  confers resistance to localized necking by causing increased resistance to further deformation when necking begins to occur.

The activation energy ( $Q$ ), is a measure of the energy required for temperature-dependent processes. For a thermally activated deformation process:

$$\dot{\epsilon} = f(\sigma)\exp(-Q/RT) \quad (\text{eqn. 2.3})$$

where  $R$  is the gas constant, and  $T$  the absolute temperature.

matrix to minimize the formation of cavities [Ref. 13]. The fine grains should consist of small equiaxed grains with smooth, rounded grain boundaries to promote grain boundary sliding. Grain growth suppresses superplasticity as larger grains impose greater diffusion distances and reduce the strain resulting from boundary sliding.

In order to prevent grain growth in superplastic forming, some form of grain boundary pinning is necessary. A fine and deformable precipitate will enhance the material's resistance to grain growth. Given that a dispersion of particles is present during elevated temperature flow, where recrystallization and grain growth occur, these particles may inhibit grain growth following the Zener-McLean relationship [Ref. 14]:

$$d = 4r/3f \quad (\text{eqn. 2.1})$$

where  $d$  is the grain size,  $r$  is the particle radius, and  $f$  is the volume fraction. This equation is based on the idea that particles sitting on grain boundaries prevent flexing of the boundary as it attempts to sweep through a field of such particles. Clearly, for a given volume fraction  $f$ , a smaller particle size should lead to a finer grain size.

Deformation at elevated temperatures is a thermally activated process, and superplasticity is observed only at

Mills [Ref. 11], extended the previous work by Becker on the Al-10% Mg-0.5% Mn alloy with a comprehensive study of superplasticity in this system. He also extended testing into the temperature range 325°C to 425°C to study grain boundary sliding effects and recrystallization in this alloy. Mills found that the high ductilities observed at temperatures above the solvus are the result of grain boundary sliding. Stengel [Ref. 12], is currently studying the effects of annealing on superplasticity in this alloy system.

#### C. SUPERPLASTIC BEHAVIOR

Superplasticity is defined as the ability of a material to deform to an exceptionally high elongation. Superplasticity is often taken to mean elongation in excess of 200% [Ref. 13]. Values greater than 1000% are common. The major requirements for superplasticity are generally agreed to be: a fine equiaxed grain structure with high angle grain boundaries, deformable second phase (if present), temperatures in the range of 0.5 - 0.7  $T_m$ , low strain rates, and a high strain rate sensitivity coefficient ( $m$ ).

A fine grain size of less than ten microns is normally required to achieve superplasticity. Also, a fine dispersion of intermetallic phases(s) is usually required to retard grain growth under warm temperature conditions. The phase(s) should be deformable and similar in strength to the

method of storing energy release at annealing temperatures of 0.6 Tm.

Johnson [Ref. 7], standardized the thermomechanical processing of the 8 - 10% aluminum magnesium alloys. In these alloys, he reported good ductility and material strength twice that of 5XXX alloys. His procedure was to solution treat the material at 440°C for nine hours, anneal for one hour at 440°C, quench, and then warm roll. Johnson used warm rolling temperatures in the range from 200°C to 340°C. He concluded that the beta phase ( $Al_8Mg_5$ ) contributed by dispersion strengthening to the high strength and good ductility found in these alloys.

Shirah [Ref. 8], improved the microstructural homogeneity by increasing the solution treatment time to 24 hours. This extended treatment minimized precipitate banding while not effecting grain growth.

Becker [Ref. 10], combined previous work, and developed the procedures for isothermal tensile testing at elevated temperatures. His testing centered around temperatures of 250°C, and 300°C. His work concentrated on the Al-8% Mg-0.4% Cu and Al-10% Mg-0.5% Mn alloys. Becker observed superplastic elongations up to 400%, and concluded that the higher magnesium content in the 10% Mg-0.5% Mn alloy stabilized grain size and extended the range of superplastic behavior to higher temperatures.

rolling portion of the thermomechanical processing sequence. Bingay [Ref. 2] performed both isothermal and non-isothermal forging prior to rolling in 15-19% magnesium containing alloys. Due to processing difficulties, subsequent work was shifted to emphasis on relatively lower magnesium alloys. Glover [Ref. 3], studied alloys containing 7-9% magnesium, and was the first to observe the characteristics of super-plastic behavior in this alloy system.

Grandon [Ref. 4], introduced a twenty-four hour solution treatment followed by an oil quench, and warm rolling at 300°C in his study of the Al-7 to 10% Mg alloys. He found that these alloys maintained good ductility, and a doubling of strength when compared with the 5XXX series alloy. Another finding was that recrystallization did not occur during warm rolling below the solvus. Speed [Ref. 5], extended Grandon's work to alloys bearing higher magnesium contents.

Chesterman [Ref. 6], studied the nature of precipitation and recrystallization in alloys with magnesium contents in the 8 - 14% range through optical microscopy. He found that recrystallization occurred only at temperatures above the solvus, and was not induced even after extensive cold working followed by annealing, provided that the annealing temperature was below the solvus. Further, he found that recrystallization was replaced by precipitation as the

## II. BACKGROUND

### A. ALUMINUM-MAGNESIUM ALLOYS

The advantages offered by aluminum alloys include their low density, ductility, and toughness. Higher strength aluminum alloys get their strength mainly from precipitation and solid solution strengthening. In these processes, the formation of a second phase retards dislocation motion.

The aluminum magnesium alloy system has been studied extensively in this laboratory and was selected in part for this work because of its good strength to weight ratio, superior ductility, lower density, and better corrosion resistance than other higher strength aluminum alloys. This alloy system also offers good high cycle fatigue behavior. Its strength can be improved through cold or warm working, and it can be easily processed.

### B. PREVIOUS WORK

Ness [Ref. 1], studied an 18% aluminum-magnesium alloy concentrating on development of material processing techniques to achieve microstructural refinement and better mechanical properties. He achieved a compression strength of 655 MPa (99 KSI) with this alloy.

A serious problem encountered with high magnesium-aluminum alloys is the elimination of cracking during the



microscopy as well as the results from the mechanical testing of the as-rolled magnesium aluminum alloys to assist in the evaluation of the test results. Review of this work and new questions are posed for subsequent investigation.

rolling. These alloys were tested in the as-rolled condition, and also subsequent to annealing treatments for various times at 300°C, and finally in the recrystallized condition after heating for one half hour at 440°C as well. Elevated temperature testing was conducted at 250°C, and 300°C.

Mills [Ref. 11], (based upon the results obtained by Becker) conducted an in-depth study of the Al-10% Mg-0.5% Mn system. Stengel [Ref. 12], is currently investigating annealing effects in the same alloy.

The processing technique developed by Johnson [Ref. 7], and the elevated temperature tensile testing procedure developed by Becker [Ref. 10], and, as modified by Mills [Ref. 11], were used to study the effect of alloying additions in the following: Al-8% Mg, Al-10% Mg, Al-8% Mg-0.4% Cu-0.5% Mn, Al-10% Mg-0.4% Cu, and Al-10%-0.2% Mn alloys. Results from Becker's work on the 8% Mg-0.4% Cu, and from Becker and Mills' work on the Al-10% Mg-0.5% Mn alloys were also used.

An electromechanical Instron machine with a Marshall three zone clamshell furnace to maintain temperature control were used for tensile testing. Optical microscopy was used to examine the microstructure of samples in the as-rolled condition. This thesis presents the data obtained from the microstructural examination conducted using optical

## I. INTRODUCTION

The purpose of this thesis was to investigate the effect of alloying additions on the elevated temperature deformation characteristics of thermomechanically processed high-magnesium aluminum magnesium alloys. Previous work by Ness [Ref. 1], Bingay [Ref. 2], Glover [Ref. 3], Grandon [Ref. 4], Speed [Ref. 5], Chesterman [Ref. 6], Johnson [Ref. 7], and Shirah [Ref. 8], have shown that thermomechanically processed high-magnesium Al-Mg alloys exhibit good ductility with high strength at ambient temperatures. McNelley and Garg [Ref. 9] have established through transmission electron microscopy that the microstructures of these alloys consists of fine, cellular dislocation structures or subgrain structures. They also reported that annealing the samples after warm rolling resulted in recovery along with possible small amounts of recrystallization to fine grains of submicron size. These results prompted further research into the elevated temperature behavior of these aluminum magnesium alloys with emphasis on their possible superplastic behavior.

Becker [Ref. 10], then investigated superplasticity in the Al-8% Mg-0.4% Cu, and the Al-10% Mg-0.5% Mn alloys. These alloys were thermomechanically processed by warm

#### ACKNOWLEDGEMENT

I would like to thank my advisor, Professor T. R. McNelley, for his expert assistance and guidance in conducting this study. Also, Doctor E. W. Lee and Mr. T. F. Kellogg whose laboratory experience, and Materials knowledge were vital to me. Finally, I would like to express my appreciation to my parents for their support throughout this research.

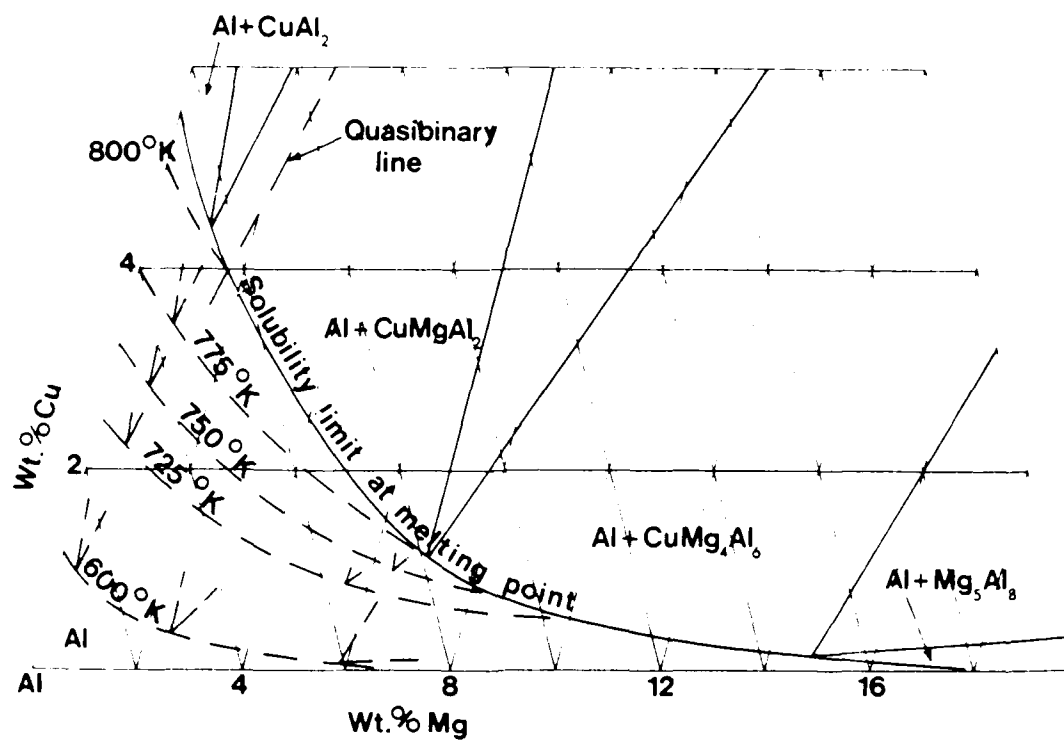


Figure 2.2. Phase Diagram for Al-Mg-Cu Alloy System

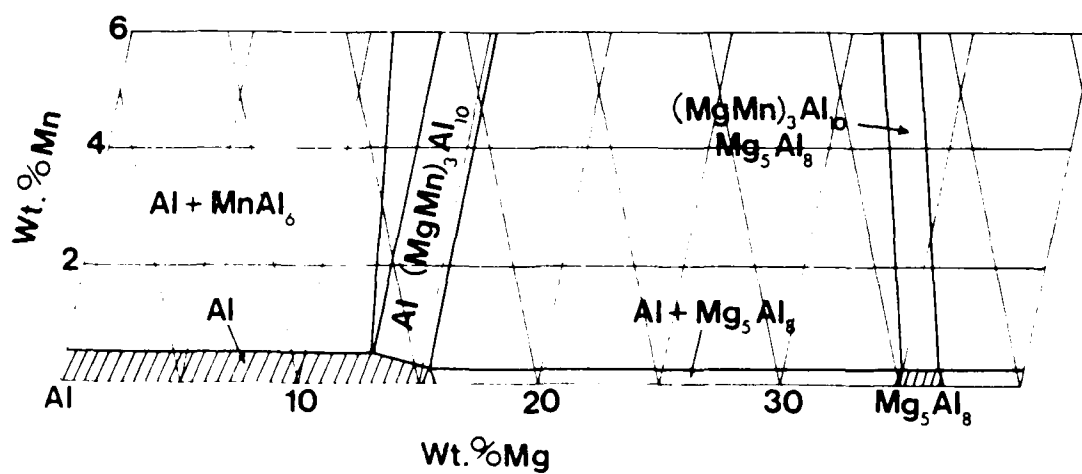


Figure 2.3. Phase Diagram for Al-Mg-Mn Alloy System

650°K, precipitation precedes recrystallization [Ref. 10]. The solid solubility of manganese in aluminum is decreased by the addition of magnesium. At higher levels of magnesium addition, the solubility becomes much smaller. The maximum solubility of magnesium is also reduced by the addition of manganese. Less than 0.08% magnesium can dissolve in  $MnAl_6$ , and little or no manganese can dissolve in the beta phase. Manganese and magnesium have an additive effect on the mechanical properties of this alloy system.

### III. EXPERIMENTAL PROCEDURE

#### A. MATERIAL PROCESSING

The compositions of the aluminum alloys investigated in this research are listed in Table I [Ref. 7]. ALCOA Technical Center produced the direct chill cast ingots using 99.99% pure aluminum and alloying was done with commercially pure magnesium, 5% beryllium-aluminum master alloy, manganese containing master alloy, Ti-B master alloy, and other commercially pure alloying additions, (i.e., Cu). Upon receipt, the ingots measured 127 mm (5 in) in diameter, and 1016 mm (40 in) in length.

TABLE I  
Alloy Composition (Weight Percent)

<u>Serial Number</u>	<u>Si</u>	<u>Fe</u>	<u>Cu</u>	<u>Mn</u>	<u>Mg</u>	<u>Ti</u>	<u>Be</u>
501301A	0.01	0.03	0.41	0.00	10.0	0.01	0.0002
501303A	0.01	0.03	0.40	0.00	8.14	0.01	0.0002
501304A	0.01	0.03	0.40	0.52	8.22	0.01	0.0002
572821A-2	0.01	0.02	0.00	0.00	8.13	0.01	0.0003
572824A-1	0.01	0.02	0.00	0.00	10.0	0.01	0.0003
572825A-1	0.01	0.02	0.00	0.22	10.0	0.01	0.0004

The ingots were sectioned to produce billets of dimensions 96 mm (3.75 in) x 32 mm (1.25 in) x 32 mm (1.25 in). These dimensions were selected to facilitate subsequent processing of the billets. The procedure for the thermomechanical processing of the billets is similar to that developed by Johnson [Ref. 7], and refined by Becker [Ref. 10]. In this procedure, billets were solution treated at 440°C for 24 hours, and upset forged at 440°C on heated platens to a final height of approximately 28 mm (1.1 in), resulting in a reduction of 73% or a true strain of approximately 1.3. This value is essentially the maximum value that could be processed on the available rolling mill. Subsequent to upset forging the billet was annealed at 440°C for one hour, and then oil quenched.

#### B. WARM ROLLING

The technique for warm rolling the billets into sheets was essentially the same as the one described by Mills [Ref. 11], who modified that used by Becker [Ref. 10], and Johnson [Ref. 7]. The billet was initially heated to 300°C prior to first rolling pass. This required a time of approximately ten minutes after the surface temperature of the sample reached 300°C. Isothermal heating of the sample is essential to prevent cracking of the forged billets during the rolling process. To achieve this, each billet was placed on a large steel plate that served as a heat



source in the furnace between rolling passes. Sample heating times varied from eight minutes between passes initially, to four minutes between passes on the last seven to eight passes. The sample remained in the furnace just long enough between passes to insure a uniform consistent temperature in the sample. The billets were rolled with the rollers lowered in increments of 1.02 mm (0.04 in) initially, and 0.762 mm (0.03 in) on the last seven to eight passes. The warm rolling process generally required from twenty-eight to thirty passes per billet to achieve the required final thickness. The temperature of the sample and the plate was monitored using thermocouples. In later rolling phases, the deformed sheet was pulled through the rolling mill with the aid of manual pressure in order to minimize warping. In the final "as-rolled" condition, each billet was rolled into a sheet about 1.8 mm (0.07 in) thick, 102 mm (4 in) wide, and 762 mm (40 in) long. The final sample reduction was approximately 94%, corresponding to a true strain of about 2.8.

The rolled sheets were cut into blanks of dimensions 63 mm (2.47 in) long, and 13 mm (0.5 in) wide using the procedure described in Becker [Ref. 10]. Each billet yielded between thirty and forty blanks. Tensile test specimens were produced by endmilling blanks in lots of five to a final gage width of approximately 3 mm (0.12 in), and a

gage length of 15 mm (0.6 in). Test specimens were fabricated by using a pattern jig as a milling guide. A sketch of the test specimen is shown in Figure 3.1.

#### C. TENSILE SPECIMEN TESTING

Tensile testing of samples was conducted using an electromechanical Instron machine. Test specimens were placed in wedge-action grips held in place by pins passing through wedges. The grip and specimen assembly were mounted into pull rods connected to the Instron machine. The grips (model #713C) were fabricated of Inconel 718 specifically for use at elevated temperatures. The grips, grip assemblies and pull rods were produced by ATS, Inc., of Butler, Pennsylvania.

Elevated temperature testing was conducted using a Marshall Model #2232 three-zone clamshell furnace. Furnace temperature was controlled by three separate controllers, one for each zone. Ceramic thermocouple sheaths were utilized to pass the thermocouples for the furnace controllers into the furnace. The controller thermocouple for the upper and lower zones of the furnace were located six inches above and below the thermocouple entrance port respectively, and approximately one inch in from the furnace heating elements. The central controller was located one inch directly inside the furnace thermocouple entry port. Glass insulation of one inch thickness was used for

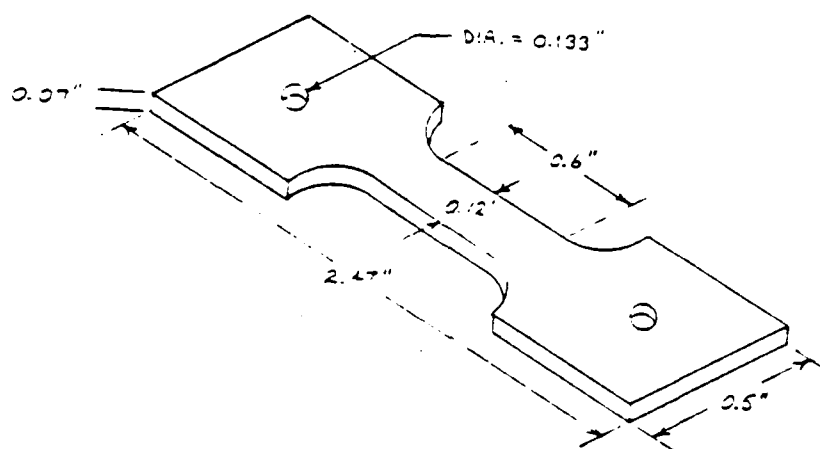


Figure 3.1. Test Specimen Geometry

insulation. Flue effect in the furnace was reduced by using two hollow circular tubes of insulation material and ceramic tiles placed around the pull rods at the top and bottom of the furnace to prevent heat loss. Thin strips of asbestos impregnated paper and glass fiber insulation were placed on the closing surfaces of the furnace. This insulation was found to be important in obtaining and maintaining a uniform temperature distribution in the test zone. Thermal insulation pads were placed over the top and under the bottom of the furnace.

Five thermocouples were installed inside the furnace to monitor temperature. A thermocouple was placed on the top pull rod, four inches above the bottom of the rod and towards the back side of the furnace. Another thermocouple was placed in contact with the specimen and just inside the upper wedge. Two additional thermocouples were placed at corresponding positions on the lower pull rod. Finally a thermocouple was also placed near, but not touching, the middle of the tensile test specimen at the start of the test. Set temperatures were adjusted to remain within 1% of the desired temperature throughout the duration of the test.

Instron crosshead speeds for the tension testing ranged from 0.005 mm/min to 127.0 mm/min (0.0002 in/min to 5.0 in/min) at temperatures of 20°C, 250°C, and 300°C. The magnification ratio used for the automatic chart recorder

was 100 for 0.05 mm/min crosshead speed, 40 for the 0.127 mm/min speed, and ten for the remaining test speeds. The clamshell furnace was heated to constant temperature for a twenty-four hour period prior to commencing a series of tests.

Testing was conducted immediately upon attaining a stable, isothermal test temperature after installation of a test specimen. At very low strain rates, the bottom pull rod temperature would slowly start to drop as the bottom pull rod moved out of the furnace. The furnace temperature was monitored and adjusted to maintain the required test temperature. Either a 1000 lb capacity, or a 2000 lb capacity Instron load cell was used. The 1000 lb load cell was necessary for adequate resolution at the higher temperatures and lower strain rates.

#### D. DATA REDUCTION

Ductility was determined by measuring both the length of the undeformed and of the fractured specimen. Raw data from the strip charts was used in the stress-strain calculations. Engineering and true stress and strain were computed from the strip chart data. The raw data from the tensile testing was reduced for analysis with the aid of a PL/C data reduction computer program run on an IBM 3033 Computer. The data reduction program was similar to that developed by Stengel [Ref. 12]. The data reduction program took into account

such variables as grip tightening, Instron machine error, and elastic strain and performed a "floating slope" calculation at each selected data point. The reduced data was loaded into computer data files for further computation, and graph plotting using the EASYPLOT routine.

#### E. METALLOGRAPHY

Samples of "as-rolled" material were mounted in standard plastic moulds with cold mounting compound. All optical microscopy specimens were polished first using 240 to 600 grit paper followed by final polishing using aluminum oxide abrasive. Graf-Sargent solution (prepared using: 15.5 ml of Nitric acid, 0.5 ml of HF, 3.0 gms  $\text{CrO}_3$ , and 84 ml of water) was used to etch each specimen. Etching time was sixty seconds. A Zeiss Universal microscope was used for both examination and photographic work. Examination of samples was done using polarized light and strain-free objective lenses. Photographs were taken at magnifications of 16X, 62X, and 125X resulting in final print magnifications of 64X, 250X, and 500X. Panatomic X 35 mm film was used for all photographic work.

#### IV. RESULTS AND DISCUSSION

##### A. OPTICAL MICROSCOPY

###### 1. General Results

Optical microscopy as a part of this work was performed on the following alloys: Al-8% Mg, Al-10% Mg, Al-10% Mg-0.4% Cu, Al-8% Mg-0.4% Cu-0.5% Mn, and Al-10% Mg-0.2% Mn. Results from Becker on the Al-8% Mg-0.4% Cu, and by Becker and Mills on the Al-10% Mg-0.5% Mn are also in this discussion [Ref. 10] and [Ref. 11]. Micrographs that follow are for materials in the "as-rolled" condition, and they show in general an elongated and banded grain structure. The microstructure is often obscured by precipitated intermetallic compounds.

McNelley and Garg [Ref. 9], have conducted Transmission Electron Microscope (TEM) work on many of the alloy compositions under consideration here. They also found the banded microstructures observed optically in these alloys. These microstructures were further revealed to consist of a cellular dislocation substructure produced by warm rolling. The precipitated intermetallic phases are not always obvious in the "as-rolled" TEM micrographs, but some TEM data on as-rolled material as well as on rolled and annealed materials suggest cell sizes of approximately 1.0

microns, and intermetallic beta phase particles of 0.2 to 0.5 microns size.

Comparison of the optical and TEM micrographs suggest that the optical microscope is unable to resolve the details of the structure. The intermetallic phase particles are actually present on a much finer scale than suggested by the optical micrographs. This appears to be the result of the manner in which the etchant works and the presence of the intermetallic phase. Further, optical micrographs are unable to reveal the grain structure. The optical microscopy does, on the other hand, provide insight into the extent of banding in these alloys, and also provides a basis for comparison of the effects of alloying on the degree of homogeneity observed in them.

## 2. Binary Alloys

Examination of micrographs of the two binary compositions investigated (8% and 10% Mg), Figures 4.1 and 4.2, two factors become apparent. First, the microstructures are heavily banded and elongated in appearance; and secondly, both the banding and amount of precipitated intermetallic phase is greater in the 10% magnesium alloy. The intermetallic beta phase ( $\text{Al}_8\text{Mg}_5$ ) is the phase dispersed in both alloys. In the rolling plane the beta is found both as a continuous phase along grain boundaries, and dispersed nonuniformly within the grains. The greater amount of



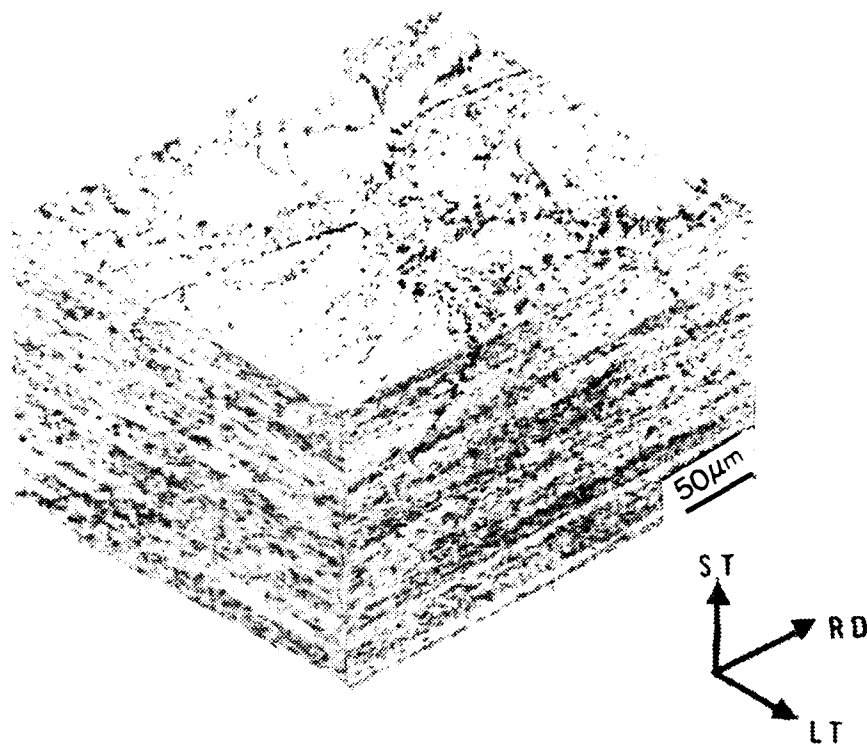


Figure 4.1. Triplanar Photomicrograph of Al-3% Mg Binary Alloy in the As-Rolled Condition, Showing Banding in Transverse and Longitudinal Planes, and Inhomogeneous Microstructure in the Rolling Plane. Graf-Sargent Etch, x250

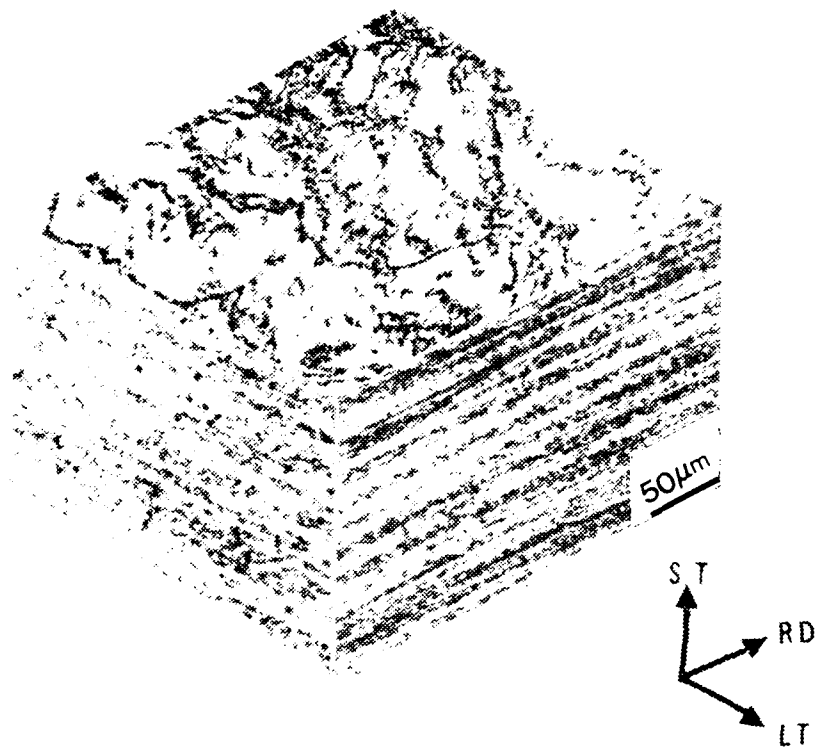


Figure 4.2. Triplanar Photomicrograph of Al-10% Mg Binary Alloy in the As-Rolled Condition, Again Showing Banding and Inhomogeneous Microstructure. Graf-Sargent Etch, x250

TABLE VII  
Mechanical Properties of Al-10% Mg-0.2% Mn Alloy

Temp (C)	Strain Rate (1/Sec)	UTS (MPa)	True Stress at 0.1 Plastic Strain (MPa)	Ductility (Percent)
20	1.39 X 10 <sup>-3</sup>	450.2	*	5.2
	1.39 X 10 <sup>-2</sup>	506.1	*	7.4
250	5.60 X 10 <sup>-5</sup>	29.1	32.1	162.7
	1.39 X 10 <sup>-4</sup>	41.6	44.1	173.0
	1.39 X 10 <sup>-3</sup>	75.5	82.0	199.0
	1.39 X 10 <sup>-2</sup>	171.5	186.3	66.0
	1.39 X 10 <sup>-1</sup>	249.0	255.5	54.3
300	1.39 X 10 <sup>-4</sup>	16.6	18.0	234.9
	1.39 X 10 <sup>-3</sup>	24.4	26.8	204.5
	1.39 X 10 <sup>-2</sup>	34.8	33.7	109.9
	1.39 X 10 <sup>-1</sup>	146.9	157.8	91.5

\* Data Unavailable.

TABLE VI

Mechanical Properties of Al-8% Mg-0.4% Cu-0.5% Mn Alloy

Temp (C)	Strain Rate (1/sec)	UTS (MPa)	True Stress at 0.1 Plastic Strain (MPa)	Ductility (Percent)
20	1.39 X 10 -3	473.9	*	16.3
	1.39 X 10 -2	474.3	*	11.8
250	1.39 X 10 -4	46.2	49.3	206.9
	1.39 X 10 -3	83.5	91.2	123.2
	1.39 X 10 -2	162.1	173.4	75.8
	1.39 X 10 -1	220.7	226.7	33.4
300	1.39 X 10 -4	24.1	23.4	213.7
	1.39 X 10 -3	44.1	48.0	315.8
	1.39 X 10 -2	46.1	94.4	155.0
	1.39 X 10 -1	151.2	157.5	77.5

\* Data Unavailable.

TABLE V  
Mechanical Properties of Al-8% Mg-0.4% Cu Alloy

Temp (C)	Strain Rate (1/sec)	UTS (MPa)	True Stress at 0.1 Plastic Strain (MPa)	Ductility (Percent)
20	5.3 X 10 <sup>-5</sup>	453.0	*	13.0
	5.3 X 10 <sup>-4</sup>	463.0	*	11.0
	5.3 X 10 <sup>-3</sup>	451.0	*	8.0
250	5.3 X 10 <sup>-5</sup>	35.0	*	312.0
	5.3 X 10 <sup>-4</sup>	66.0	*	130.0
	5.3 X 10 <sup>-3</sup>	119.0	131.3	123.0
300	5.3 X 10 <sup>-5</sup>	22.0	*	210.0
	5.3 X 10 <sup>-4</sup>	30.0	*	224.0
	5.3 X 10 <sup>-3</sup>	63.0	79.2	152.0

\* Data unavailable

TABLE IV  
Mechanical Properties of Al-10% Mg-0.4% Cu Alloy

Temp (C)	Strain Rate (1/sec)	UTS (MPA)	True Stress at 0.1 Plastic Strain (MPA)	Ductility (Percent)
20	1.39 X 10 <sup>-3</sup>	456.7	*	10.8
	1.39 X 10 <sup>-2</sup>	450.5	*	10.9
250	5.60 X 10 <sup>-5</sup>	35.5	38.4	200.2
	1.39 X 10 <sup>-4</sup>	34.0	37.2	458.5
	1.39 X 10 <sup>-3</sup>	77.0	83.7	213.6
	1.39 X 10 <sup>-2</sup>	139.4	151.8	88.7
	1.39 X 10 <sup>-1</sup>	160.5	167.6	64.5
300	1.39 X 10 <sup>-4</sup>	11.9	12.7	378.3
	1.39 X 10 <sup>-3</sup>	30.5	33.3	421.0
	1.39 X 10 <sup>-2</sup>	71.4	72.4	157.3
	1.39 X 10 <sup>-1</sup>	146.8	161.5	106.9

\* Data Unavailable.

TABLE III  
Mechanical Properties of Al-10% Mg Alloy

Temp (C)	Strain Rate (1/sec)	UTS (MPA)	True Stress at 0.1 Plastic Strain (MPA)	Ductility (Percent)
20	1.39 X 10 -3	482.0	*	8.2
	1.39 X 10 -2	467.4	*	9.7
250	5.60 X 10 -5	36.1	39.9	138.0
	1.39 X 10 -4	43.0	47.1	119.8
	1.39 X 10 -3	80.2	88.5	155.7
	1.39 X 10 -2	148.6	156.7	87.6
300	1.39 X 10 -1	231.1	241.1	46.3
	1.39 X 10 -4	27.2	29.5	205.2
	1.39 X 10 -3	36.8	40.6	175.3
	1.39 X 10 -2	83.4	90.9	102.7
		72.8	153.5	75.0

\* Data Unavailable.

TABLE II  
Mechanical Properties of Al-8% Hg Alloy

Temp (C)	Strain Rate (1/sec)	UTS (MPa)	True Stress at 0.1 Plastic Strain (MPa)	Ductility (Percent)
20	1.39 X 10 <sup>-4</sup>	399.6	440.2	16.4
	1.39 X 10 <sup>-3</sup>	386.6	418.8	22.0
	1.39 X 10 <sup>-2</sup>	381.2	416.0	19.8
250	1.39 X 10 <sup>-4</sup>	53.9	61.8	234.2
	1.39 X 10 <sup>-3</sup>	104.5	114.0	254.5
	1.39 X 10 <sup>-2</sup>	178.9	187.0	43.4
	1.39 X 10 <sup>-1</sup>	206.2	221.8	33.8
300	1.39 X 10 <sup>-4</sup>	28.2	30.8	157.9
	1.39 X 10 <sup>-3</sup>	63.0	66.6	181.9
	1.39 X 10 <sup>-2</sup>	114.2	119.5	139.7
	1.39 X 10 <sup>-1</sup>	159.1	165.0	41.6



system decreases as the manganese content increases. The same effect is true for manganese when increasing the copper content. The high content of magnesium, copper, and manganese in this system would lead to reduced solubilities for all three in the alloy. This would result in the precipitation of more intermetallic phase particles. According to the phase diagram, this system could contain as many as four equilibrium phases. Possible candidates for the coarser intermetallic phase are  $\text{CuMg}_4\text{Al}_6$  and  $\text{MnAl}_6$  with the more likely candidate being the  $\text{CuMg}_4\text{Al}_6$ .

## B. MECHANICAL TEST RESULTS

### 1. General Remarks

Stress-Strain data was obtained as outlined in the experimental section. Stress-Strain data for 8% Mg with 0.4% Cu and 10% Mg, 0.5% Mn aluminum alloys was obtained from Becker [Ref. 10], and Mills [Ref. 11]. Tables containing the results of the mechanical testing are listed in Tables II through VIII. Plots of this data appear in the discussion, and in the appendices. Appendix A contains the plots for the 8% Mg alloy, Appendix B, the 10% Mg alloy, and so forth through Appendix F. The plots available in each appendix are: engineering stress-engineering strain at 20°C, 250°C, and 300°C; true stress-true strain at the same temperatures; log true stress-log true strain at 250°C, and 300°C; and ductility-log strain rate.

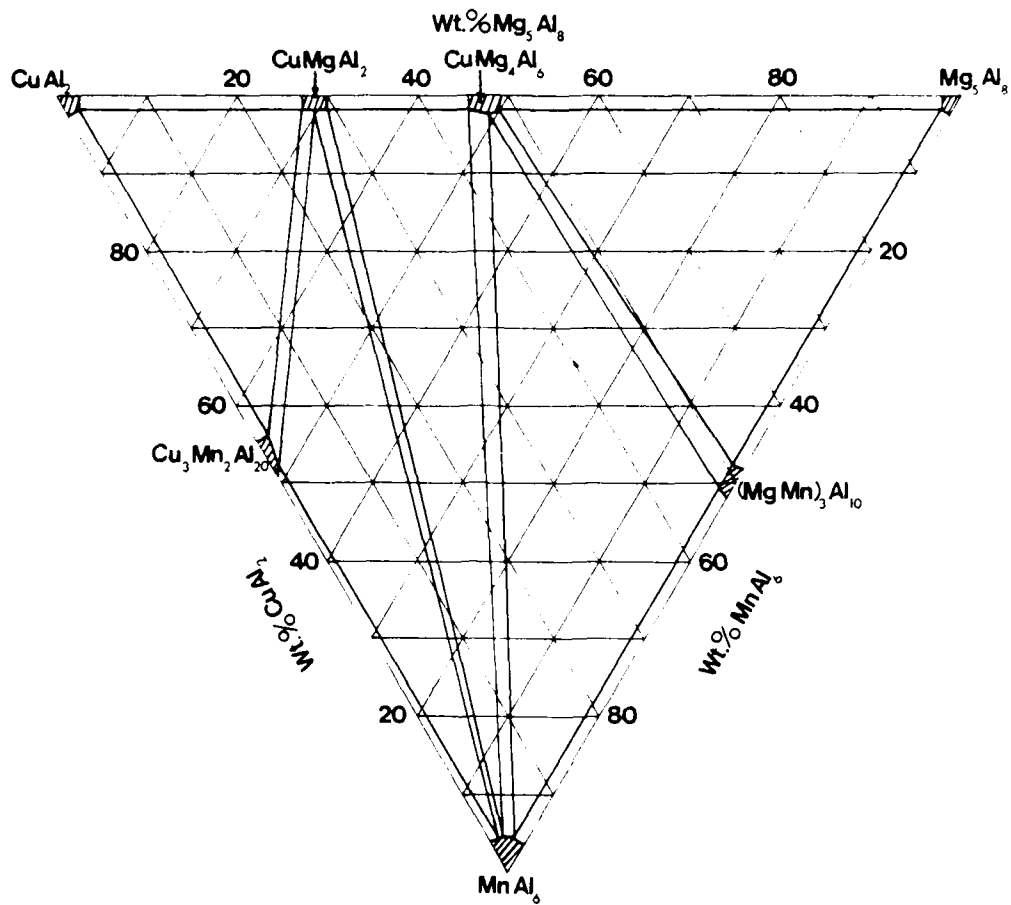


Figure 4.6. Phase Diagram for the Al-Cu-Mg-Mn Alloy System.

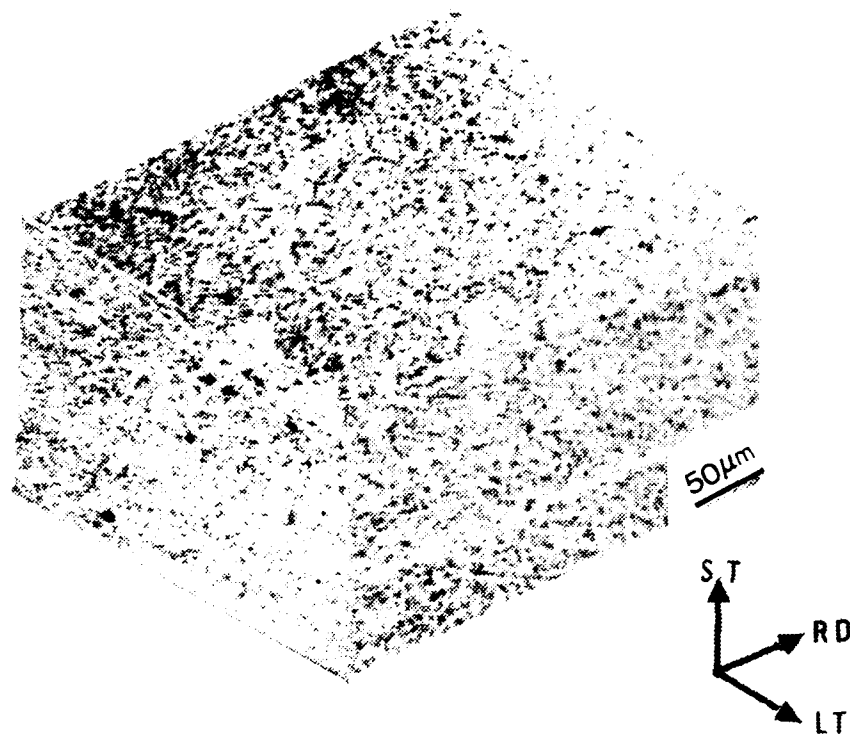


Figure 4.5. Triplanar Photomicrograph of Al-8% Mg-0.4% Cu-0.5% Mn Alloy in the As-Rolled Condition Showing the Homogenizing Effect of the Copper and Manganese Additions; Slight Banding in the Transverse and Longitudinal Planes. Graf-Sargent, x250.

precipitate should be  $\text{CuMg}_4\text{Al}_6$ . The phase diagram for the Al-Cu-Mg system is illustrated in Figure 2.2. The  $\text{CuMg}_4\text{Al}_6$  intermetallic phase might have been carried over from the "as-cast" condition, or might have been precipitated during processing, due to the decreased solubility of both copper and magnesium in aluminum with the ternary addition of copper. In summary, the addition of copper has a substantial homogenization effect over microstructure when compared with the binary alloys and also appears to introduce a third phase,  $\text{CuMg}_4\text{Al}_6$ .

#### 5. Copper and Manganese Addition

The addition of both copper and manganese to the 8% magnesium system had the expected results based on the foregoing observations (see Figure 4.5). We see less banding present than in the Al-8% Mg-0.4% Cu alloy, but more than was found in the Al-10% Mg-0.4% Cu alloy. Manganese is a strong grain refiner in aluminum alloys. The intermetallic phases in this structure are finer, and more widely dispersed than in the Al-8% Mg-0.4% Cu case. Like the Al-10% Mg-0.4% Cu alloy, there is the "coarser" second precipitate present. In the 8% alloy with copper and manganese the precipitate is larger than the precipitate found in the Al-10% Mg-0.4% Cu alloy. A phase diagram for this system can be found in Figure 4.6. Mondolfo [Ref. 16], indicates that the solubility of copper in the Al-Mg-Cu-Mn

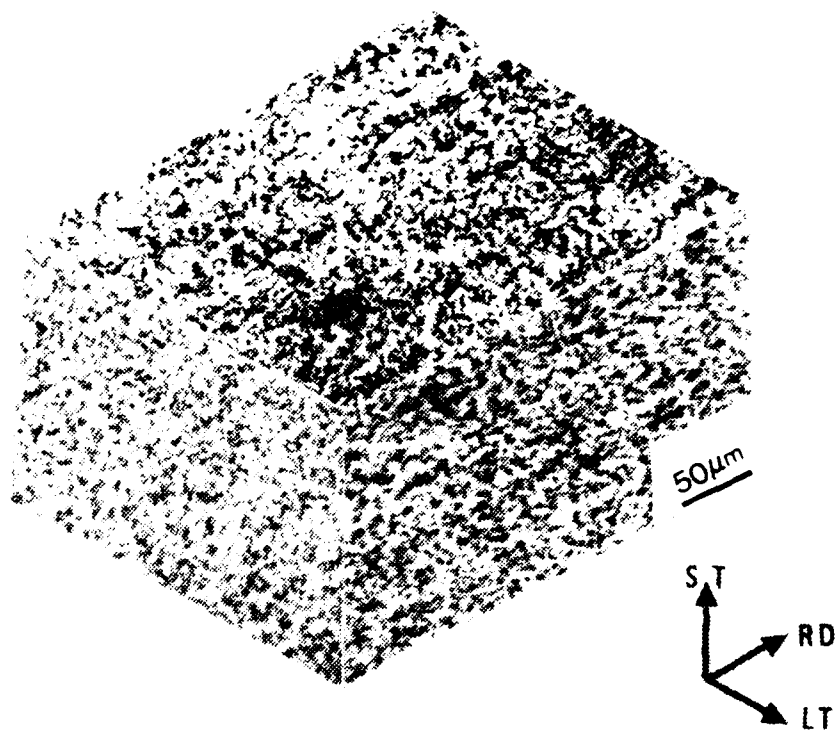


Figure 4.4. Triplanar Photomicrograph of Al-10% Mg-0.4% Cu Alloy in the As-Rolled Condition Showing the Homogenizing Effect of the Copper Addition. Graf-Sargent Etch, x250.

for this alloy system may be found in Figure 2.3. It is also evident in these micrographs that manganese homogenizes the structure. Banding is evident in the 0.2% manganese alloy, and especially notable in the non-uniform beta dispersion when viewed in the rolling plane. At 0.5% manganese, both features are much less notable although slight banding may still be seen. The mechanism for this enhanced homogeneity is not clear. For large manganese additions, as noted above, there appears a relatively fine third phase,  $MnAl_6$ . This phase may refine the matrix grain structure and may also present preferred sites for beta phase formation in the alloy. However, based on the phase diagram, 0.2% manganese should remain in solution.

#### 4. Copper Alloying Additions

From the optical micrographs (Figure 4.4), the addition of copper also has a substantial homogenizing effect on the alloy microstructure. Here, again, the amount of magnesium present would appear as well to have a pronounced effect on the appearance of the microstructure. In the Al-8% Mg-0.4% Cu alloy, banding is still quite evident, while in the 10% alloy the banding is not as noticeable. In the 10% Mg alloy there is a fine dispersion of precipitated beta phase, with what appears to be a coarser dispersion of a different intermetallic phase superimposed. According to Mondolfo [Ref. 16], this coarse

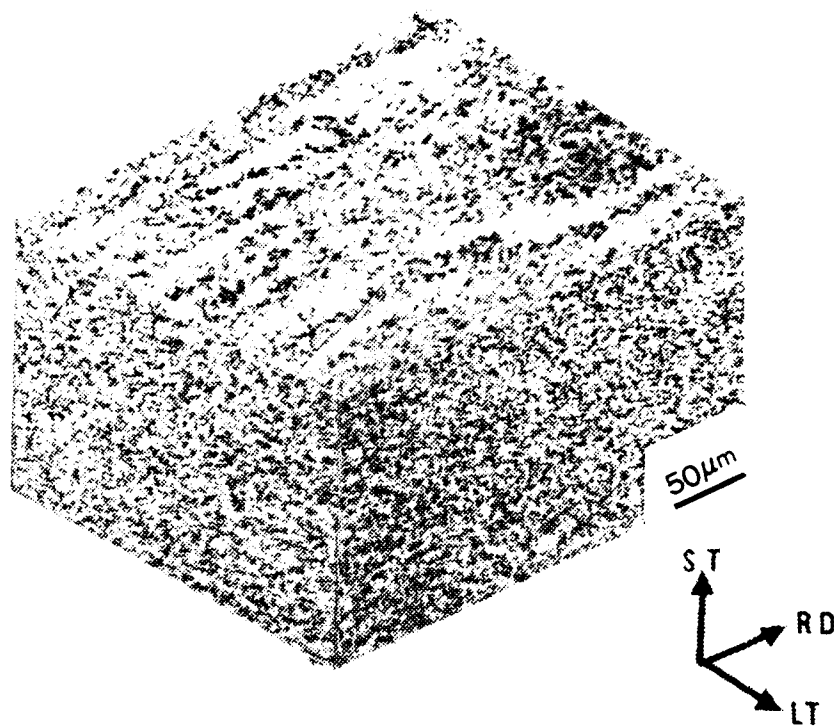


Figure 4.3. Triplanar Photomicrograph of Al-10% Mg-0.2% Mn Alloy in the As-Rolled Condition Showing the Homogenizing Effect of the Manganese Addition; However, the Rolling Plane Microstructure is Still Slightly Inhomogeneous at this Mn Content. Graf-Sargent Etch, x250

dispersion of beta in the higher percent magnesium alloy is expected due to the larger amount of magnesium present. A phase diagram for the Al-Mg alloy system is shown in Figure 2.1, and lever rule calculations suggests about ten volume percent beta phase for an Al-10% Mg alloy rolled at 300°C. In fact, McNelley and Garg [Ref. 9], found this to be the case. In the 8% Mg alloy, the lever rule suggests only about three volume percent beta would be present if precipitation to the equilibrium magnesium content of the solid solution occurs.

### 3. Manganese Alloying Additions

Substantial work on the Al-10% Mg-0.5% Mn alloy has been done by Becker [Ref. 10], and Mills [Ref. 11], and this data appears in the appendices. In this work a lower manganese content of 0.2% was investigated. Manganese additions have a very pronounced homogenization effect on Al-Mg alloys. A triplanar micrograph representation of this alloy may be found in Figure 4.3. Manganese is a very effective grain refiner in aluminum alloys [Ref. 16]. Selected area diffraction experiments discussed in an unpublished work by Garg indicates that the manganese bearing precipitate is  $MnAl_6$ . In the rolling plane of the 0.2% Mn alloy there is an elongated structure with precipitate free zones in regions that are made up of a dispersion of intermetallic precipitates. The phase diagram



TABLE VIII  
Mechanical Properties of Al-10% Mg-0.5% Mn Alloy

Temp (C)	Strain Rate (1/sec)	UTS (MPa)	True Stress at 0.1 Plastic Strain (MPa)	Ductility (Percent)
20	5.6 X 10 <sup>-4</sup>	414.0	*	3.0
	5.6 X 10 <sup>-3</sup>	478.0	*	3.2
	5.6 X 10 <sup>-2</sup>	503.0	*	3.2
250	1.39 X 10 <sup>-4</sup>	28.4	36.0	269.0
	1.39 X 10 <sup>-3</sup>	59.2	78.0	228.0
	1.39 X 10 <sup>-2</sup>	105.0	134.0	142.0
	1.39 X 10 <sup>-1</sup>	191.0	218.0	54.8
300	1.39 X 10 <sup>-4</sup>	11.4	14.0	258.0
	1.39 X 10 <sup>-3</sup>	25.9	32.0	391.0
	1.39 X 10 <sup>-2</sup>	61.3	83.0	160.0
	1.39 X 10 <sup>-1</sup>	120.0	154.0	85.2

\* Data Unavailable.

## 2. Magnesium Alloying Additions

The effect of magnesium on mechanical properties at the 8 and 10% alloy addition levels is shown in Figures 4.7 through 4.11. In the 8% magnesium alloy, the strength of the material decreases as the test temperature increases (Figure 4.7). At 300°C, the 8% magnesium alloy is near the solvus, and the magnesium is tending to go back into solution. A result of this effect would be a relatively small volume fraction of beta phase to retard grain growth, and in addition that the beta present would tend to coarsen with time at this temperature. From the Zener equation mentioned previously, the net result would be coarsening of the grain structure. An increase in grain size will suppress grain boundary sliding, and result in dislocation creep processes dominating, leading to reduced ductility. The same effects are at work in the ten percent magnesium alloy (Figure 4.8), but to a lesser extent perhaps, given the larger Mg content. With more Mg, a larger volume fraction of beta would be present and lead to a finer grained, weaker material. The 10% alloy is in fact weaker than the 8% alloy at 300°C (Figure 4.9), and also at 250°C (Figure 4.10), although the difference in strength is not large at either temperature.

Only limited superplasticity as evaluated by the ductility is observed in the eight and ten percent magnesium

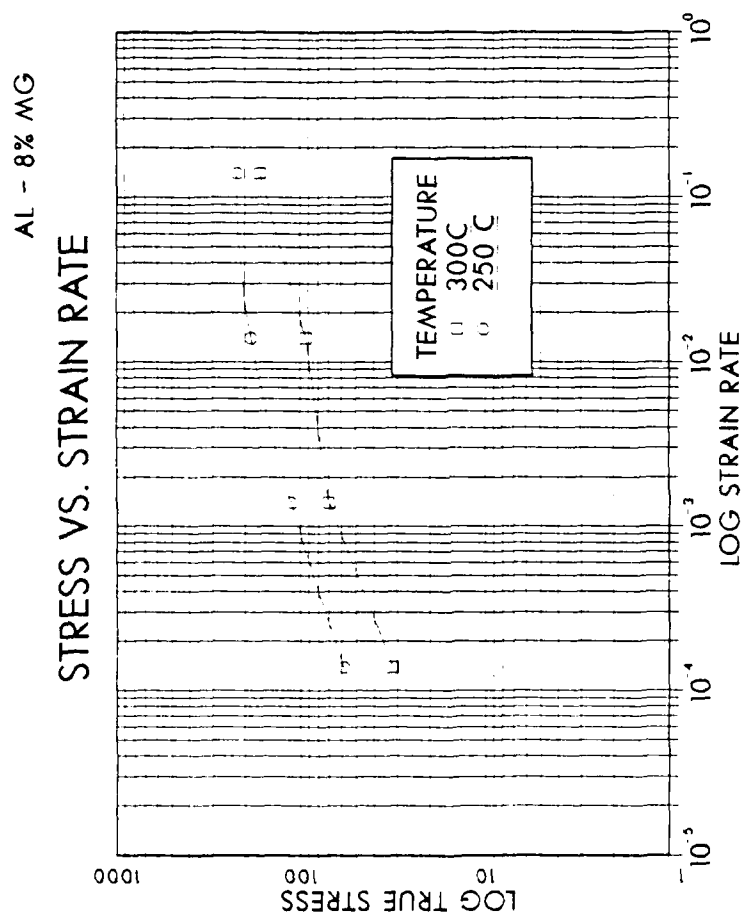


Figure 4.7. True Stress at 0.1 Strain versus Strain Rate for Tensile Tests on Al-8% Mg Alloy Conducted at 250 and 300°C. The Al-8% Mg Alloy is Slightly Stronger at 250°C than it is at 300°C.

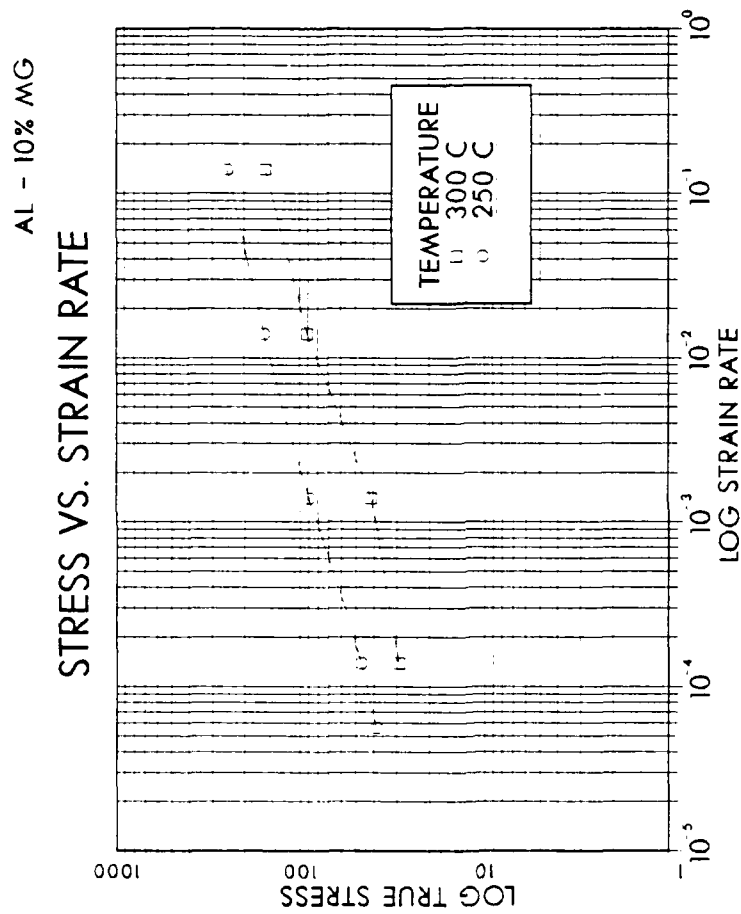


Figure 4.8. True Stress at 0.1 Strain versus Strain Rate for Tensile Tests on Al-10% Mg Alloy Conducted at 250 and 300°C Again Showing that the 10% Mg Alloy is Slightly Stronger at 250°C than it is at 300°C.

# EFFECT OF MG AT 300C

## STRESS VS. STRAIN RATE

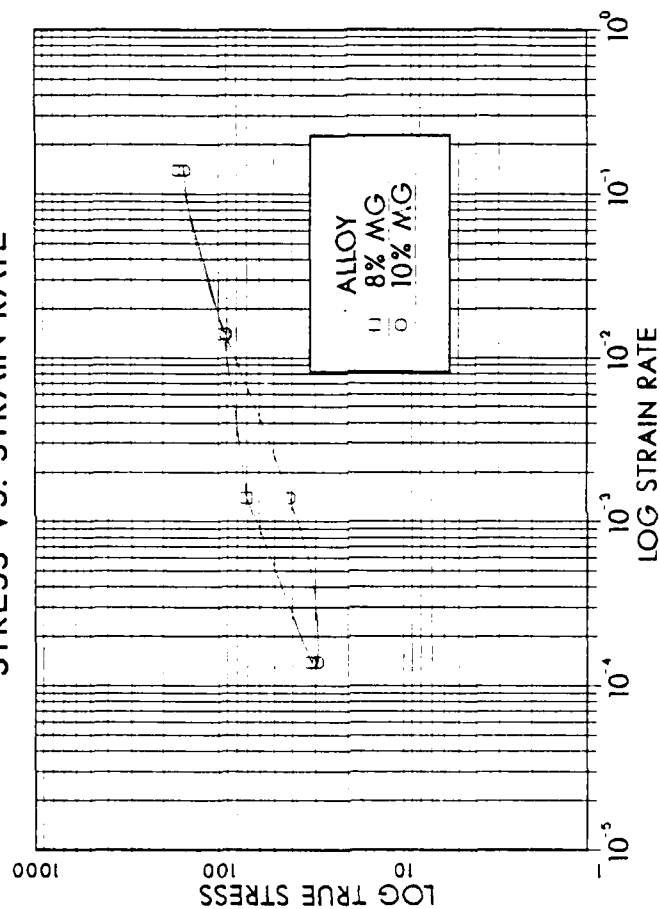


Figure 4.9. True Stress at 0.1 Strain versus Strain Rate for Tensile Tests at 300°C Comparing the Effect of Magnesium Addition at 8% and 10% Levels; Showing that the 8% Mg Alloy is Slightly Stronger.

# EFFECT OF MG AT 250C

## STRESS VS. STRAIN RATE

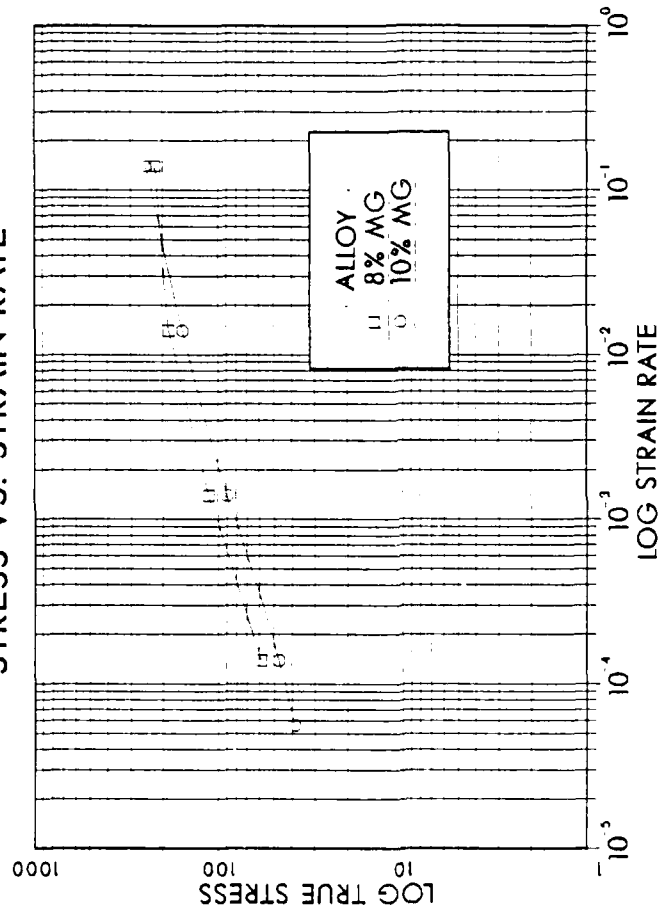


Figure 4.10. True Stress at 0.1 Strain versus Strain Rate for Tensile Tests at 250°C Comparing the Effect of Magnesium Addition at 8% and 10% Levels; Showing that the 8% Alloy is Slightly Stronger.

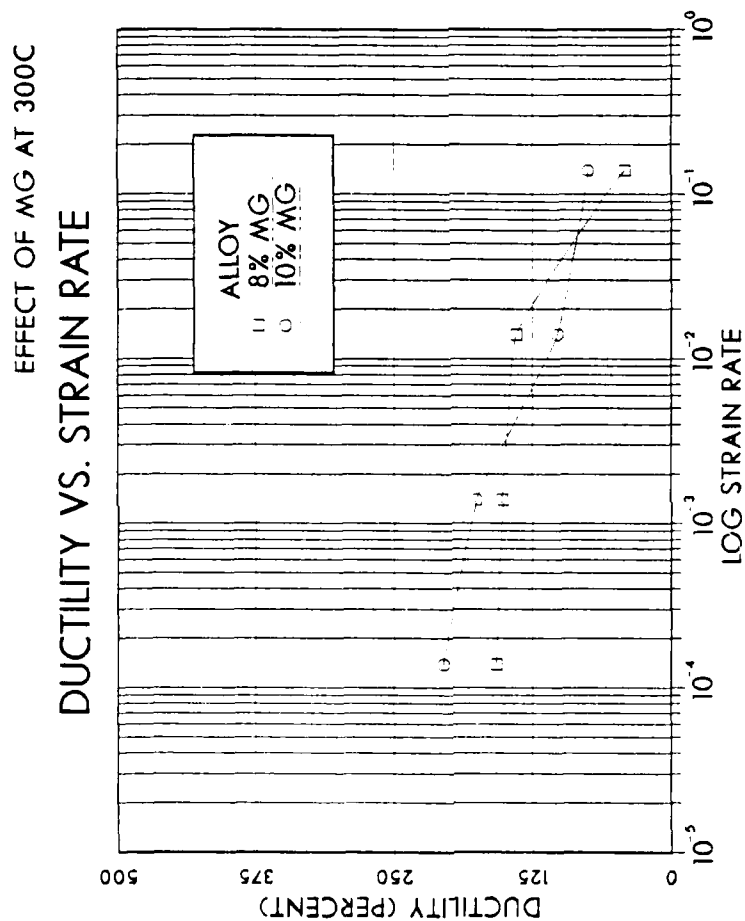


Figure 4.11. Ductility versus Strain Rate for Tensile Tests at 300°C Comparing the Effect of the Magnesium Addition at the 8% and 10% Levels Showing that the 8% Mg Alloy is Slightly More Ductile.

aluminum alloys. As the percentage of magnesium increases, there is more beta phase present as noted above, and therefore, more refinement, and an attendant ductility increase. However, this effect also is not large. It would be inferred from this that the beta phase by itself is of limited use in refining and stabilizing the grain structure of these alloys. Both of the binary alloys would appear to behave essentially as Al-Mg solid solution alloys with a coarse dispersion of particles having limited effect on the mechanical properties.

### 3. Manganese Alloying Additions

The effect of a 0.2% manganese addition on a 10% magnesium-aluminum alloy is shown in Figures 4.12 and 4.13. The same data for a 0.5% manganese addition is shown in Figures 4.14 and 4.15. Comparative data for these two alloys is shown in Figures 4.16 and 4.17. From the data in Figures 4.12 and 4.14, it is seen that the Al-10% Mg, 0.5% Mn alloy is weaker at 300°C than it is at 250°C, and that it is also weaker at all temperatures than the 10% binary alloy. The ductility data indicates (Figures 4.13 and 4.15) that these alloys are more ductile at the 300°C test temperature. The 10% Mg alloy with 0.2% manganese is more ductile at room temperature than is the 0.5% manganese alloy. From the data presented in Figure 4.16, there is a progressive weakening of this material as the percent



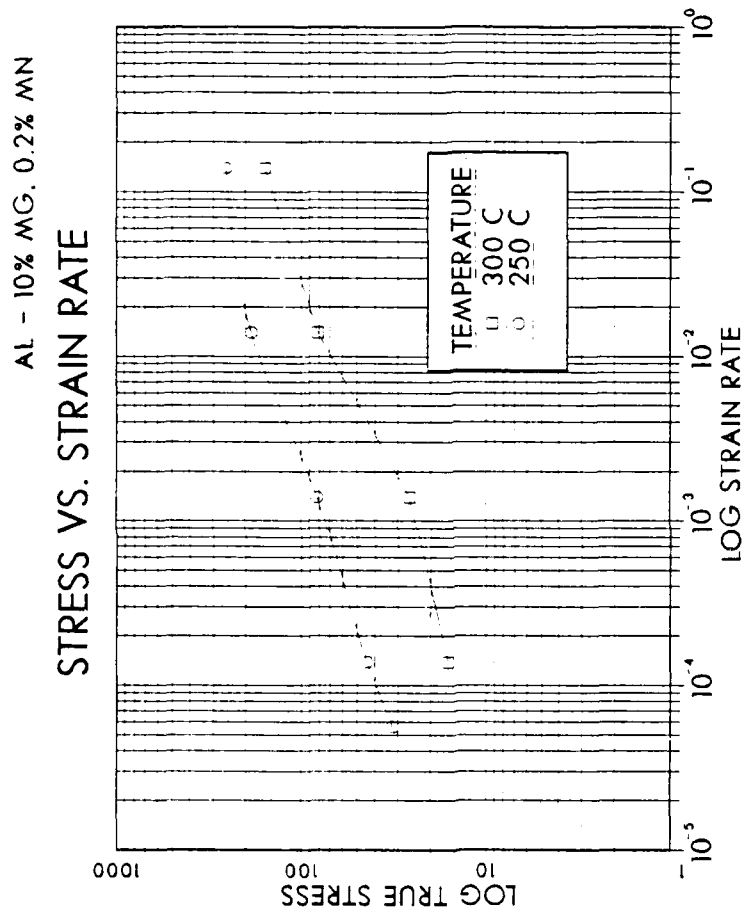


Figure 4.12. True Stress at 0.1 Strain versus Strain Rate for Tensile Tests on Al-10% Mg-0.2% Mn Alloy Conducted at 250 and 300°C. This Alloy is Stronger at 250°C than it is at 300°C.

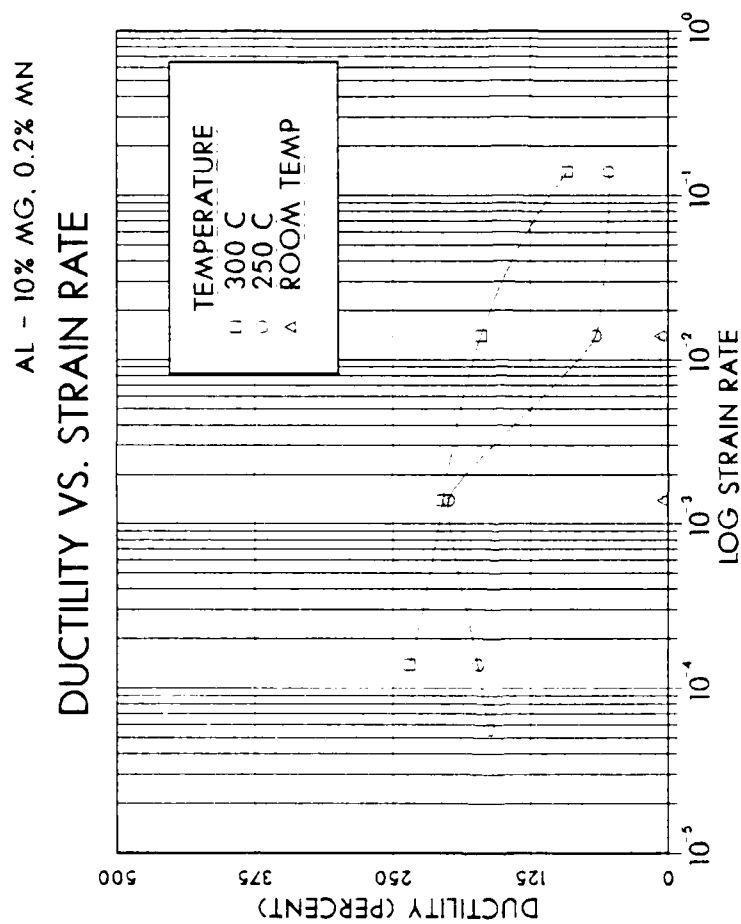


Figure 4.13. Ductility versus Strain Rate for Tensile Tests on Al-10% Mg-0.2% Mn Alloy, Tests Conducted at Room Temperature, 250°C, and 300°C.

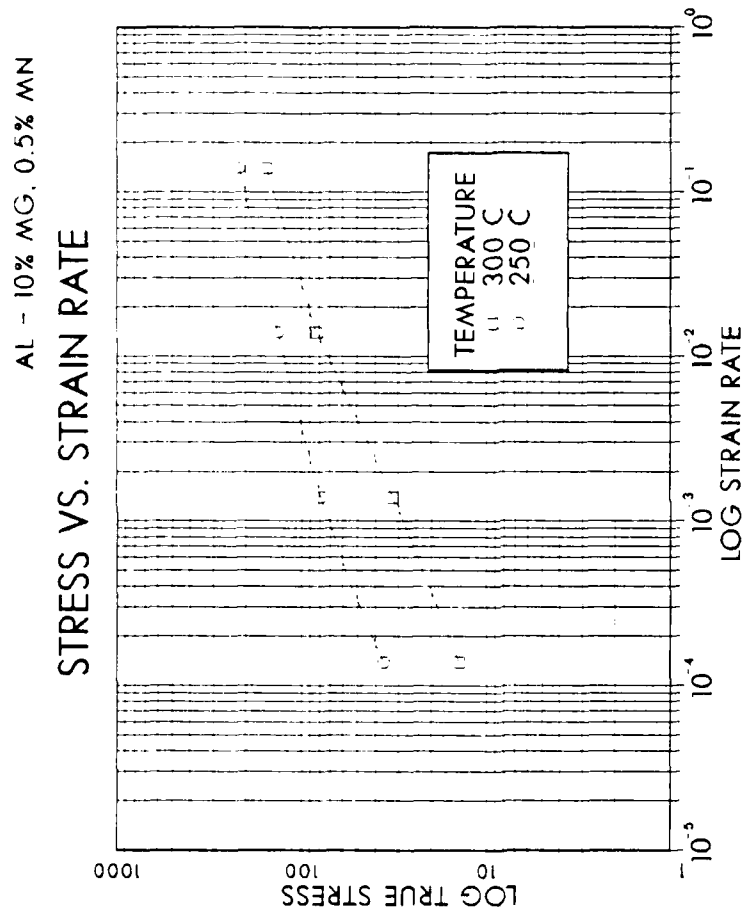


Figure 4.14. True Stress at 0.1 Strain versus Strain Rate for Tensile Tests on Al-10% Mg-0.5% Mn Alloy Conducted at 250 and 300°C. This Alloy is Stronger at 250°C than it is at 300°C.

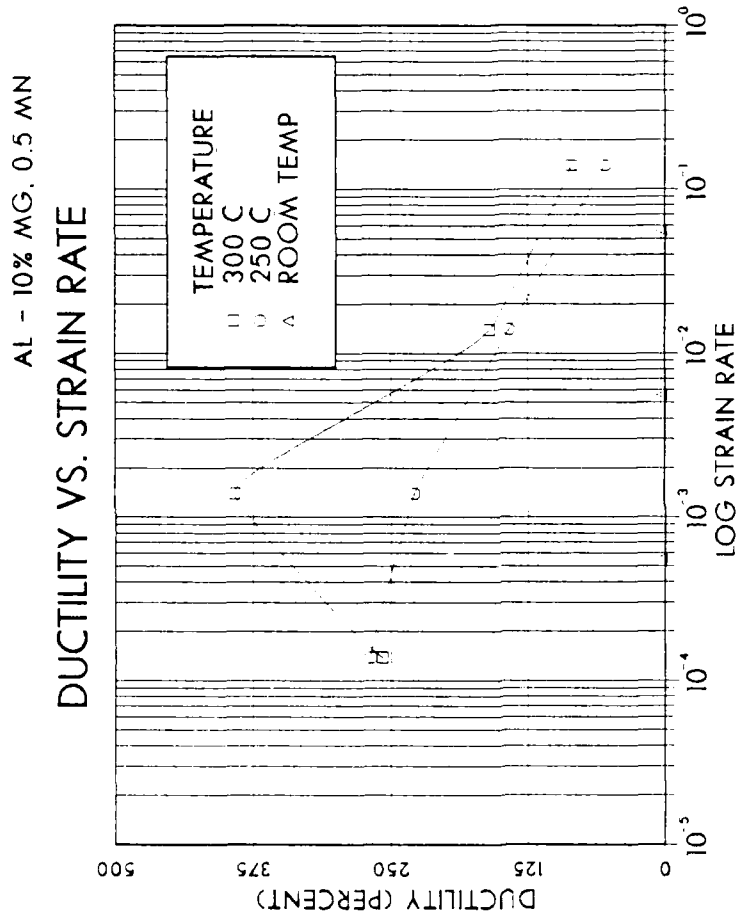


Figure 4.15. Ductility versus Strain Rate for Tensile Tests on Al-10% Mg-0.5% Mn Alloy, Tests Conducted at Room Temperature, 250°C, and 300°C, Showing the Large Increase in Ductility at 300°C.

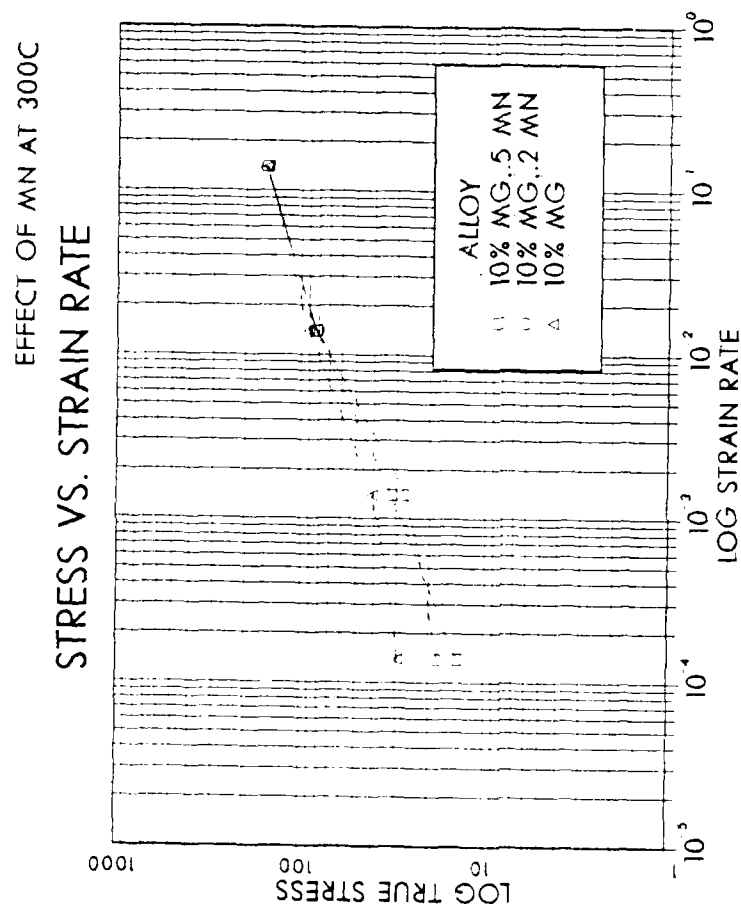


Figure 4.16. True Stress at 0.1 Strain versus Strain Rate for Tensile Tests Conducted at 300°C Showing the Comparative Effects of Increasing Mn Content on Strength in the 10% Mg Alloy.

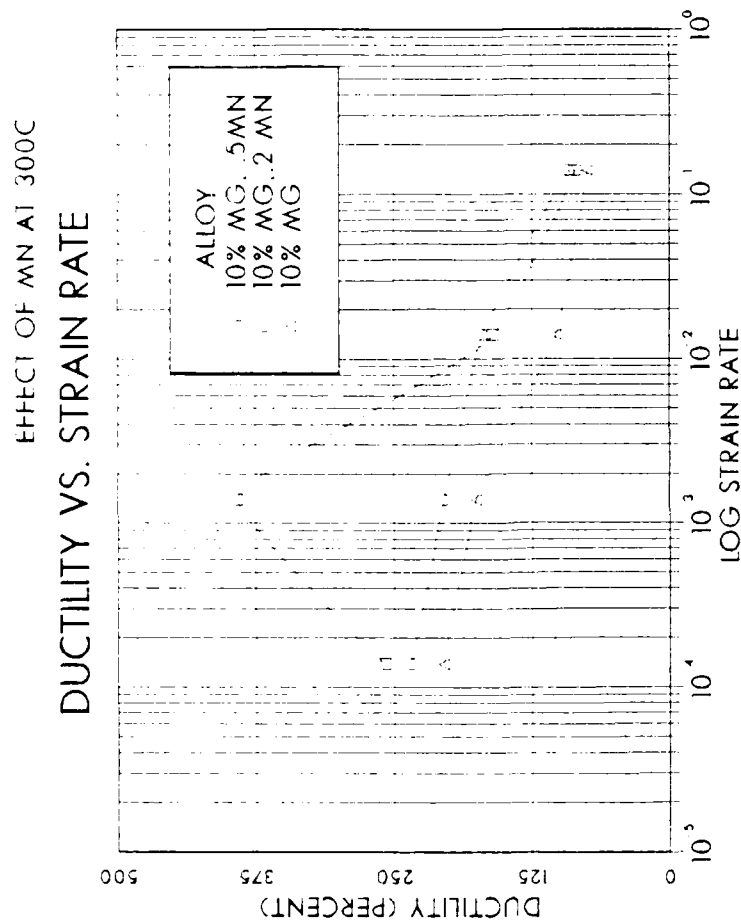


Figure 4.17. Ductility versus Strain Rate for Tensile Tests Conducted at 300°C Showing the Comparative Effects of Increasing Mn Content on Ductility. There is a Pronounced Increase in Ductility in the 10% Mg Alloy for a 0.5% Mn Addition.

AL-8% MG-0.4CU-0.5MN ALLOY

# DUCTILITY VS. STRAIN RATE

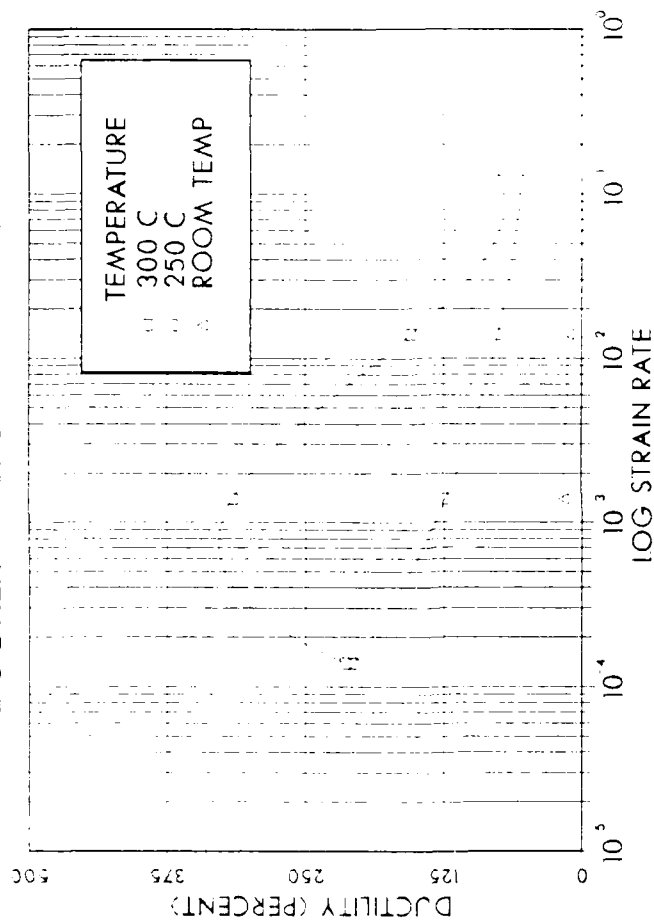


Figure 4.28. Ductility versus Strain Rate for Tensile Tests on Al-8% Mg-0.4% Cu-0.5% Mn Alloy, Tests Conducted at Room Temperature, 250°C, and 300°C, Showing the Large Increase in Ductility Observed at 300°C.

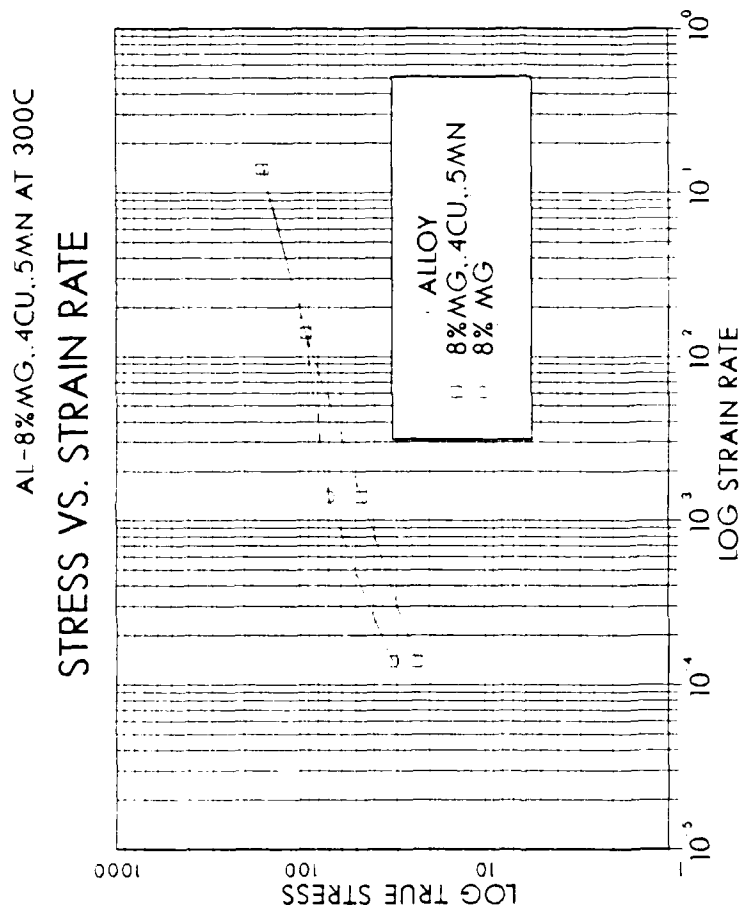


Figure 4.27. True Stress at 0.1 Strain versus Strain Rate for Tensile Tests Conducted at 300°C Comparing the 8% Mg and the 8% Mg-0.4% Cu-0.5% Mn Alloys Showing that the 8% Mg Alloy is Slightly Stronger than is the 8% Mg-0.4% Cu-0.5% Mn Alloy.



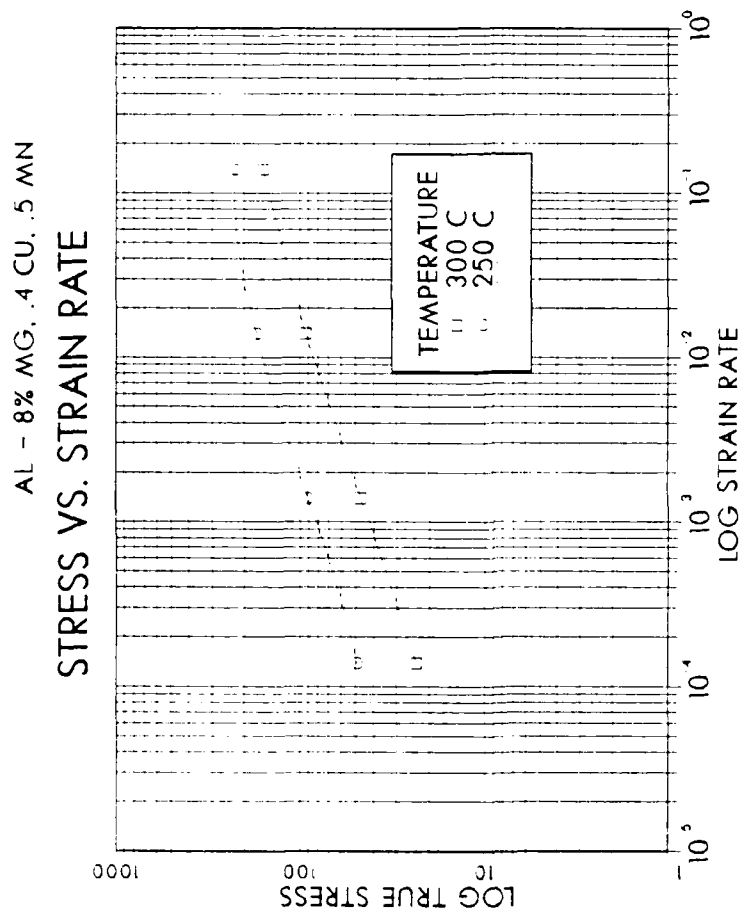


Figure 4.26. True Stress at 0.1 Strain versus Strain Rate for Tensile Tests on Al-8% Mg-0.4% Cu-0.5% Mn Alloy Conducted at 250 and 300°C Showing that the Alloy is Slightly Stronger at 250°C than it is at 300°C.

CU - MN ADDITIONS AT 300C

### DUCTILITY VS. STRAIN RATE

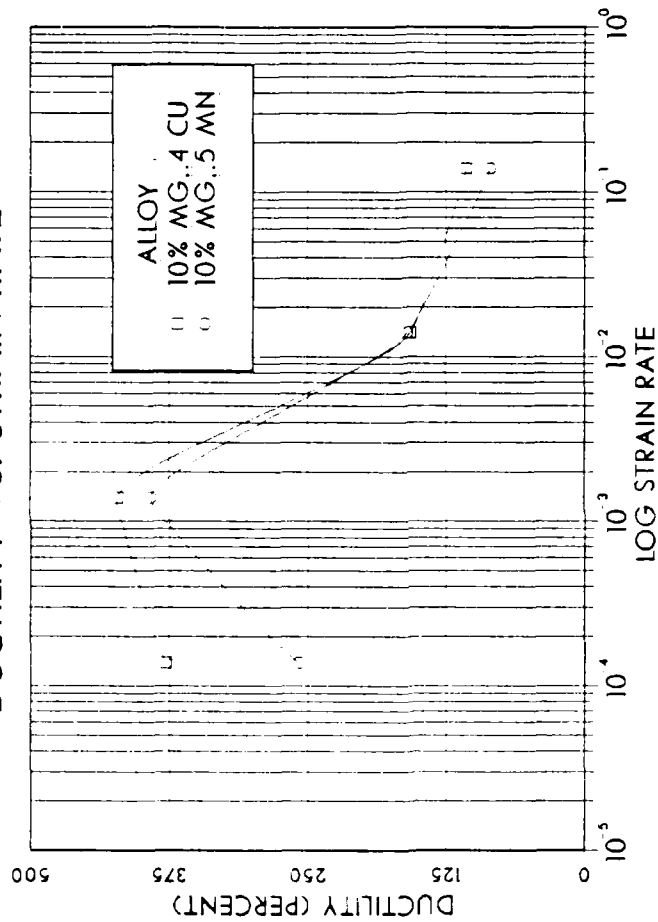


Figure 4.25. Ductility versus Strain Rate for Tensile Tests Conducted at 300°C. Comparing the Effects of Cu and Mn Additions on the 10% Mg Alloy, and also showing that the Cu Addition Results in a Slightly Enhanced Ductility.

content, the greater the amount of copper that precipitates out of solid solution.

The copper addition appears to be just as effective as the manganese addition in enhancing the ductility of these alloys on a per weight percentage basis (Figure 4.25). Copper has a similar effect to manganese, in that it progressively weakens the material probably by micro-structure refinement. Further, the copper addition offers slightly higher elongations under elevated temperature testing conditions than does the manganese. Finally, it also has a relatively small effect on ambient temperature ductility, decreasing it from 10-12% elongation for a binary alloy at room temperature to 7-9% for the copper containing alloy. In contrast, the manganese bearing alloy exhibits ductility of only 3% at room temperature.

#### 5. Copper and Manganese Addition

The Al-8% Mg, 0.4% Cu, 0.5% Mn alloy is shown in Figure 4.26. It is weaker at all temperatures than the eight percent binary alloy, the effect being more pronounced at lower strain rates (Figure 4.27). In fact, the alloy is almost identical to the 10% magnesium binary alloy in strength. The Al-8% Mg-0.4% Cu-0.5% Mn alloy shows higher ductilities at 300°C than it does at 250°C (Figure 4.28), again like the 10% Mg alloys and in contrast to the 8% Mg alloys. There is an increase in ductility over those

10% Mg binary alloy at 300°C. The eight percent alloy is stronger than the 10% alloy (Figure 4.21). An extensive discussion of the superplasticity observed in the Al-8% Mg-0.4% Cu alloy is available in Becker [Ref. 10].

The Al-8% Mg-0.4% Cu alloy is more ductile than is the eight percent binary alloy at low strain rates at 300°C, but not substantially so (Figure 4.22). The effect on ductility of the copper addition in the 10% Mg alloy is more dramatic (Figure 4.23). This effect is most pronounced at low strain rates. In Figure 4.24, the effects of a 0.4% copper addition at both the eight and ten percent magnesium levels are shown. The effect of the copper addition is much greater at the 10% magnesium level. From this we can infer that not only is the alloying addition, in this case copper, important, but rather the alloying addition along with a high magnesium level, i.e., 10% Mg.

In summary, the copper addition has a small effect on the 8% alloy, but a large one on the 10% alloy. At 250°C, the 8% alloy with copper is noticeably weaker. It appears that the effect of the copper addition is to homogenize, refine and stabilize the beta phase. At 300°C the principal effect on the 8% Mg alloy is coarsening and re-solution of the beta, while in the 10% Mg alloy the structure is more stable given the relatively larger beta content. It would appear that the higher the magnesium

AL - MG - CU ALLOY AT 300C

### DUCTILITY VS. STRAIN RATE

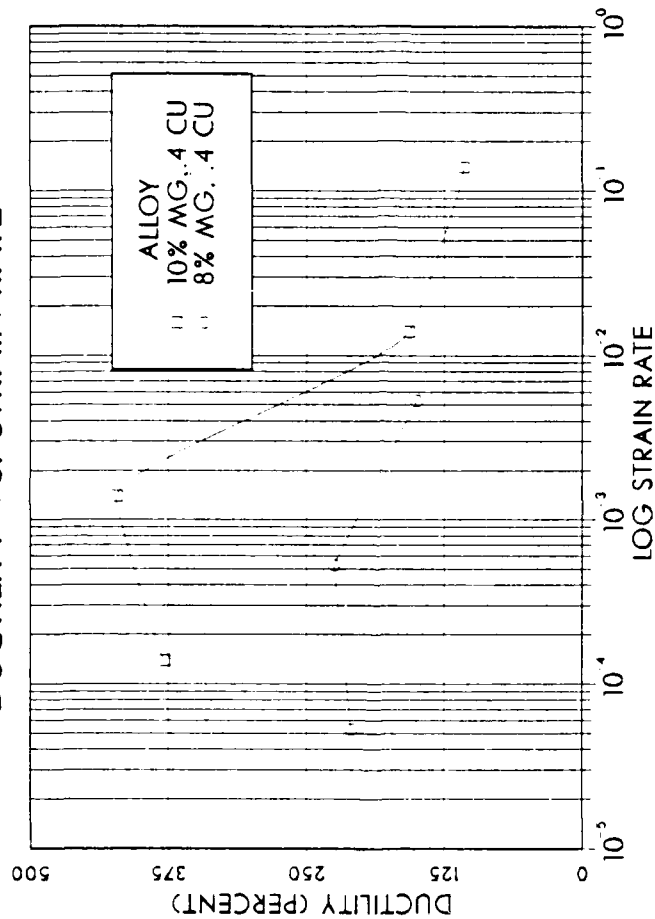


Figure 4.24. Ductility versus Strain Rate for Tensile Tests Conducted at 300°C Comparing the 8% Mg-0.4% Cu and the 10% Mg-0.4% Cu Alloys. Again Showing the Pronounced Increase in Ductility Observed in the 10% Mg-0.4% Cu Alloy.

AL - MG - CU ALLOY AT 300C

### DUCTILITY VS. STRAIN RATE

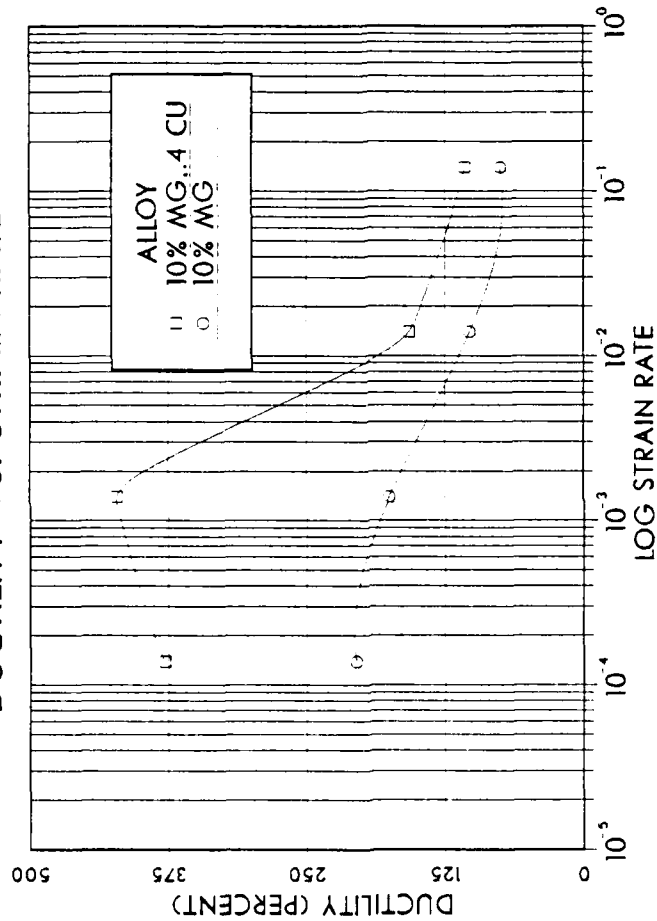


Figure 4.23. Ductility versus Strain Rate for Tensile Tests Conducted at 300°C Comparing the 10% Mg and the 10% Mg-0.4% Cu Alloys Showing the Pronounced Ductility Increase in the 10% Mg-0.4% Cu Alloy.

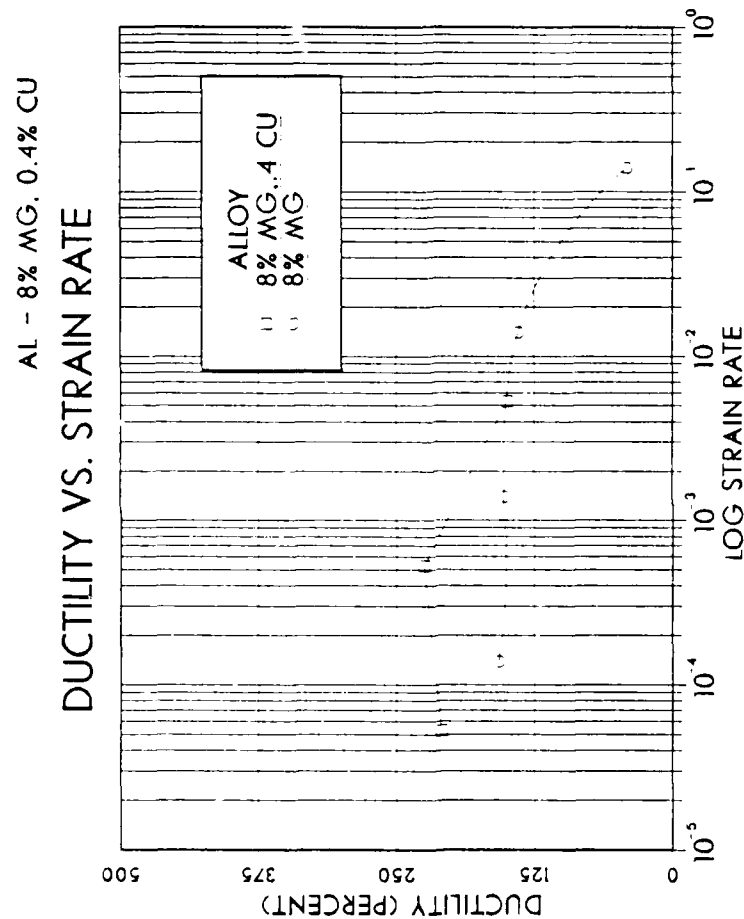


Figure 4.22. Ductility versus Strain Rate for Tensile Tests Conducted at 300°C Comparing the 8% Mg and the 8% Mg-0.4% Cu Alloys. The 8% Mg-0.4% Cu Alloy is Slightly more Ductile.

AL - MG - CU ALLOY AT 300C

### STRESS VS. STRAIN RATE

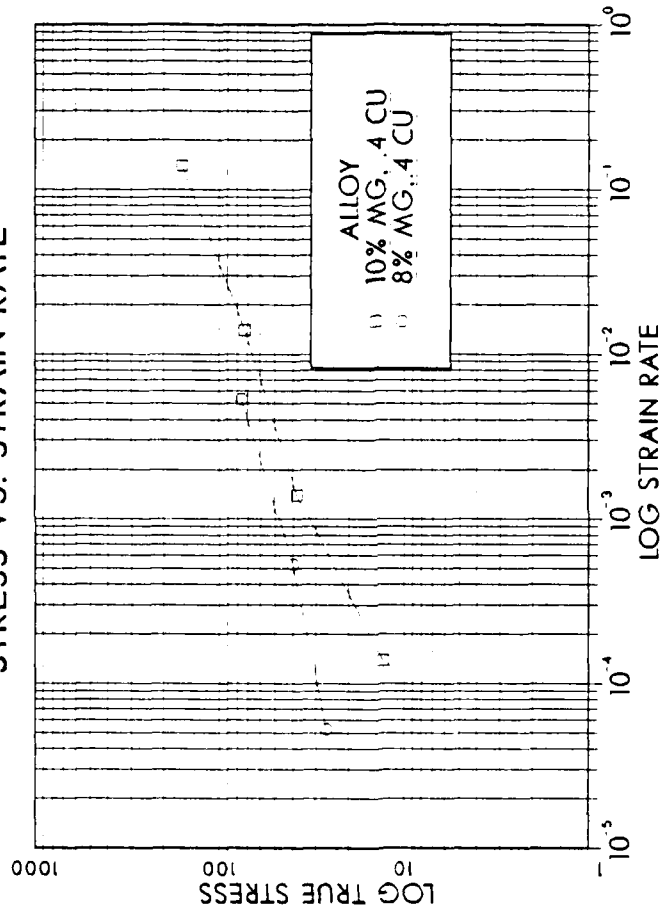


Figure 4.21. True Stress at 0.1 Strain versus Strain Rate for Tensile Tests Conducted at 300°C Comparing the Effect of Increasing Magnesium Content on Strength of the Al-Mg Alloy with a 0.4% Cu Addition, Showing that the 8% Alloy is Slightly Stronger than is the 10% Alloy.



AL - MG - CU ALLOY AT 300C

# STRESS VS. STRAIN RATE

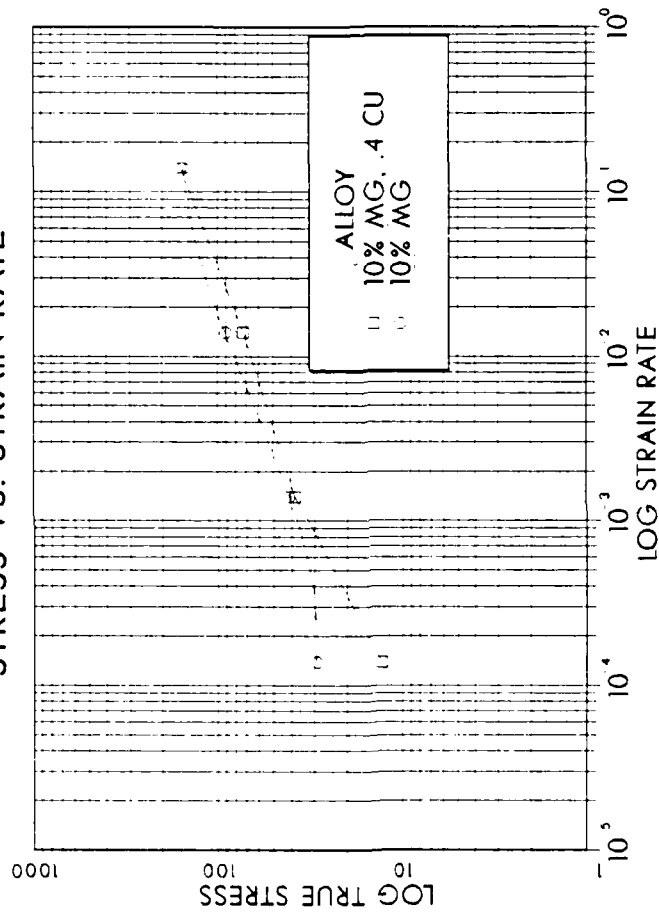


Figure 4.20. True Stress at 0.1 Strain versus Strain Rate for Tensile Tests Conducted at 300°C Comparing the Effects of Copper Addition on Strength in the 10% Mg Alloy, and also Showing that the 10% Mg Binary Alloy is Slightly Stronger than the 10% Mg Alloy with Copper Addition.

AL-10% MG. 0.4% CU

# STRESS VS. STRAIN RATE

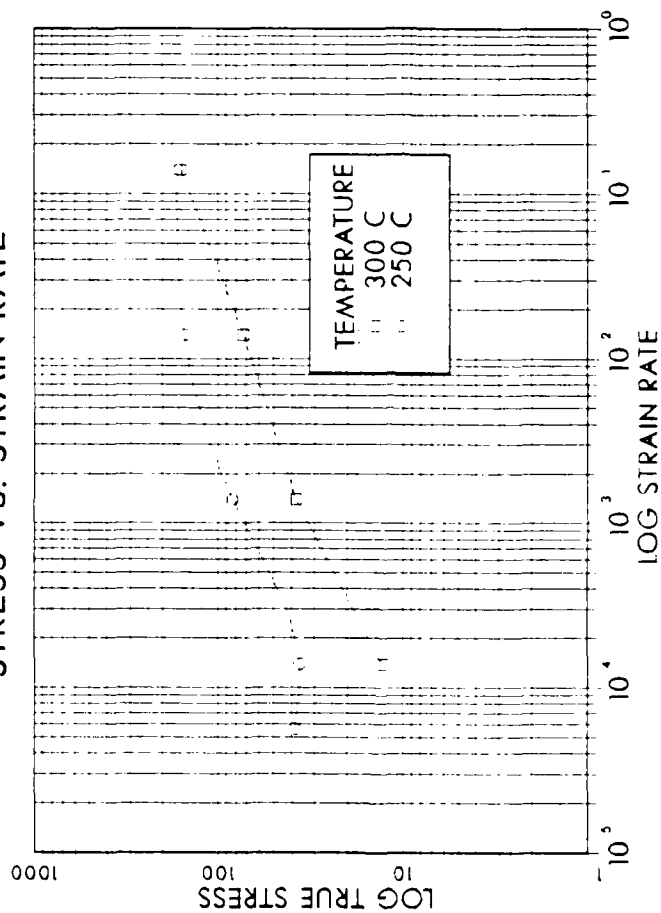


Figure 4.19. True Stress at 0.1 Strain versus Strain Rate for Tensile Tests on Al-10% Mg-0.4% Cu Alloy Conducted at 250 and 300°C Showing that the Alloy is Stronger at 250°C than it is at 300°C.

AL - 8% MG, 0.4% CU

# STRESS VS. STRAIN RATE

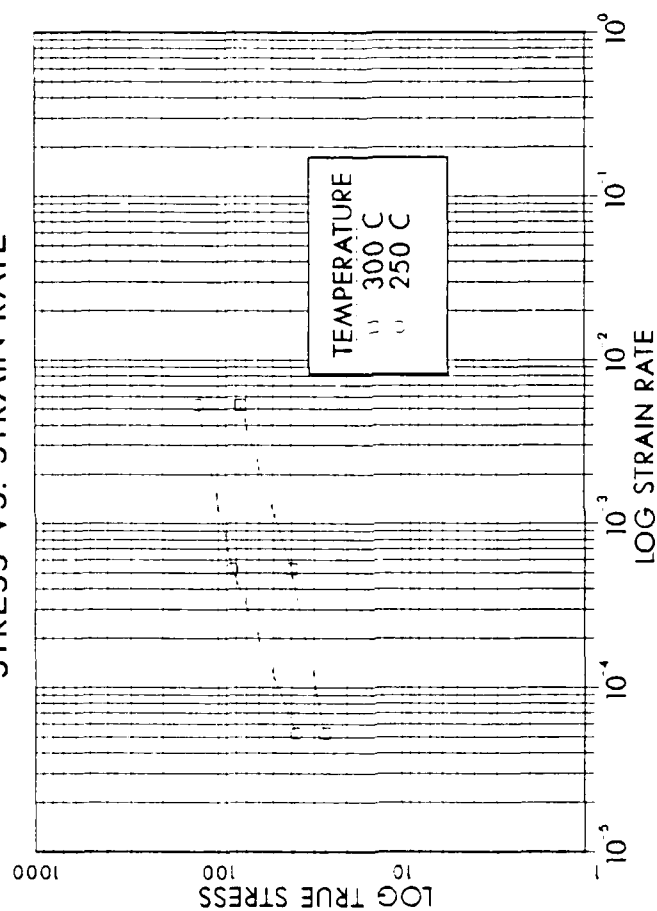


Figure 4.18. True Stress at 0.1 Strain versus Strain Rate for Tensile Tests on Al-8% Mg-0.4% Cu Alloy Conducted at 250 and 300°C Showing that the Alloy is Stronger at 250°C than it is at 300°C.

manganese is increased. This effect is more pronounced at the lower strain rates than it is at the higher values for strain rate.

The 0.2% manganese containing alloy appears to be an intermediate stage in the microstructural refinement process. At the 0.2% Mn level, the manganese is still in solid solution, and may therefore have little or no effect on the beta phase, while at the 0.5% Mn addition level we are seeing a decreased solubility of both magnesium and manganese due to the manganese addition. Manganese that precipitates out of solid solution as a third phase may refine the material's grain structure during hot working, consequently providing more nucleation sites for the beta phase during warm rolling. This would lead to a finer, more stable beta phase. Figure 4.17 shows the large jump in ductility values observed in the Al-10% Mg-0.5% Mn alloy over those obtained in the Al-10% Mg-0.2% Mn, and Al-10% Mg binary alloys.

#### 4. Copper Alloying Additions

The effects of copper alloying additions on the mechanical properties of eight and ten percent magnesium alloys are shown in Figures 4.18 through 4.24. As shown in Figures 4.18 and 4.19, both alloys exhibit normal temperature dependence of the flow stress. As shown in Figure 4.20, the Al-8% Mg-0.4% Cu alloy is slightly weaker than the

observed in both the 8% and 10% binary alloys, although the effect is less pronounced relative to the 10% binary alloy (Figure 4.29). A possible effect of the combined copper and manganese addition is to reduce the solubility of magnesium in the material. Thus, this alloy behaves like a higher magnesium alloy. The Mn may also assist in refining the grain structure in conjunction with refinement of the beta by the Cu.

#### 6. Summary of Mechanical Test Data

It should be kept in mind that the strength data was obtained at a strain rate of 0.1 while the ductility data reflects behavior of the alloy at much larger strains. As such, the effect of the alloying elements on strength, while notable, is not as pronounced as the effect on ductility. It is surmised that the alloying additions refine and homogenize the structure during the warm rolling; the Mn, at least, appears most completely effective when some of it is out of solution as  $MnAl_6$ . This would likely refine the matrix grain structure. The Cu also is present in precipitated form, it may also assist in refining the beta as it is soluble in it.

With regard to ductility, the binary alloys most likely coarsen during plastic deformation, and the addition of either Cu, Mn, or both, may retard such coarsening. This would enhance the ductility of the alloy if such coarsening

AL-8% MG..4 CU..5 MN AT 300 C

# DUCTILITY VS. STRAIN RATE

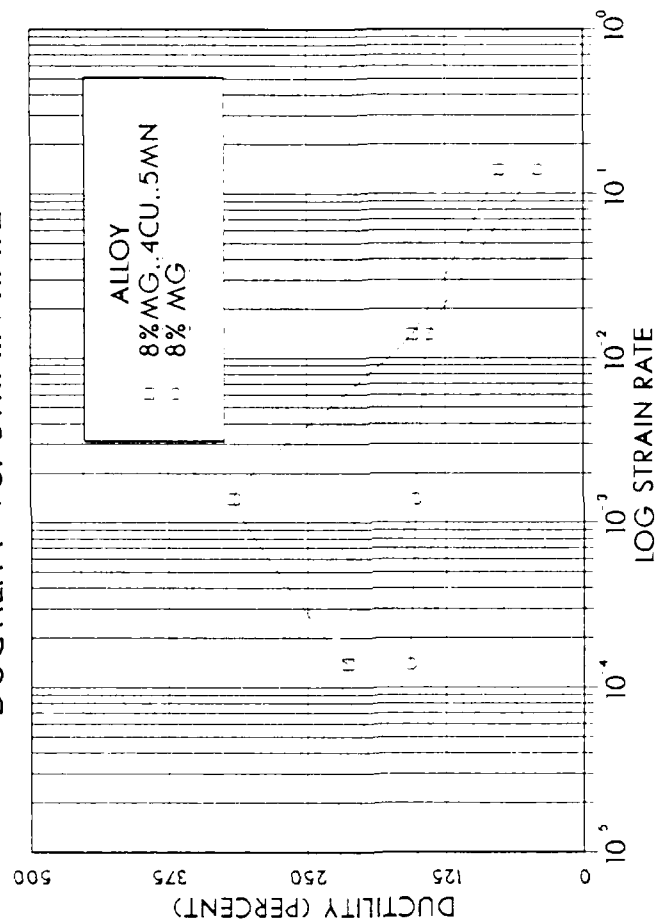


Figure 4.29. Ductility versus Strain Rate for Tensile Tests Conducted at 300°C Comparing the 8% Mg and the 8% Mg-0.4% Cu-0.5% Mn Alloys Showing the Pronounced Ductility Increase in the 8% Mg-0.4% Cu-0.5% Mn Alloy.

at strains beyond 0.1 results, otherwise causing suppression of superplastic mechanisms. In reviewing the test data, the slopes of log stress versus log strain rate curves (the  $m$  values) do not vary as much as does the ductility data, again indicating that coarsening (or lack of it) at large strains is an important factor in determining the final ductility.

## V. CONCLUSIONS

The following conclusions are drawn from this research:

- 1) the microstructures of the thermomechanically processed Al-8% Mg and Al-10% Mg binary alloys consisted of banded, inhomogeneous dispersions of the intermetallic beta phase;
- 2) as the percentage magnesium increased in the binary alloys, there was a mild enhancement in their superplastic properties;
- 3) the addition of copper to the binary alloys homogenized and refined their microstructures;
- 4) the Al-10% Mg-0.4% Cu alloy was the most superplastic alloy observed in this research;
- 5) the addition of manganese to the binary alloy has the same effect on microstructure as the addition of copper when added on the same weight percent basis, i.e., it homogenizes and refines the microstructure;
- 6) the Al-10% Mg-0.5% Mn alloy produces superplastic response under tensile test conditions at elevated temperatures;
- 7) the addition of copper does not degrade room temperature ductility as much as does the addition of manganese;
- 8) the addition of both 0.4% Cu and 0.5% Mn to the Al-8% Mg binary alloy produces the same strength characteristics found in alloys with higher magnesium contents.

The following recommendations for further study are made: 1) a detailed study of the effect of copper addition



on these alloys; 2) further study into the effects of strain on grain coarsening, and other structural changes at elevated temperatures; 3) that detailed activation energy data on the alloys studied in this work be obtained, and compared with the results for the Al-10% Mg-0.5% Mn alloy obtained by Mills, to examine the effect of alloying addition on activation energy; 4) study of the Al-10% Mg-0.4% Cu-0.5% Mn alloy for comparison to the 8% alloy with these alloying additions.

# APPENDIX A

## Mechanical Test Data on Al-8% Mg Alloy

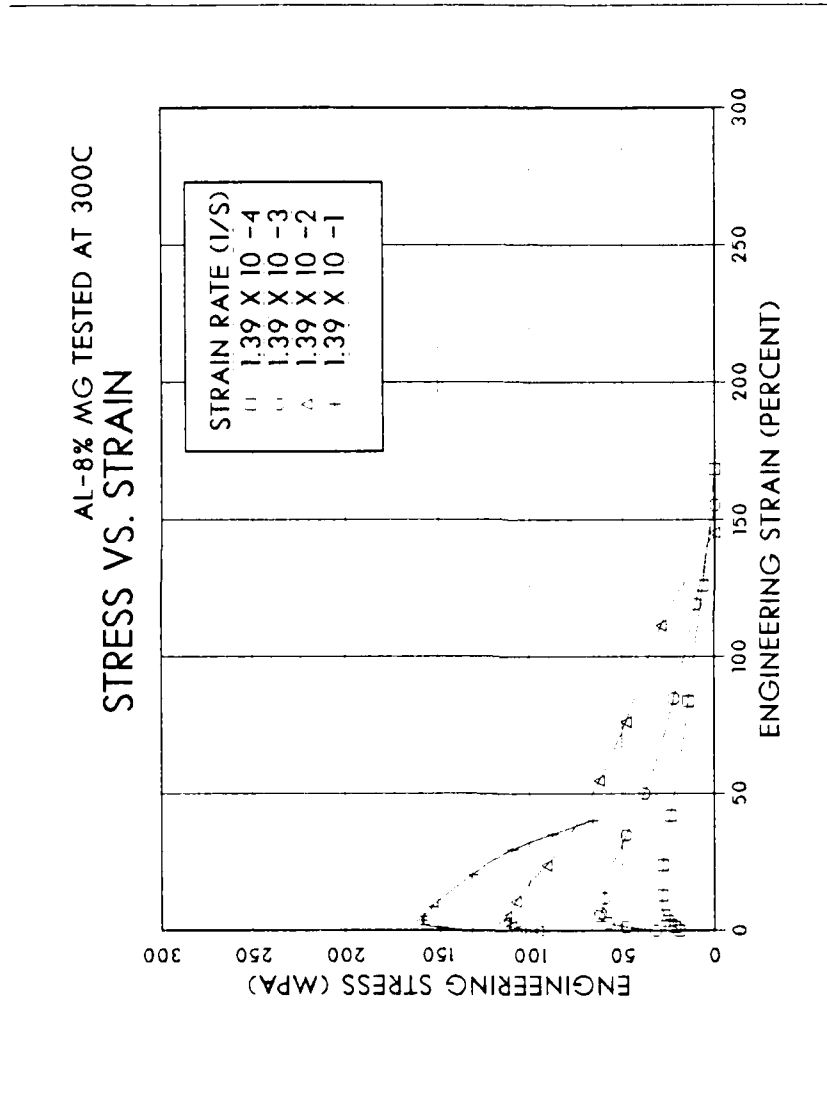


Figure A.1. Engineering Stress versus Engineering Strain Data for Testing Conducted at 300°C for Al-8% Mg Alloy, in the As-Rolled Condition.

AL - 8% MG TESTED AT 250C

# STRESS VS. STRAIN

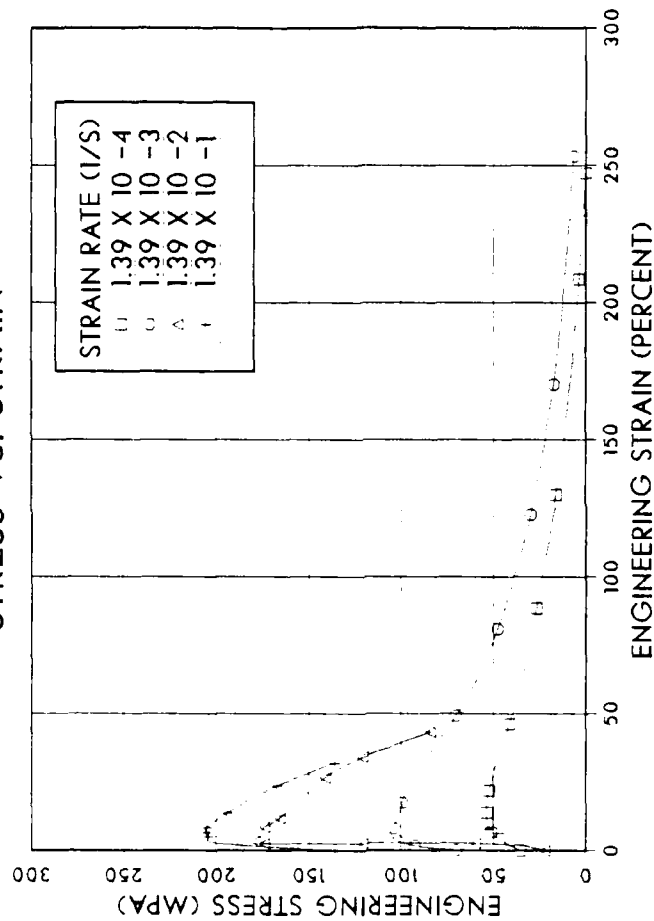


Figure A.2. Engineering Stress versus Engineering Strain Data for Tensile Tests Conducted at 250°C for Al-8% Mg Alloy in the As-Rolled Condition.

AL - 8% MG TESTED AT 20C

# STRESS VS. STRAIN

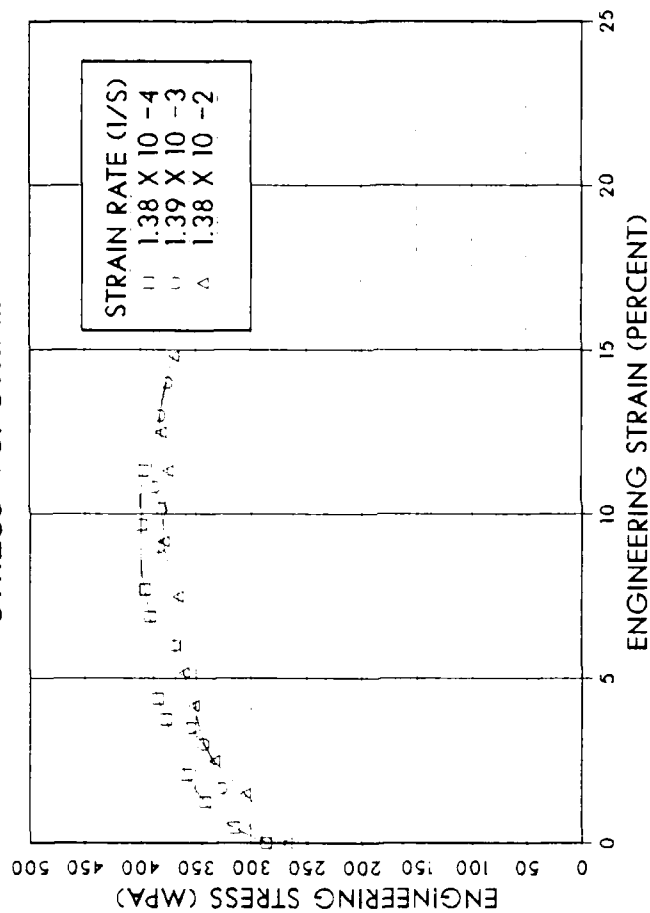


Figure A.3. Engineering Stress versus Engineering Strain Data for Tensile Tests Conducted at 20°C for Al-8% Mg Alloy in the As-Rolled Condition.

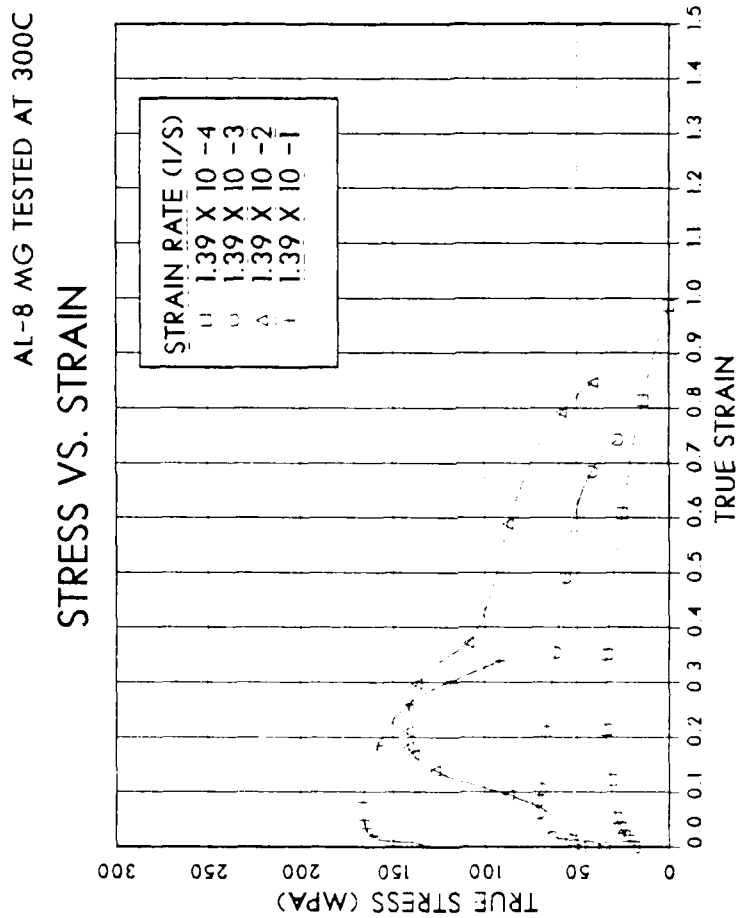


Figure A.4. True Stress versus True Strain Data for Tensile Tests Conducted at 300°C for Al-8% Mg Alloy in the As-Rolled Condition.

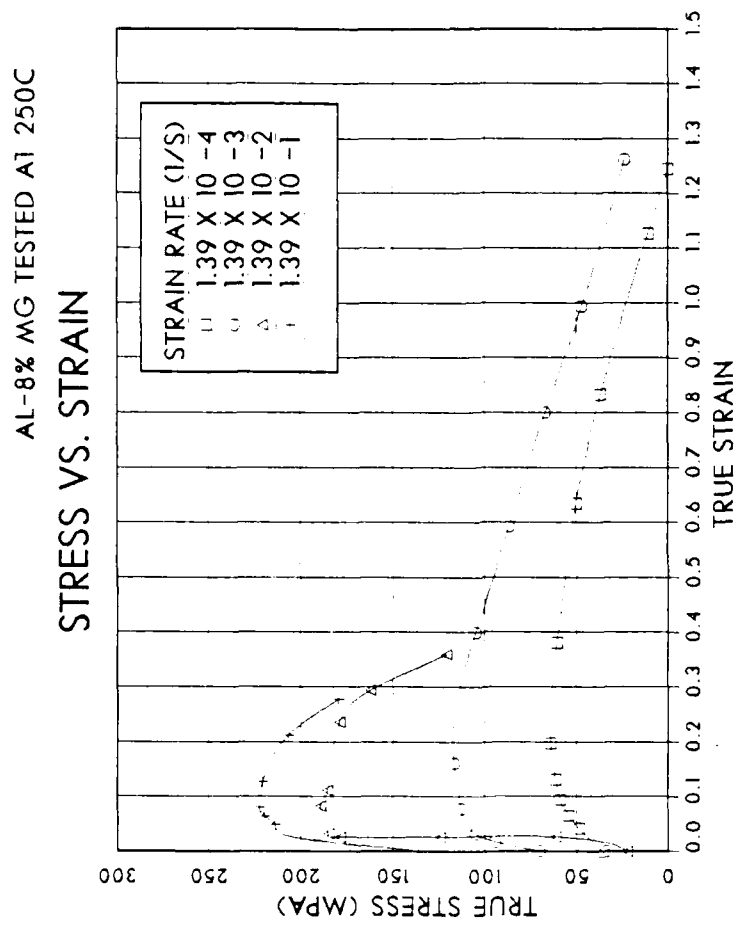


Figure A.5. True Stress versus True Strain Data for Tensile Tests Conducted at 250°C for Al-8% Mg Alloy in the As-Rolled Condition.

AL-8% MG TESTED AT 20C

# STRESS VS. STRAIN

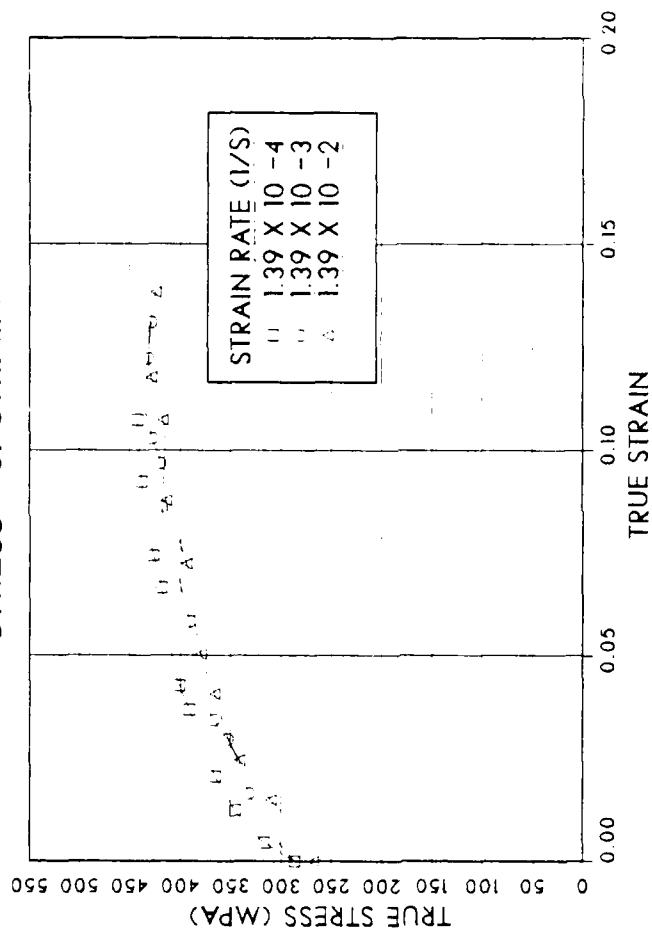


Figure A.6. True Stress versus True Strain Data for Tensile Tests Conducted at 20°C on Al-8% Mg Alloy in the As-Rolled Condition.

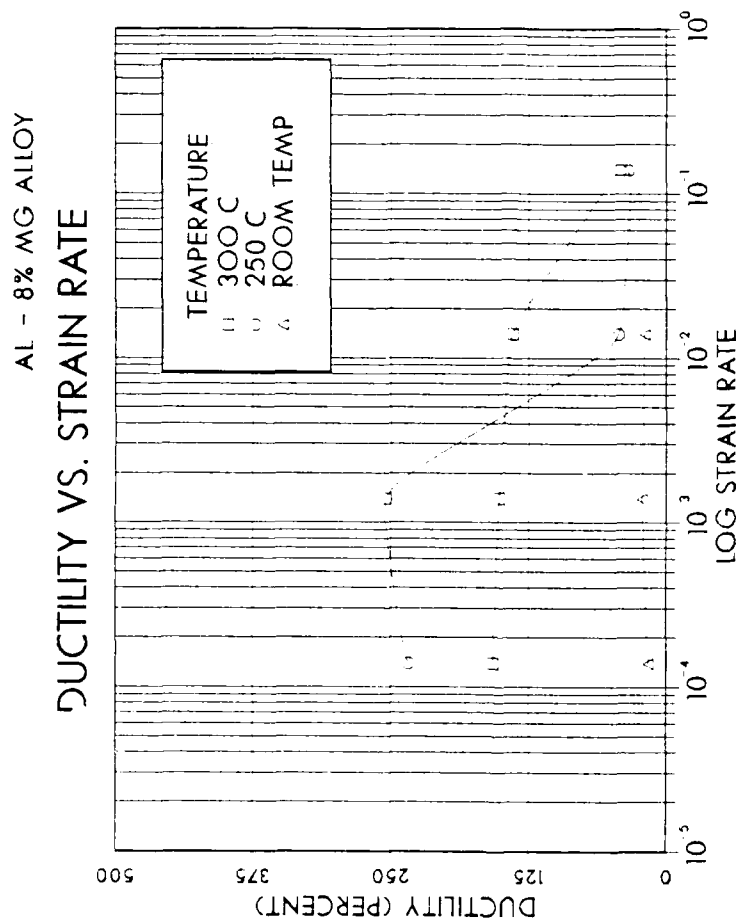


Figure A.7. Ductility versus Strain Rate for Tensile Tests on Al-8% Mg Alloy, Tests Conducted at Room Temperature, 250°C, and 300°C.



# APPENDIX B

## Mechanical Test Data on Al-10% Mg Alloy

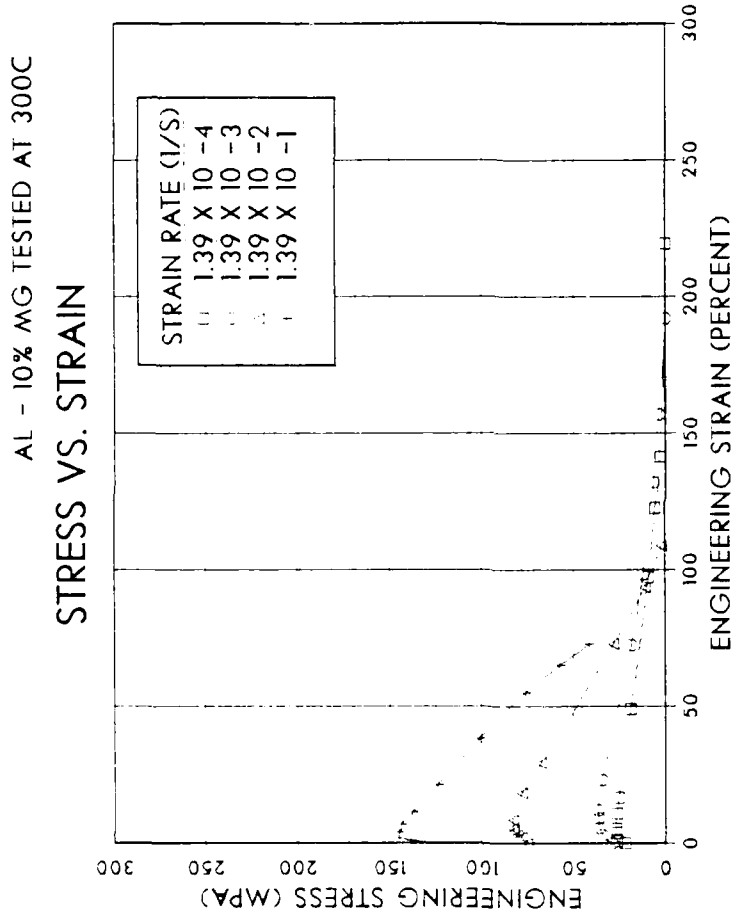


Figure B.1. Engineering Stress versus Engineering Strain Data for Tensile Tests Conducted at 300°C on Al-10% Mg Alloy in the As-Rolled Condition.

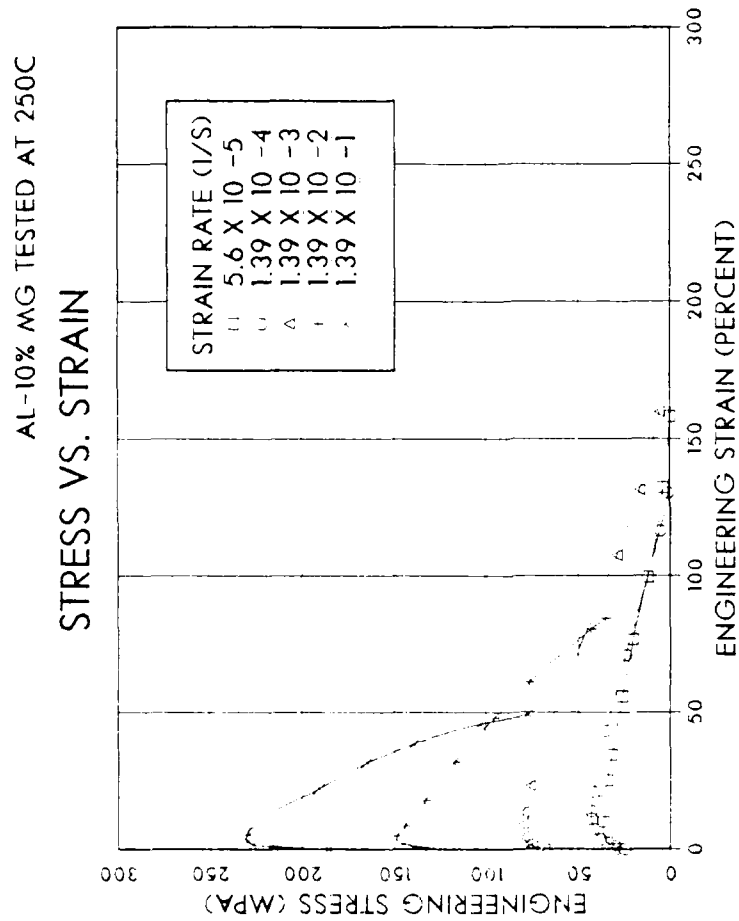


Figure B.2. Engineering Stress versus Engineering Strain Data for Tensile Tests Conducted at 250°C on Al-10% Mg Alloy in the As-Rolled Condition.

AD-A155 142

THE EFFECT OF ALLOY ADDITIONS ON SUPERPLASTICITY IN  
THERMOMECHANICALLY PR. (U) NAVAL POSTGRADUATE SCHOOL  
MONTEREY CA R J SELF DEC 84

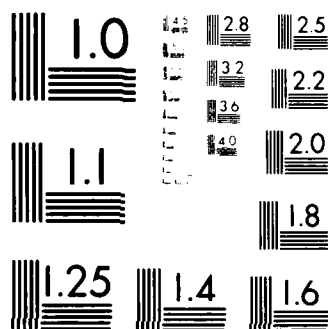
2/2

UNCLASSIFIED

F/G 11/6

NL

					END							
					PAID							
					DATE							



MURPHY RESOLUTION TEST CHART  
 U.S. GOVERNMENT PRINTING OFFICE: 1963 O

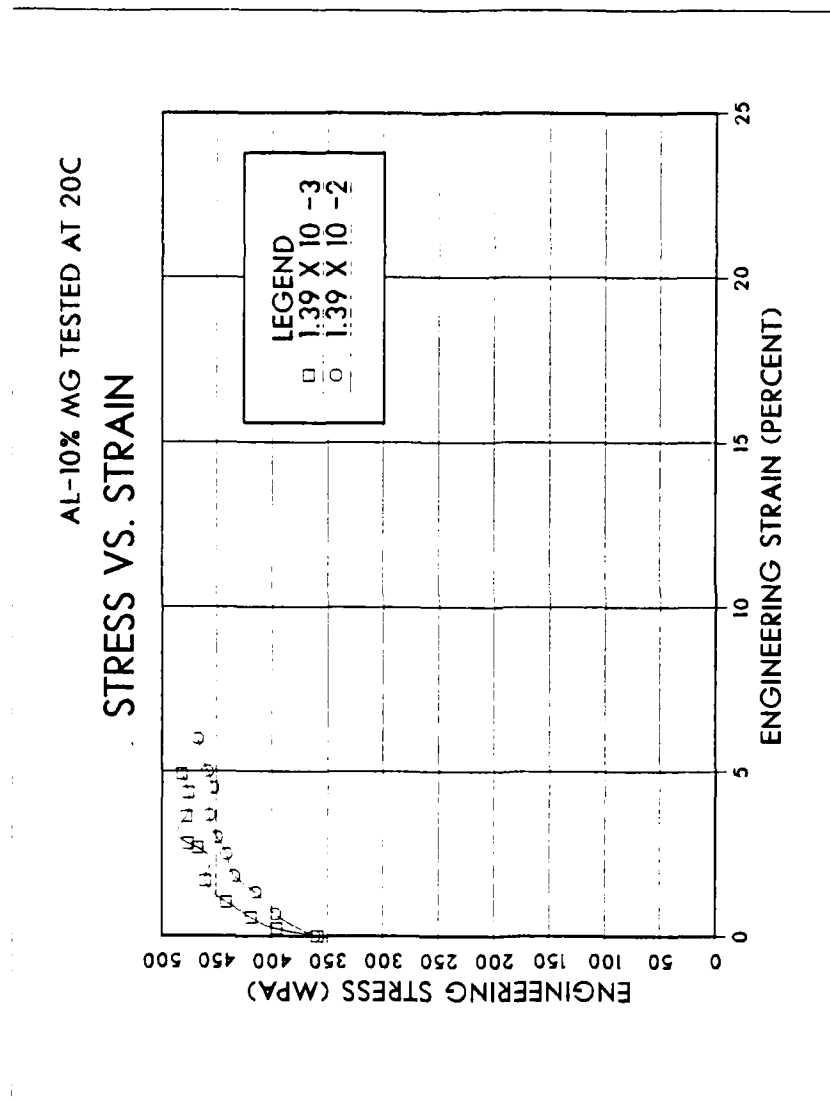


Figure B.3. Engineering Stress versus Engineering Strain Data for Tensile Tests Conducted at 20°C on Al-10% Mg Alloy in the As-Rolled Condition.

AL-10% MG TESTED AT 300C

# STRESS VS. STRAIN

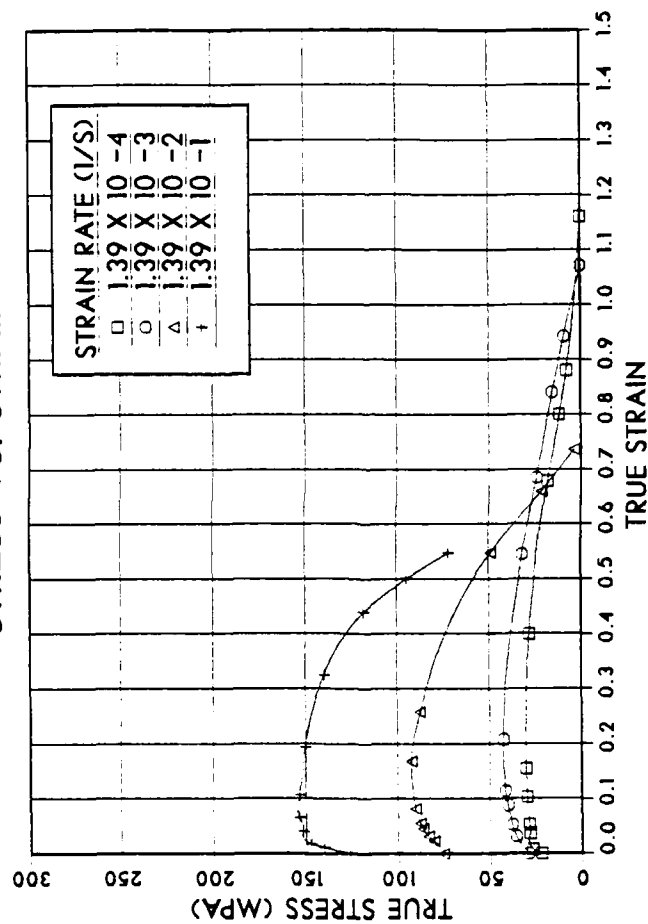


Figure B.4. True Stress versus True Strain Data for Tensile Tests Conducted at 300°C on Al-10% Mg Alloy in the As-Rolled Condition.

AL-10% MG TESTED AT 250C

# STRESS VS. STRAIN

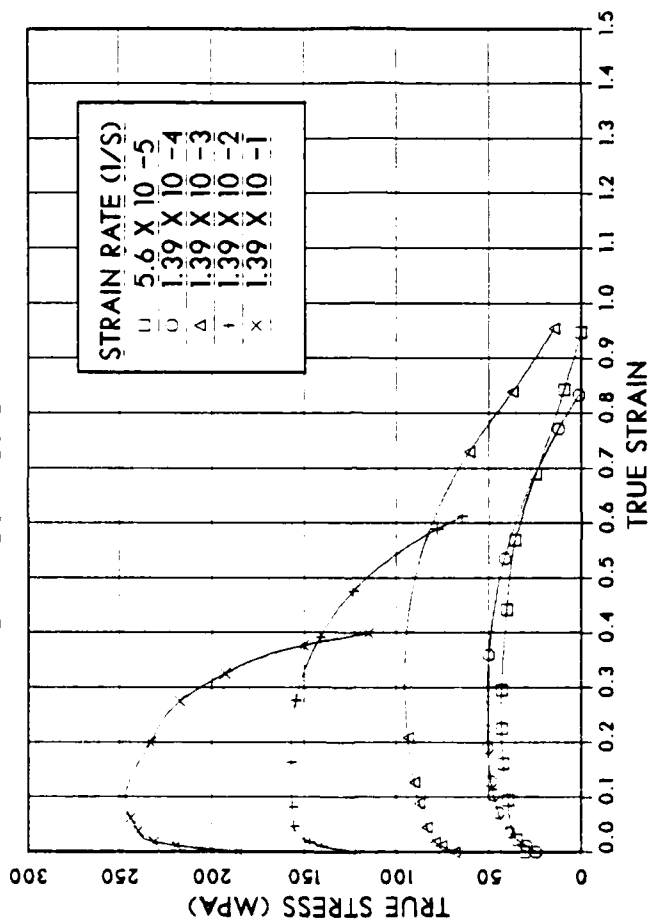


Figure B.5. True Stress versus True Strain Data for Tensile Tests Conducted at 250°C on Al-10% Mg Alloy in the As-Rolled Condition.

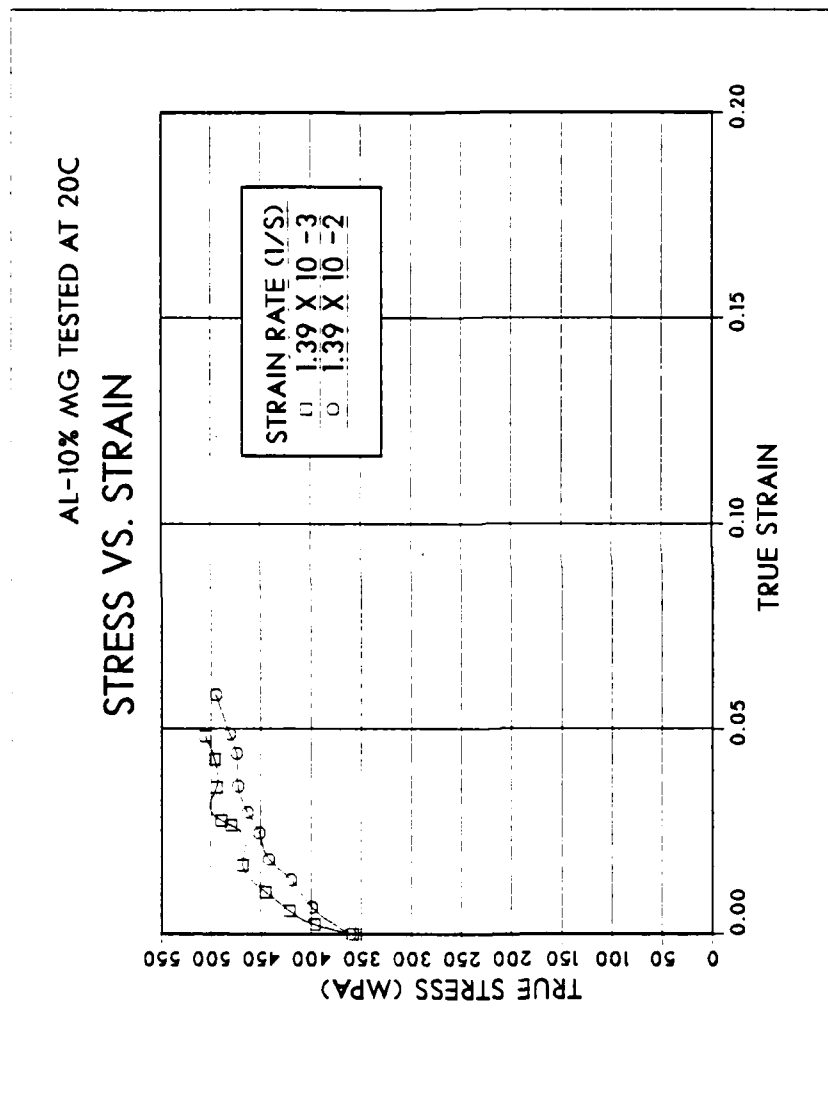


Figure B.6. True Stress versus True Strain Data for Tensile Tests Conducted at 20°C on Al-10% Mg Alloy in the As-Rolled Condition.



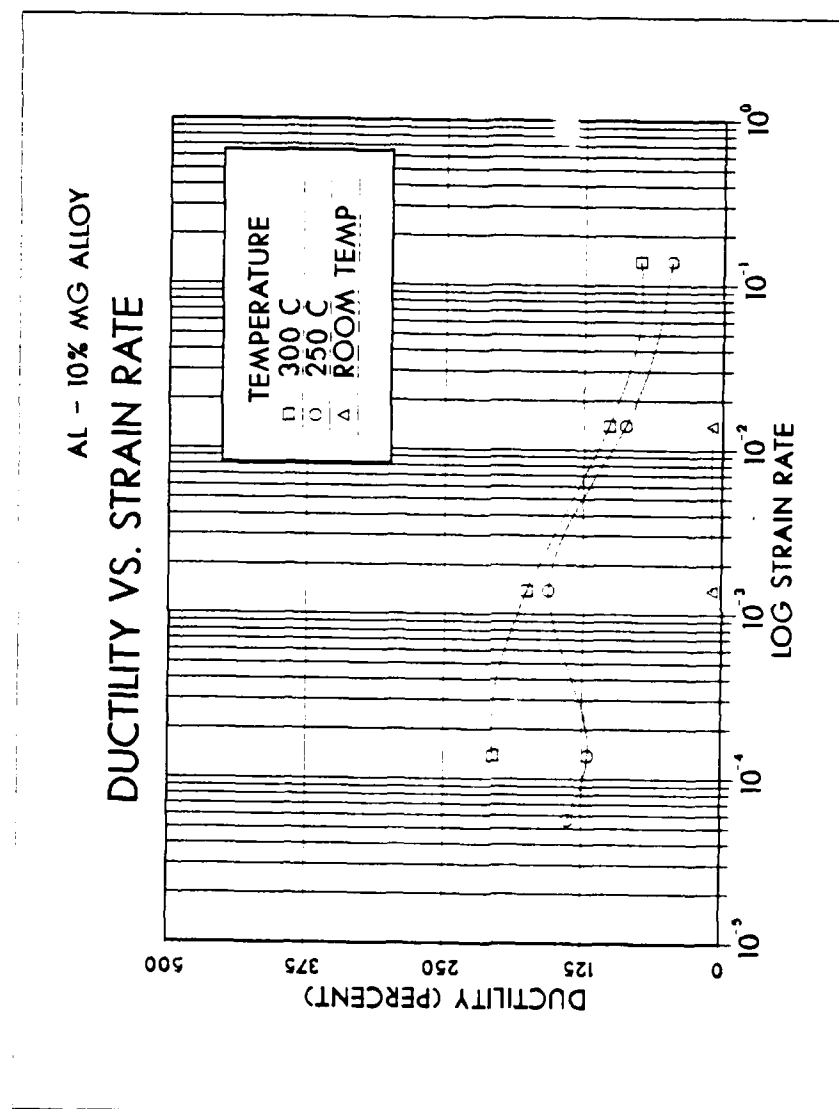


Figure B.7. Ductility versus Strain Rate for Tensile Tests on Al-10% Mg Alloy, Tests Conducted at Room Temperature, 250°C, and 300°C.

# APPENDIX C

## Mechanical Test Data on Al-10% Mg-0.4% Cu Alloy

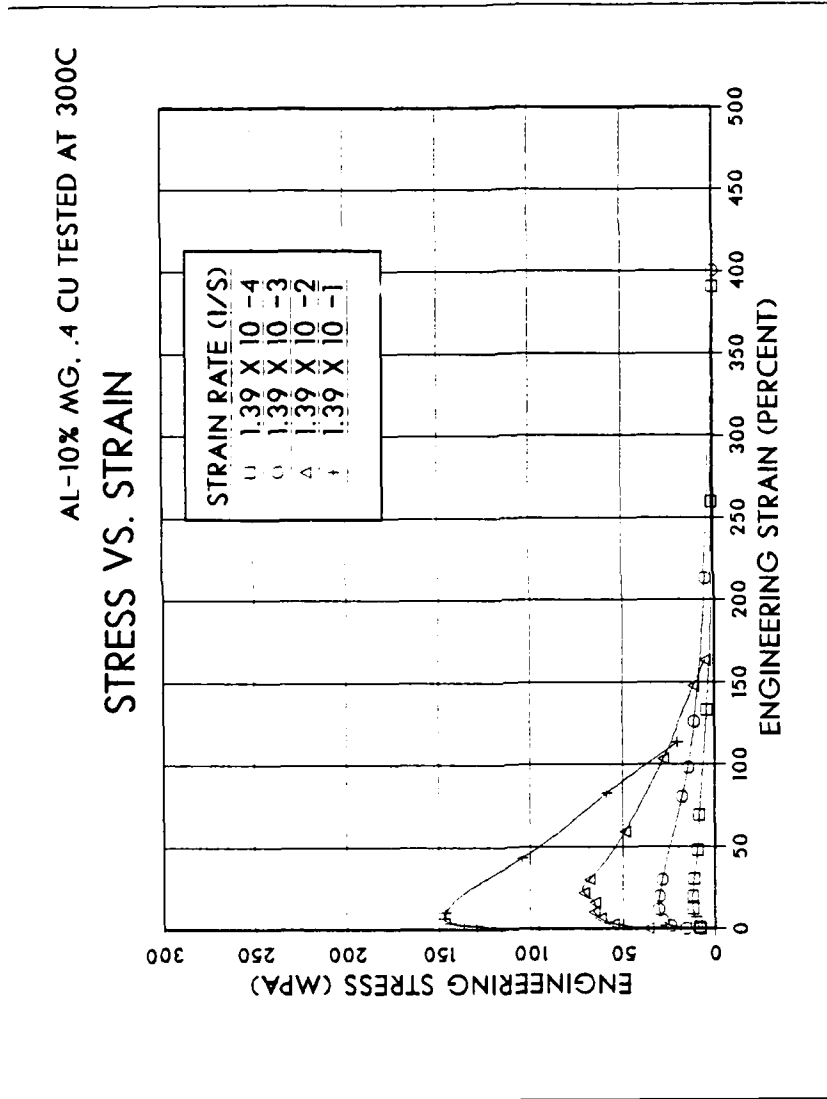


Figure C.1. Engineering Stress versus Engineering Strain for Tensile Tests Conducted at 300°C on Al-10% Mg-0.4% Cu Alloy in the As-Rolled Condition.

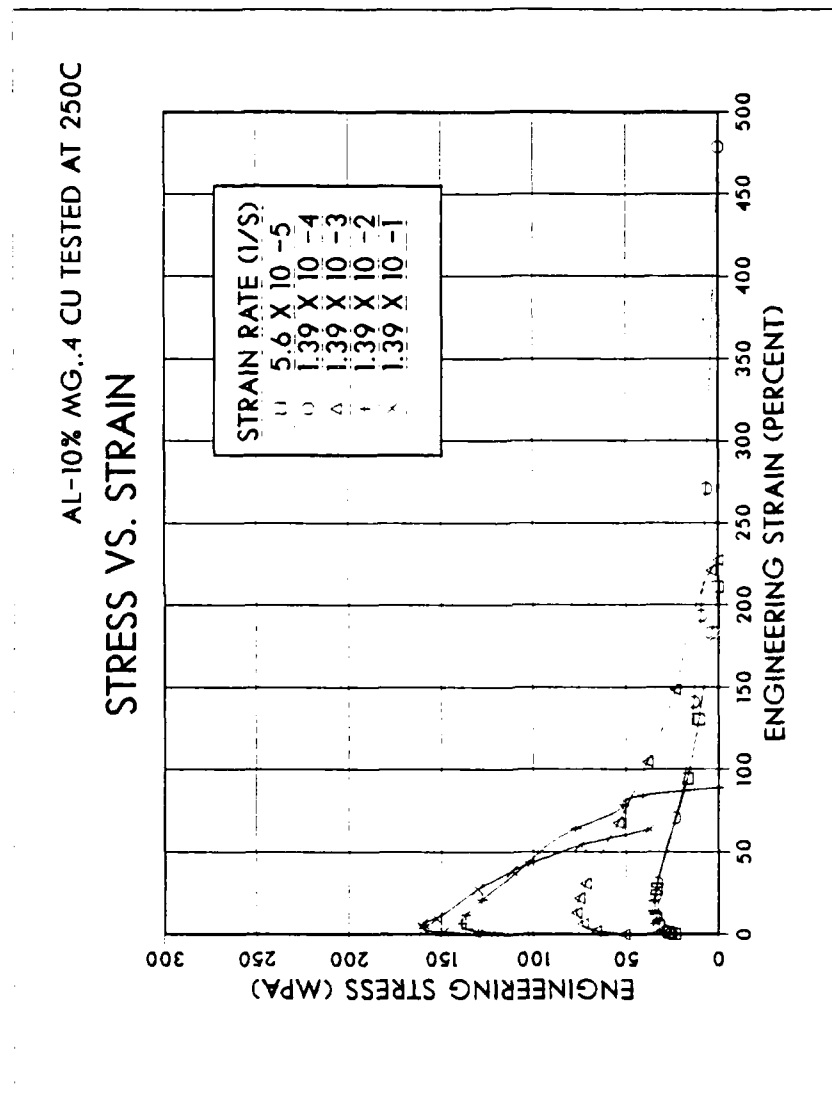


Figure C.2. Engineering Stress versus Engineering Strain for Tensile Tests Conducted at 250°C on Al-10% Mg-0.4% Cu Alloy in the As-Rolled Condition.

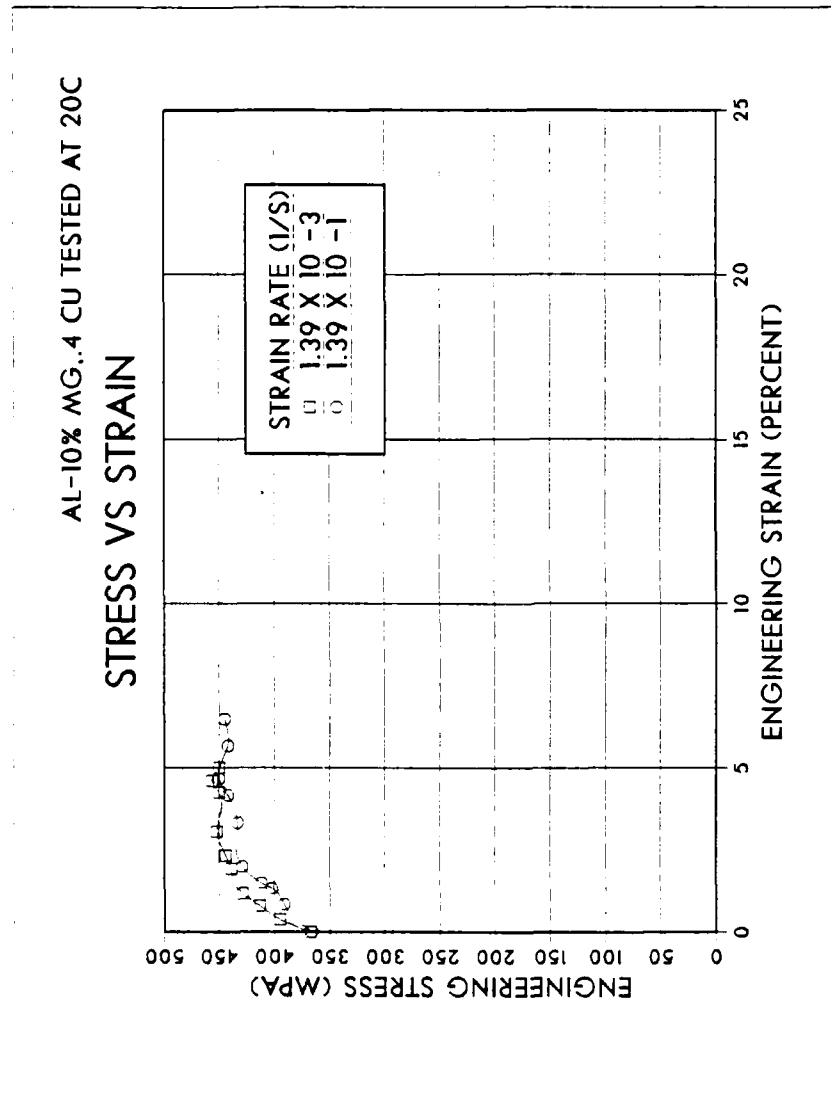


Figure C.3. Engineering Stress versus Engineering Strain for Tensile Tests Conducted at 20°C on Al-10% Mg-0.4% Cu Alloy in the As-Rolled Condition.

AL-10% MG, .4 CU TESTED AT 300C  
STRESS VS. STRAIN

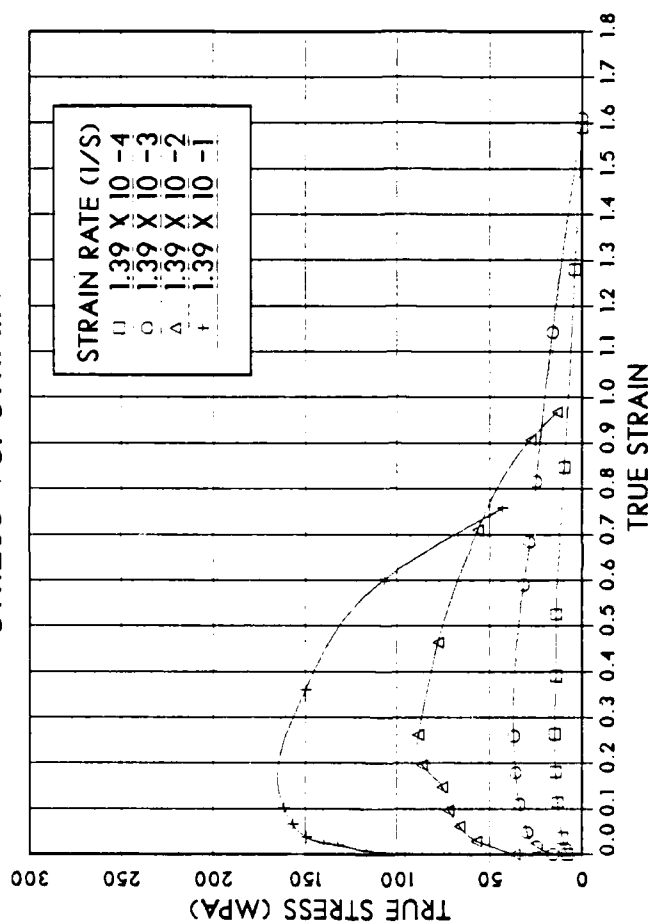


Figure C.4. True Stress versus True Strain Data for Tensile Tests Conducted at 300 C on Al-10% Mg-0.4% Cu Alloy in the As-Rolled Condition.

AL-10% MG. .4 CU TESTED AT 250C  
STRESS VS. STRAIN

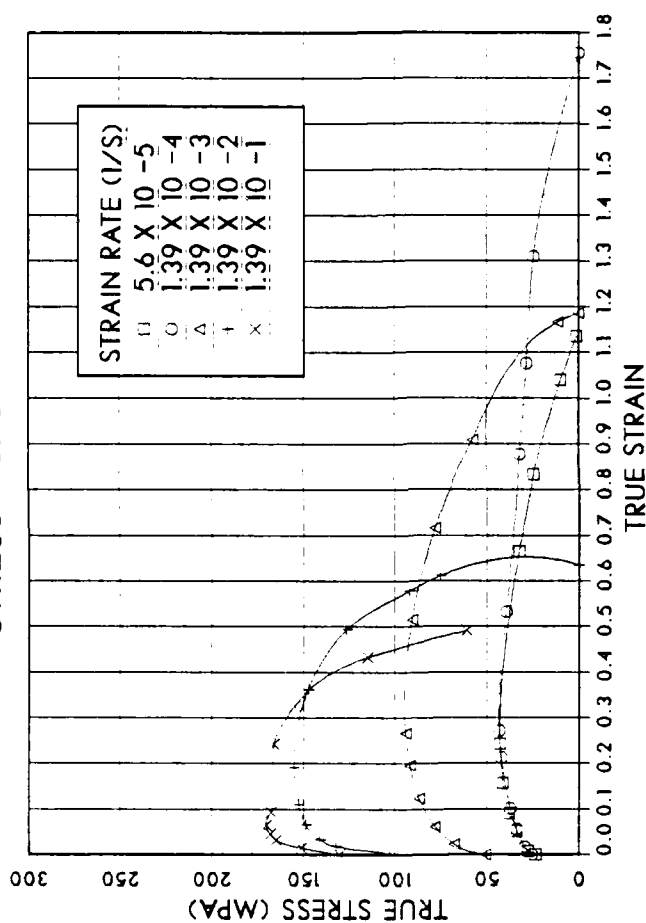


Figure C.5. True Stress versus True Strain Data for Tensile Tests Conducted at 250°C on Al-10% Mg-0.4% Cu Alloy in the As-Rolled Condition.

AL-10% MG. .4 CU TESTED AT 20C

# STRESS VS. STRAIN

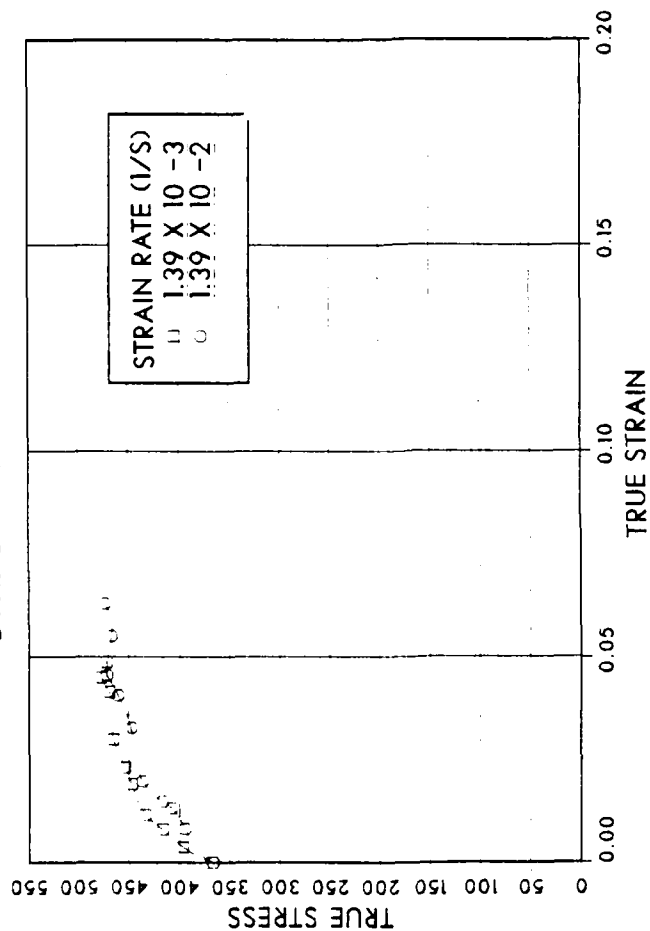


Figure C.6. True Stress versus True Strain Data for Tensile Tests Conducted at 20°C on Al-10% Mg-0.4% Cu Alloy in the As-Rolled Condition.

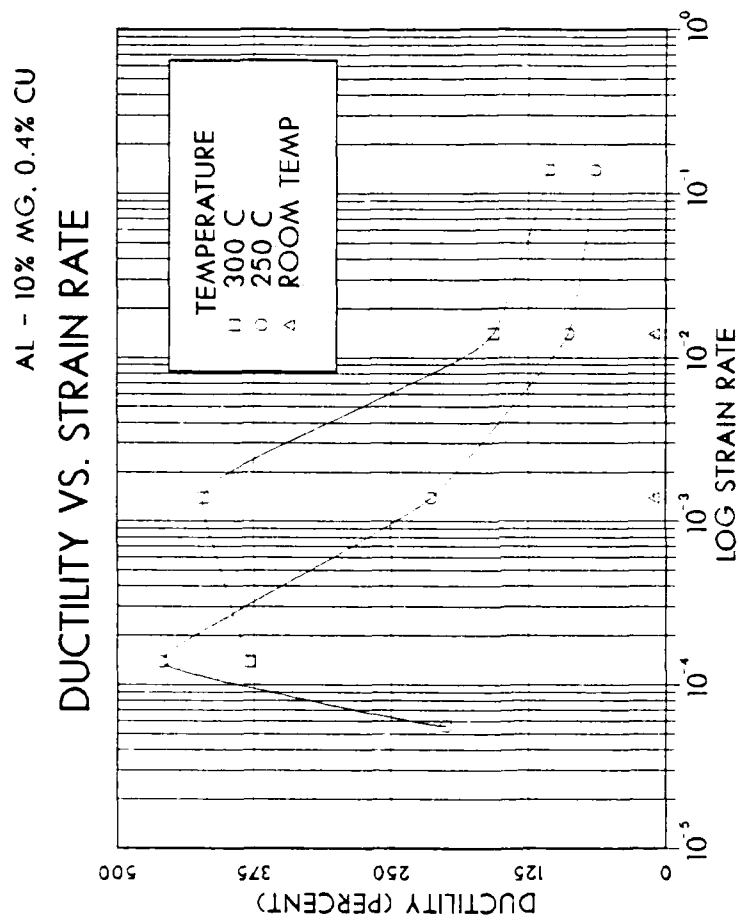


Figure C.7. Ductility versus Strain Rate for Tensile Tests on Al-10% Mg-0.4% Cu Alloy, Tests Conducted at Room Temperature, 250°C, and 300°C.



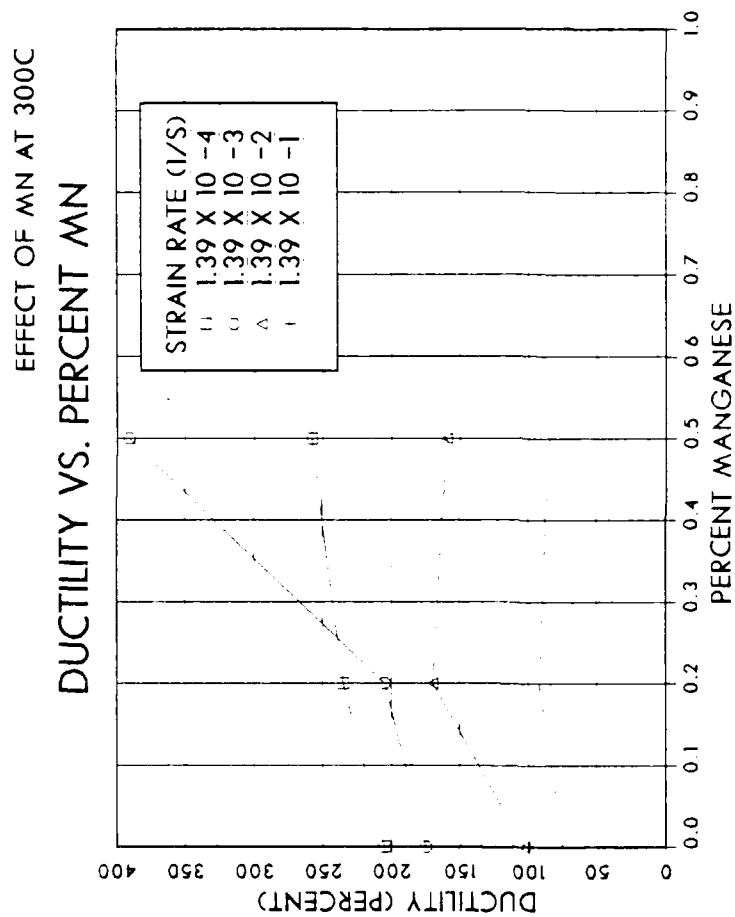


Figure F.2. Ductility versus Percent Mn Addition Data for Tensile Tests Conducted at 300°C for Mn Additions to the 10% Mg Binary Alloy in the As-Rolled Condition.

# APPENDIX F

## Mechanical Test Data on the Effect of Mn Addition on Al-10% Mg Alloy

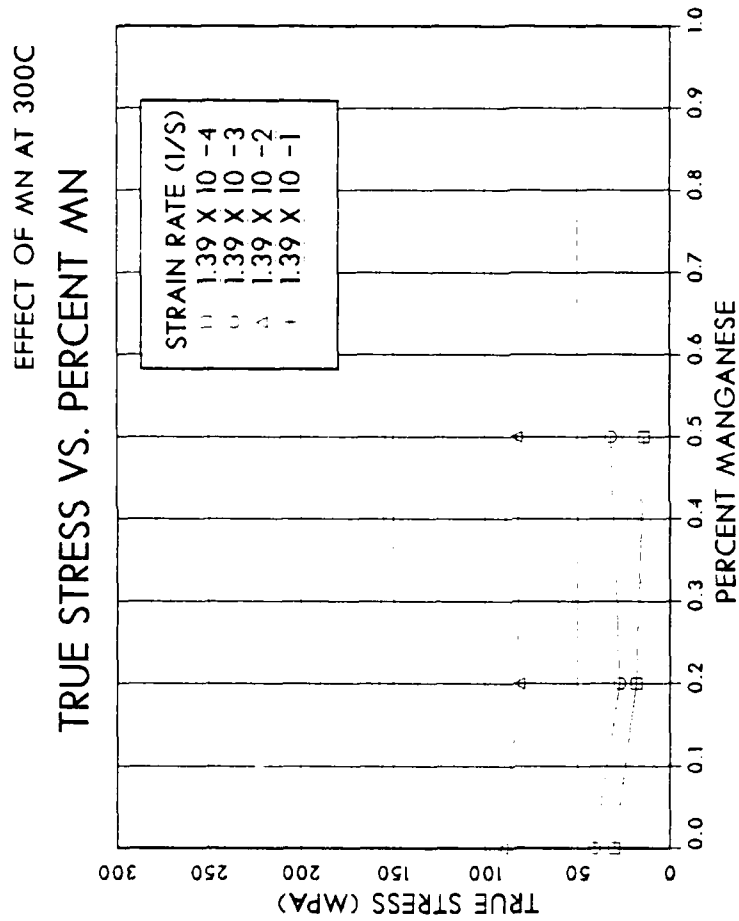


Figure F.1. True Stress versus Percent Mn Addition Data for Tensile Tests Conducted at 300°C on Mn Additions to the 10% Mg Binary Alloy in the As-Rolled Condition.

AL-8%MG..4CU..5MN TESTED AT 20C

# STRESS VS. STRAIN

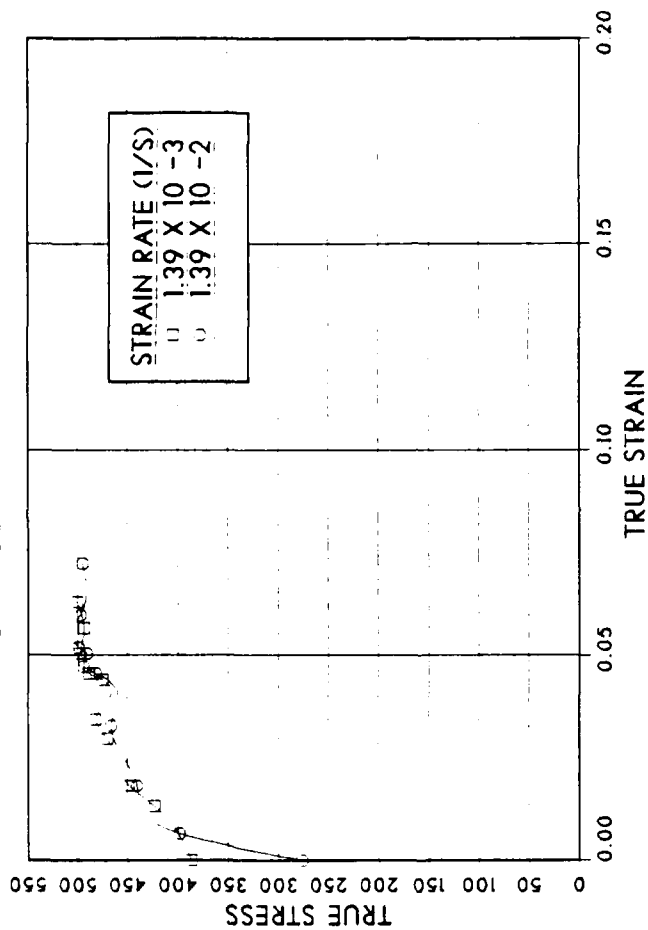


Figure F.6. True Stress versus True Strain Data for Tensile Tests Conducted at 20°C on Al-8% Mn-0.4% Cu-0.5% Mn Alloy in the As-Rolled Condition.

AL-8%MG..4CU..5MN TESTED AT 250C

# STRESS VS. STRAIN

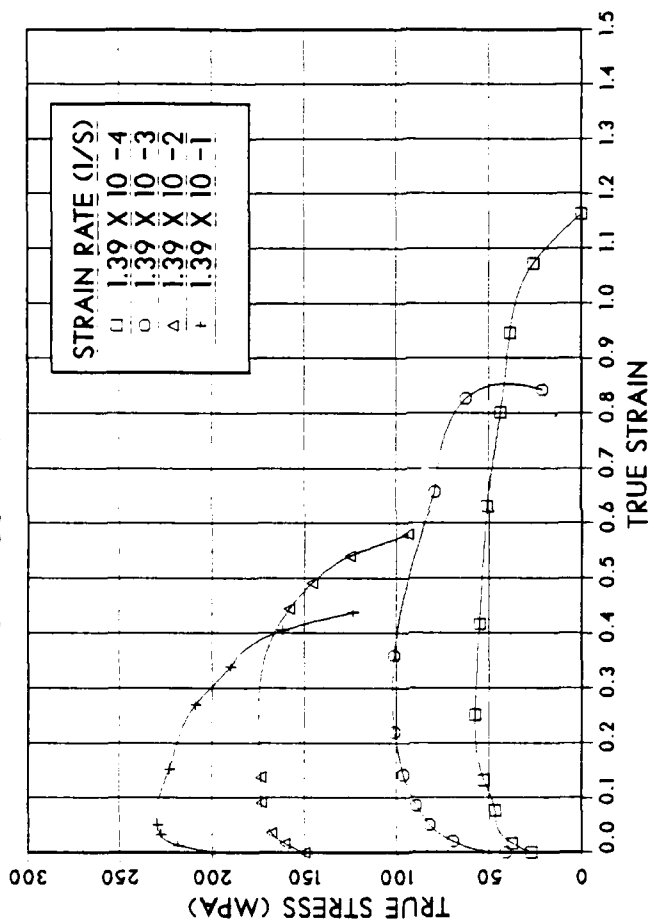


Figure E.5. True Stress versus True Strain Data for Tensile Tests Conducted at 250°C on Al-8% Mn-0.4% Cu-0.5% Mn Alloy in the As-Rolled Condition.

AL-8%MG..4CU..5MN TESTED AT 300C

# STRESS VS. STRAIN

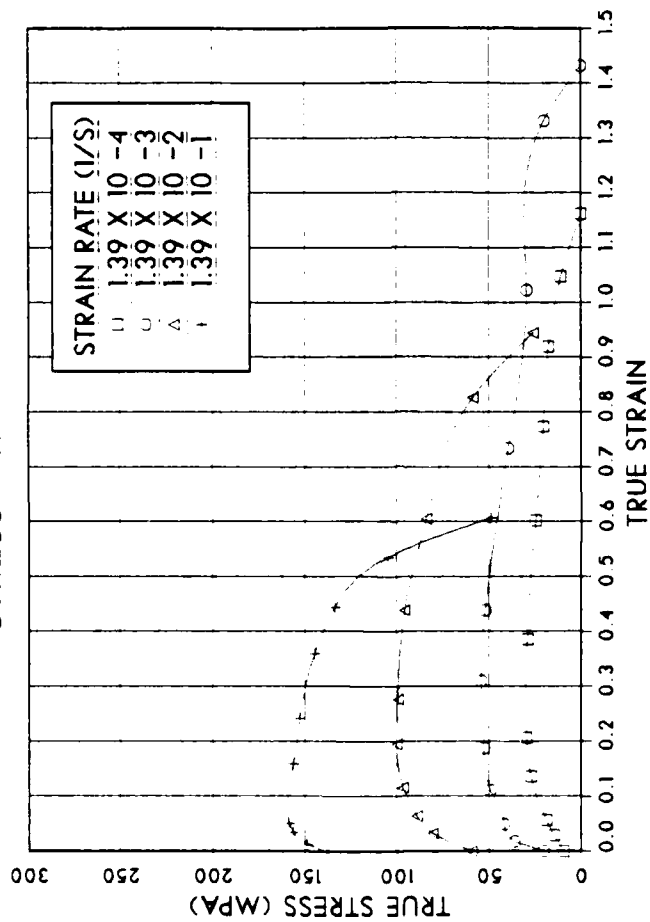


Figure E.4. True Stress versus True Strain Data for Tensile Tests Conducted at 300°C on Al-8% Mn-0.4% Cu-0.5% Mn Alloy in the As-Rolled Condition.

AL-8%MG..4CU..5MN TESTED AT 20C

# STRESS VS. STRAIN

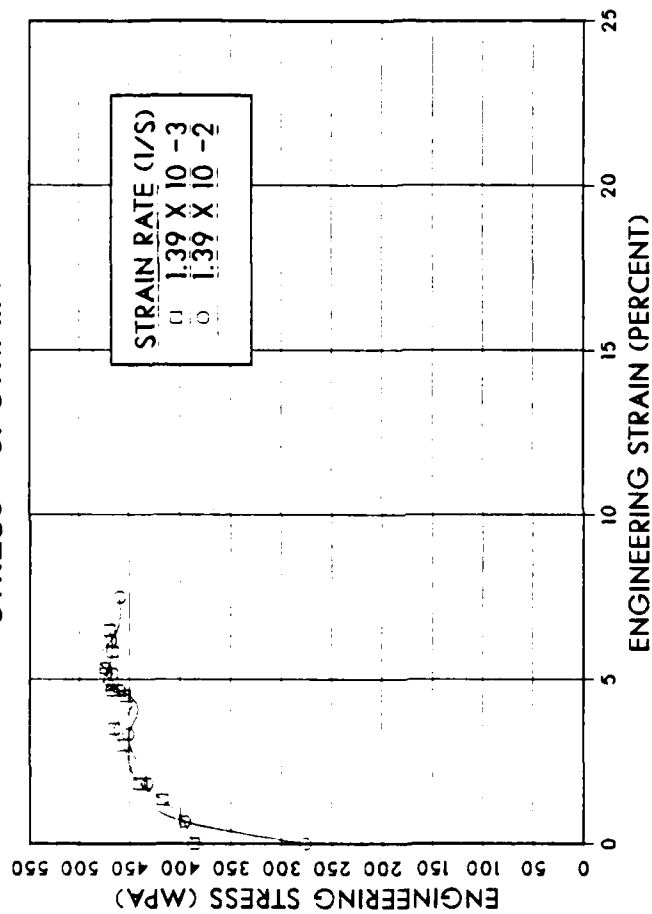


Figure E.3. Engineering Stress versus Engineering Strain Data for Tensile Tests Conducted at 20°C on Al-8% Mg-0.4% Cu-0.5% Mn Alloy in the As-Rolled Condition.

AL-8%MG..4CU..5MN TESTED AT 250C

# STRESS VS. STRAIN

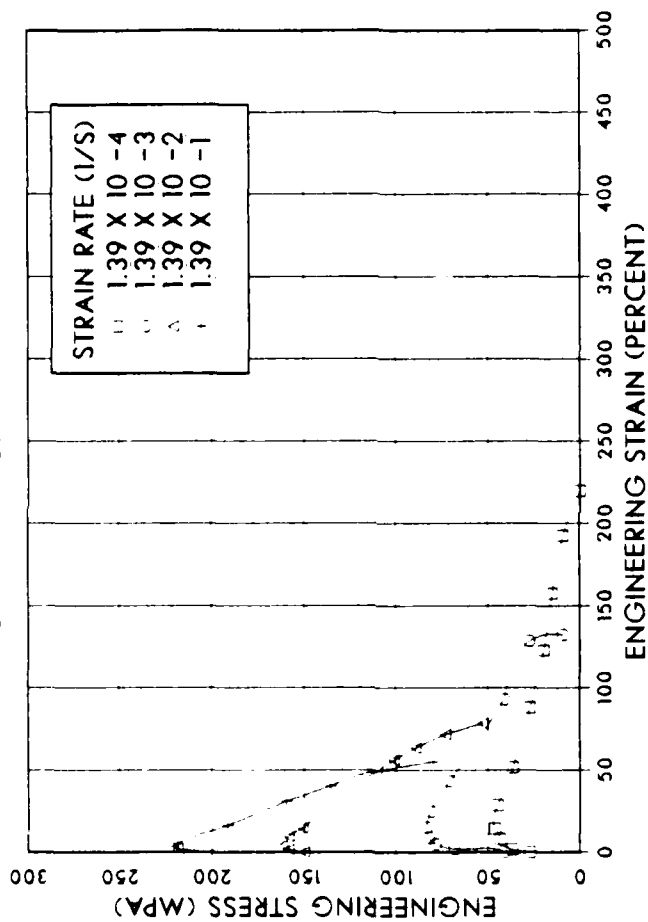


Figure E.2. Engineering Stress versus Engineering Strain Data for Tensile Tests Conducted at 250°C on Al-8% Mg-0.4% Cu-0.5% Mn Alloy in the As-Rolled Condition.

# APPENDIX E

Mechanical Test Data on Al-8% Mn-0.4% Cu-0.5% Mn Alloy

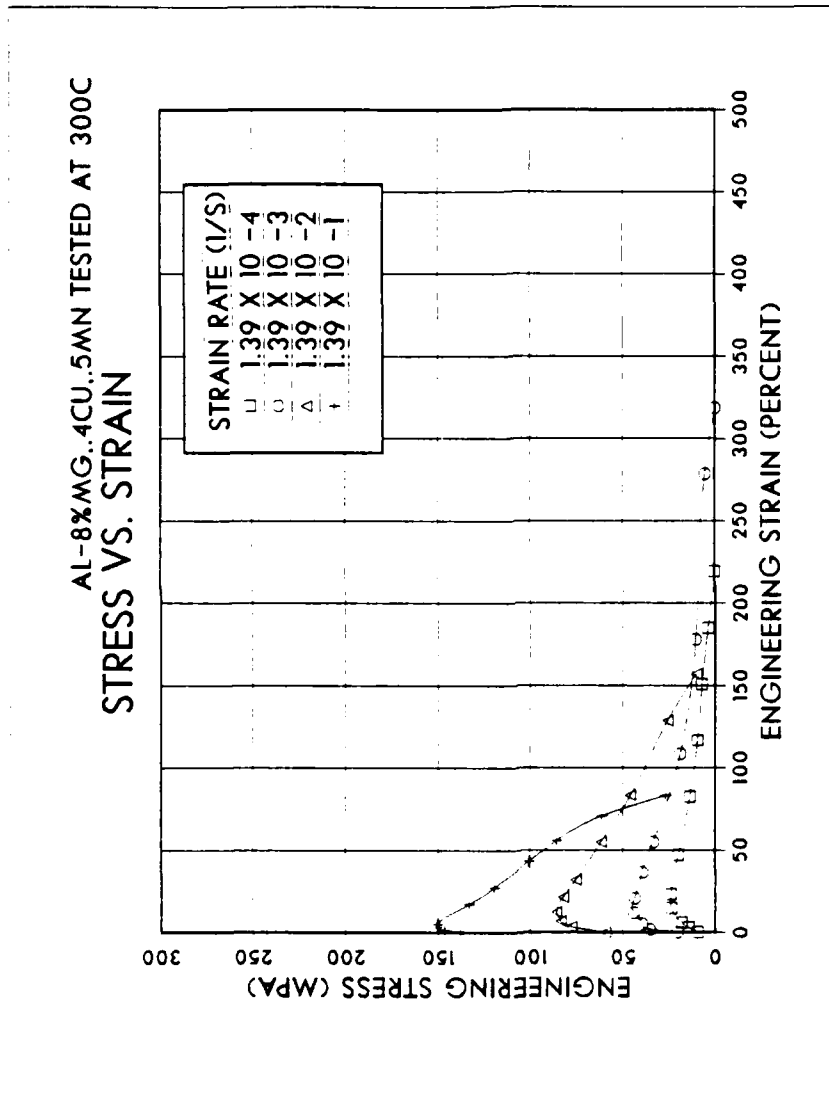


Figure E.1. Engineering Stress versus Engineering Strain for Tensile Tests Conducted at 300°C on Al-8% Mg-0.4% Cu-0.5% Mn Alloy in the As-Rolled Condition.



AL-10% MG. .2 MN TESTED AT 20C

# STRESS VS. STRAIN

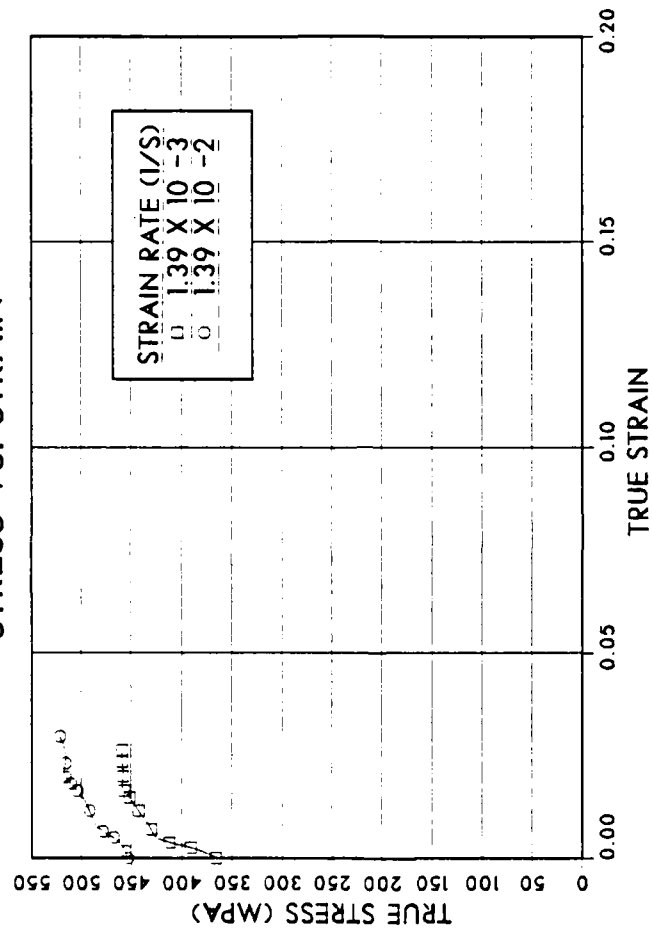


Figure D.6. True Stress versus True Strain Data for Tensile Tests Conducted at 20 C on Al-10% Mg-0.2% Mn Alloy in the As-Rolled Condition.

AL-10% MG, 2 MN TESTED AT 250C

# STRESS VS. STRAIN

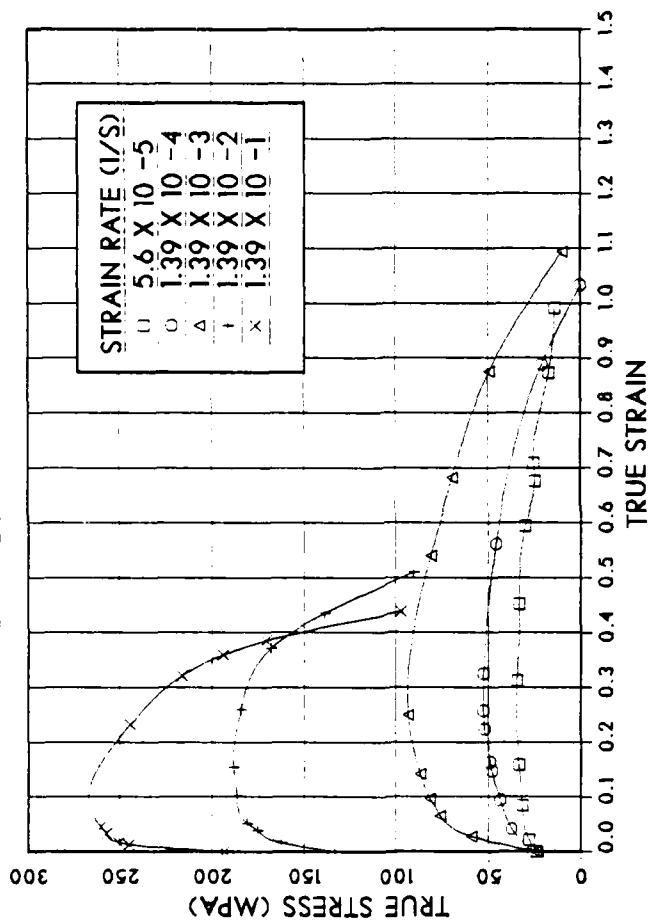


Figure D.5. True Stress versus True Strain Data for Tensile Tests Conducted at 250°C on Al-10% Mg-0.2% Mn Alloy in the As-Rolled Condition.

AL-10% MG, .2 MN TESTED AT 300C

# STRESS VS. STRAIN

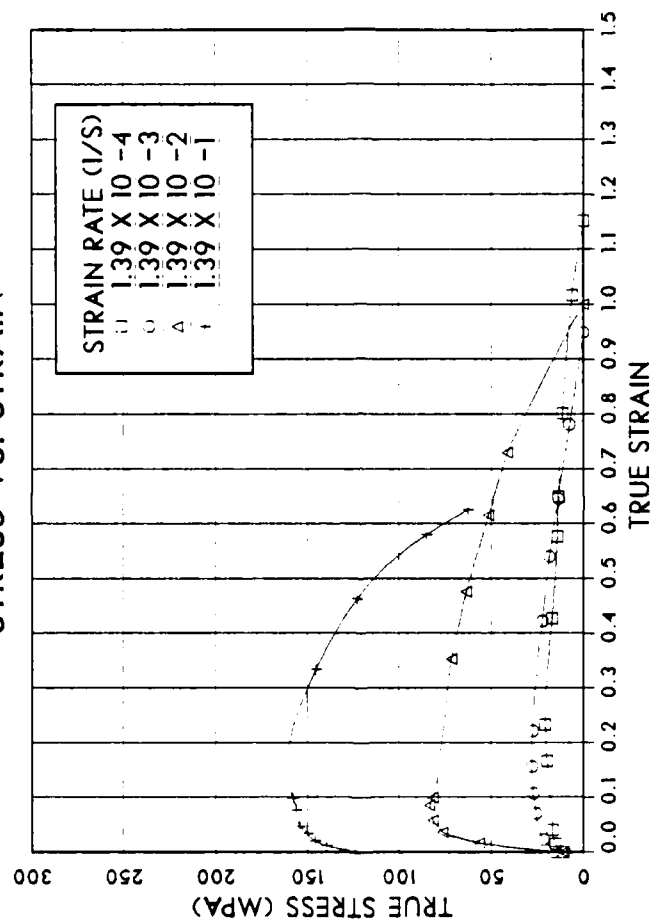


Figure D.4. True Stress versus True Strain Data for Tensile Tests Conducted at 300°C on Al-10% Mg-0.2% Mn Alloy in the As-Rolled Condition.

AL-10% MG, .2MN TESTED AT 20C

# STRESS VS. STRAIN

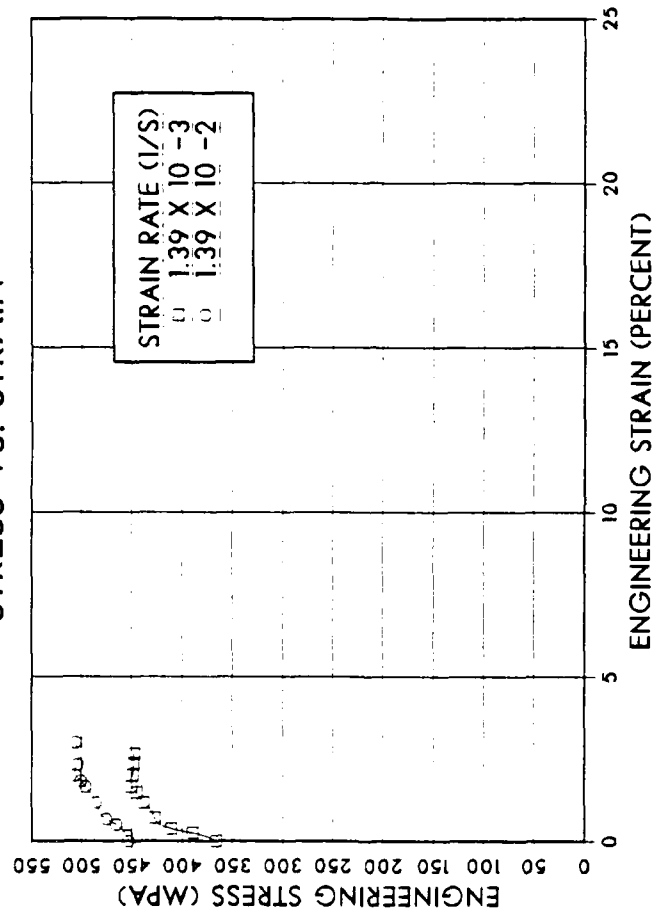


Figure D.3. Engineering Stress versus Engineering Strain Data for Tensile Tests Conducted at 20°C on Al-10% Mg-0.2% Mn Alloy in the As-Rolled Condition.

AL-10%MG, .2 MN TESTED AT 250C

# STRESS VS. STRAIN

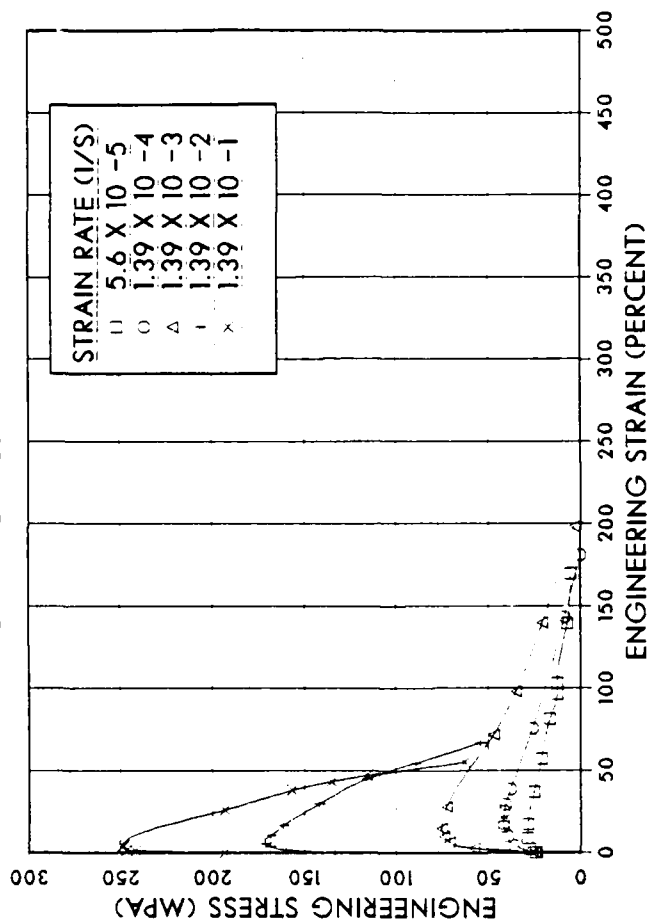


Figure D.2. Engineering Stress versus Engineering Strain Data for Tensile Tests Conducted at 250°C on Al-10% Mg-0.2% Mn Alloy in the As-Rolled Condition

# APPENDIX D

## Mechanical Test Data on Al-10% Mg-0.2% Mn Alloy

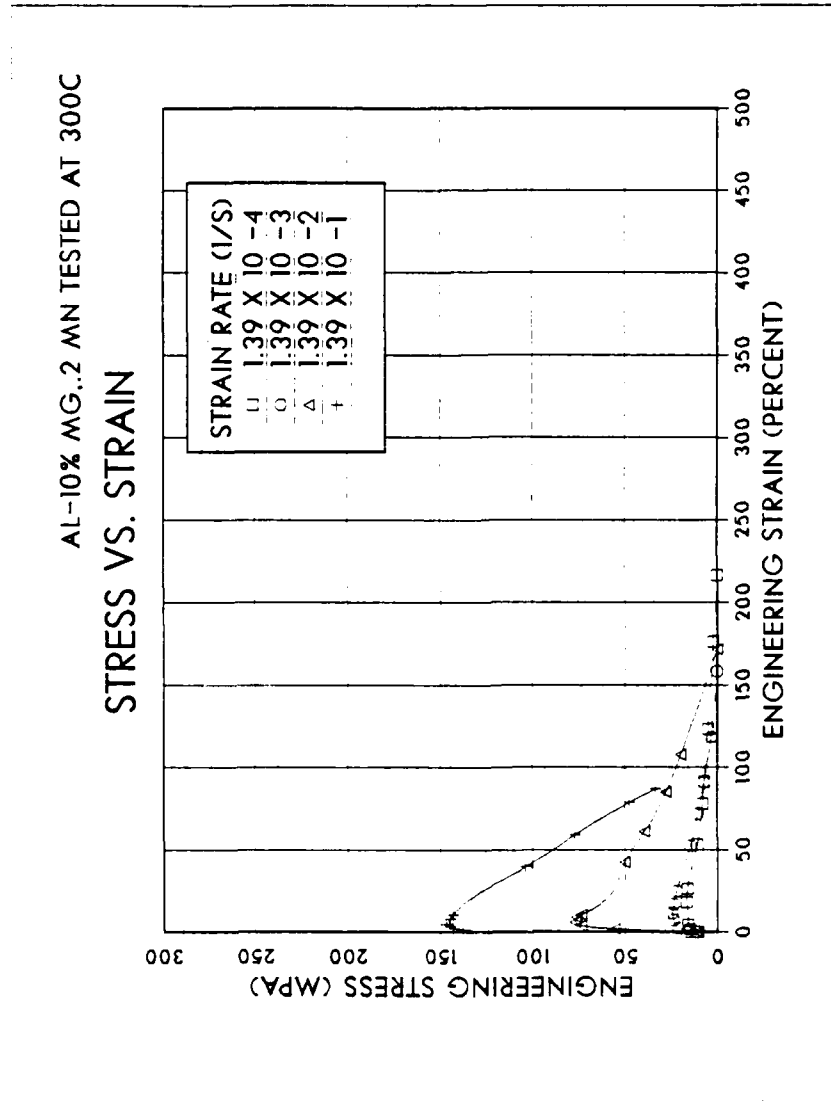


Figure D.1. Engineering Stress versus Engineering Strain Data for Tensile Tests Conducted at 300°C on Al-10% Mg-0.2% Mn Alloy in the As-Rolled Condition

EFFECT OF MN AT 250C

TRUE STRESS VS. PERCENT MN

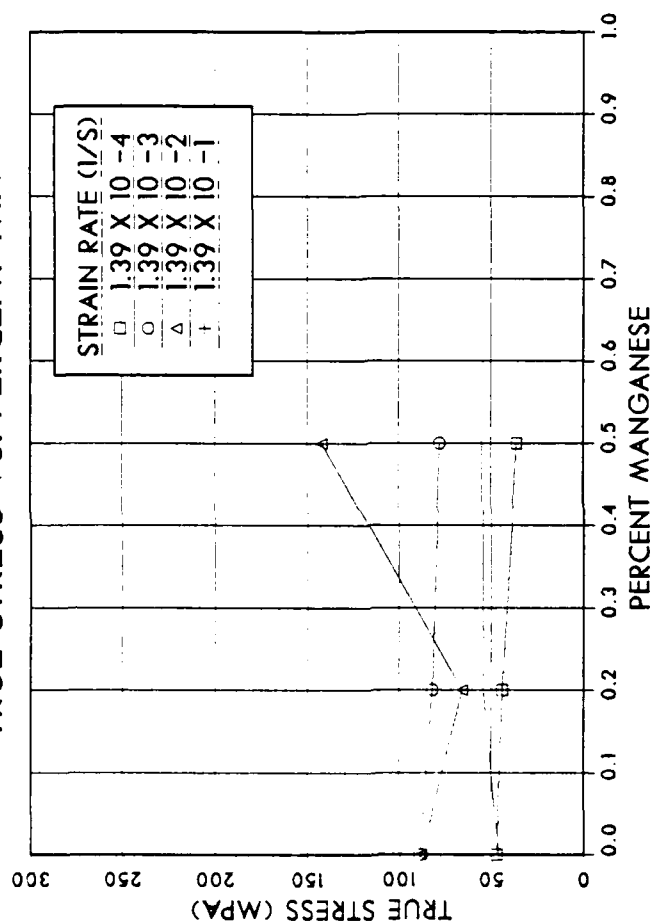


Figure F.3. True Stress versus Percent Mn Addition Data for Tensile Tests Conducted at 250°C for Mn Additions to the 10% Mg Binary Alloy in the As-Rolled Condition.

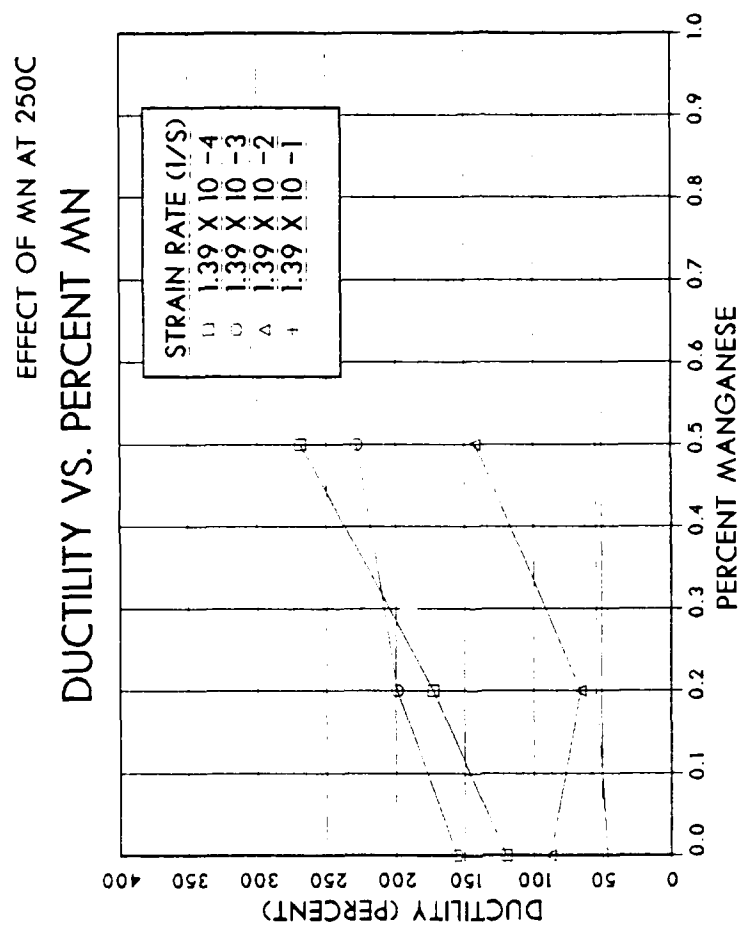


Figure F.4. Ductility versus Percent Mn Addition Data for Tensile Tests Conducted at 250°C for Mn Additions to the 10% Mg Binary Alloy in the As-Rolled Condition.



## LIST OF REFERENCES

1. Ness, F.G., Jr., High Strength to Weight Aluminum-18 Weight Percent Magnesium Alloy Through Thermomechanical Processing, M.S. Thesis, Naval Postgraduate School, Monterey, California, December 1976.
2. Bingay, C.P., Microstructural Response of Aluminum--Magnesium Alloys to Thermomechanical Processing, M.S. Thesis, Naval Postgraduate School, Monterey, California, December 1977.
3. Glover, T.L., Effects of Thermomechanical Processing on Aluminum-Magnesium Alloys Containing High Weight Percent Magnesium, M.S. Thesis, Naval Postgraduate School, Monterey, California, December 1977.
4. Grandon, R.A., High Strength Aluminum-Magnesium Alloys: Thermomechanical Processing, Microstructure, and Tensile Mechanical Properties, M.S. Thesis, Naval Postgraduate School, Monterey, California, December 1976.
5. Speed, W.G., An Investigation into the Influence of Thermomechanical Processing on Microstructure and Mechanical Properties of High Strength Aluminum--Magnesium Alloys, M.S. Thesis, Naval Postgraduate School, Monterey, California, December 1976.
6. Chesterman, C.W., Jr., Precipitation, Recovery and Recrystallization Under Static and Dynamic Conditions for High Magnesium Aluminum Magnesium Alloys, M.S. Thesis, Naval Postgraduate School, Monterey, California, March 1980.
7. R. B. Johnson, The Influence of Alloy Composition and Thermomechanical Processing Procedure on Microstructural and Mechanical Properties of High-Magnesium Aluminum Magnesium Alloys, M.S. Thesis, Naval Postgraduate School, Monterey, California, June 1980.
8. Shirah, R.H., The Influence of Solution Time and Quench Rate on the Microstructure and Mechanical Properties of High-Magnesium Aluminum-Magnesium Alloys, M.S. Thesis, Naval Postgraduate School, Monterey, California, December 1981.

9. McNelley, T.R. and Garg, A., "Development of Structure and Mechanical Properties in Al-10.2% Mg by Thermomechanical Processing," Scripta Metallurgica, v. 13, pp. 917-920, 1984.
10. Becker, J., Superplasticity in Thermomechanically Processed High Magnesium, Aluminum-Magnesium Alloys, M.S. Thesis, Naval Postgraduate School, Monterey, California, March 1984.
11. Mills, M.E., Superplasticity in a Thermomechanically Processed Aluminum-10.2% Mg, 0.5% Mn Alloy, M.S. Thesis, Naval Postgraduate School, Monterey, California, September 1984.
12. Stengel, A., Effects of Annealing Treatments on Superplasticity in a Thermo-Mechanically Processed Aluminum-10.2% Mg, 0.52% Mn Alloy, M.S. Thesis, Naval Postgraduate School, Monterey, California, December 1984.
13. Bly, D.C., Sherby, O.D., and Young, C.M., "Influence of Thermal Mechanical Treatments on the Mechanical Properties of a Finely Spheroidized Eutectic Composition Steel," Material Science and Engineering, v. 12, pp. 41-46, 1973.
14. Zener, C., as quoted by C.S. Smith, "Grains, Phases, Phase and Interphases: An Interpretation of Microstructure," Transactions American Institute of Metallurgical Engineering, v. 175, pp. 15-51, 1948.
15. Sherby, O.D., and Burke, P.M., "Mechanical Behavior of Crystalline Solids at Elevated Temperatures," Progress in Materials Science, v. 13, p. 325, 1968.
16. Mondolfo, L.F., Aluminum Alloys: Structure and Properties, Butterfield and Co. (publishers), 1976.
17. Holt, D.L., and Backofen, W.A., "Superplasticity in Al-Cu Eutectic Alloy," Transactions of American Society for Metals, v. 59, pp. 755-767, 1966.

# INITIAL DISTRIBUTION LIST

	<u>No. Copies</u>
1. Defense Technical Information Center Cameron Station Alexandria, Virginia 22314	2
2. Library, Code 0142 Naval Postgraduate School Monterey, California 93943	2
3. Department Chairman, Code 69Mx Department of Mechanical Engineering Naval Postgraduate School Monterey, California 93943	1
4. Professor T.R. McNelley, Code 69Mc Department of Mechanical Engineering Naval Postgraduate School Monterey, California 93943	5
5. Mr. Richard Schmidt, Code AIR 320A Naval Air Systems Command Naval Air Systems Command Headquarters Washington, D.C. 20361	1
6. LT Richard J. Self, USN 6607 Green Gables Avenue San Diego, California 92119	3

**END**

**FILMED**

7-85

**DTIC**